CLARO

Undergraduate Interdisciplinary Journal

Vol. VIII
Spring, 2020

Red Rocks Community College

RED ROCKS
COMMUNITY COLLEGE

Claro

Undergraduate Interdisciplinary Journal

Vol VIII

Claro
Trefny Honors
Red Rocks Community College
Lakewood, CO 80228

Editor, Design, Layout & Formatting
Barbra Sobhani, Director, Trefny Honors

Cover Design
Danea Fidler

Table of Contents

Part I Creative Work

Part II Undergraduate Research

Part I
Creative Work

Have Ani Luck?:
Adventures in Birdwatching

Brendan Burns
ENG 122 Composition II Fall 2017

I pulled my car up next to a curve in the road, placed it in park and got out onto the hot black asphalt. It was 1 o'clock on a Tuesday and after a long and dirty shift at the zoo, I had decided to take a detour home in an attempt to find a rare bird nearby. The sun, poised high in the air, beat down upon me with its heated rays as I opened up the side door of the car and got my red hip-pack containing my camera out. I debated internally whether or not to bring my tan brim hat. It had protected my head from the sun in the lowland desert of Qatar and its immediate rays atop alpine summits, however it did look very dorky. For all I knew the prettiest teenage bird-nerd could be out there and have the same quarry as me. I ended up taking it; deciding that this adaptation to the heat would suit me better than potentially finding a mate.

I began trekking, or in a less adventurous reality, awkwardly walking in my grey, bulky waterproof boots through a small yellowish-green lot up to a slanted barbwire fence where two elderly men were standing. The size of their camera lenses dwarfed my own, sticking out roughly a foot and a half from the base of their cameras. I gave a still wave as I walked forward exclaiming, "I'm guessing we're here for the same thing." Typically when more than two people are together, holding cameras in an area where a rare bird was spotted they automatically know what you're talking about. When this happens it provides a brief but favorable feeling that you're not the only person interested in this odd hobby. "Yep, haven't seen him yet today but he was here yesterday", the larger of the two men replied. The other man also pitched in and pointed claiming that "a young fella went down that way lookin' for it." I looked both directions and seeing the way where the man pointed I decided to go the opposite direction figuring that nobody had gone that way before and perhaps he may have been looking in the wrong place.

I've always considered myself a bit of a frontiersman, especially when it comes to birding. I've always been one to go the opposite direction of others, exploring new regions as I go. I figure that if nobody has gone a direction and still can't find the same goal, perhaps then I'm exploring the region where the animal has gone. This logic proved useful in January when looking for a pink-footed goose at a crowded lake full two thousand Canadian geese. It was quite literally trying to find a needle in a haystack. Despite the cold weather, high tech birders with large telephonic lenses and expensive binoculars dotted the circumference of the lake, looking for the same one goose. My mother and I had looked around for roughly two hours and saw nothing. While she went back to sit in the warmth of

the car I continued searching. After another thirty minutes almost realizing failure, I sat down on a large granite rock and peered through a small pair of BassPro binoculars at the sea of geese, not expecting to see one different from the others. To my extreme luck, the place I sat provided a near-perfect view of a goose not quite like the rest of them. A smile pushed back my frozen cheeks as I drew my camera and began photographing the rare animal. Other birders had passed this location up however by exploring the area on my own I was able to find the bird first and bring it to other birder's attention.

Today, however, I walked along this barbwire fence, my eyes peeled on the green creek flowing steadily below me. The intense cold of January served me only in memory as the fiery sharpness of the sun continued. Today my grandfather's binoculars hung at my chest. These binoculars carried my extended vision and memories of the man who got me into birdwatching. Back on the porch of his Wyoming home together we would watch the wild deer and turkeys roam their open wooded backyard. We spied on the line of bird feeders set intricately along the hillside and the colorful birds that stopped to rest there We would often make bets (using whatever pennies and dimes I was able to pick up as I traveled) on any species discrepancy we had on the bright orange and blue birds that landed on his feeder. Most of the time I won. Today I'm not sure if he was letting me win or is he just called every orange bird an "oriole." If it wasn't for him and the love of birds he instilled in me, I most likely wouldn't be pursuing a bird that day.

I stopped and put the binoculars up to my eyes, looking for any movement other than the persistent flow of the stream. Nothing. I continued on, periodically stopping and gazing through the metal lenses. This particular bird hadn't made it easy for itself to be seen. The bird in question was a Groove-billed ani, a bird native to Central and South America. Similar looking to a grackle or a small crow, the Groove-billed ani shares the metallic black feathering however differs by the shape of its beak. Instead of the crow's narrow "ballpoint pen" looking beak, the Groove-billed ani's beak resembles a thick silver almond that fades into a large eye and a stylish black plumage. This individual was clearly lost. He must have taken a wrong turn in Mexico, saw mountains and flew northwards, not realizing a difference in climate due to the unusually hot temperatures that persisted in Colorado this year. He had not adjusted well to this newfound paparazzi of "bird people" that he had attained. To the best of his efforts he tried to remain hidden as much as possible, a behaviour which at the moment I resented however within two days of being initially spotted, he already had over 70 sighting reports on Ebird (a sort of hub to track species data in the area) and to add to the magnitude of the effect of his arrival, almost every person who reported seeing it had commented "MOB!" beneath their sighting (which in reality was probably no more than 8 people however that may be a lot for this famously introverted community).

As I plodded on, I ditched the concrete pavement in favor of the brush. The dirt provided a closer view to the creek which I was now directly adjacent to and removed the disturbance of bicyclists going by at high speeds. Despite this, the brush also provided refuge to mosquitos which hovered above my skin, eager to get a taste of my mammalian blood. To combat this, I found a sagebrush and rubbed its acerbic leaves on my skin, eliminating this new inconvenience almost immediately. The size of the foliage grew to my shoulders as I approached the stream. I looked up onto the ridge with the barbed wire fence I had come down upon. A young fellow with curly hair and rounded glasses looked eagerly down at the stream, most definitely searching for the ani as well. He suspended searching this location and moved on while I stealthily moved through the grass below. It's not that I didn't want to be seen, more as if with respect to his birding experience that he would not see "The rare teenage *Homo sapien sapien*" in what was surely not his natural habitat.

I saw a bridge up ahead which I crossed after taking a few photos of the bleach white egrets that waded in the water near me. I disappointedly began my way back to the car, accepting defeat to the well-hidden bird. I figured if I didn't see it on the return track then it wasn't meant to be. I continued uphill and proceeded to take periodic breaks, looking at the stream below hoping to catch a miracle of a sighting. No avail. Heading back to where I started, I found three people instead of two standing near the fence. One of the people was immediately familiar and was the man from before but the others were new to their search. They were both women who also looked familiar but from a distance I could not figure out how. As I approached and my eyes focused in I realized they were both zookeepers I had worked with before. Katie, a tall red-head with a big grin and Hannah, a short young keeper with a safari-themed conical straw hat, waved over at me. We were all equally surprised to see ourselves in the same random piece of land at the same time. It was the serendipitous sensation of "in all the places and at any time what are the odds that we would be here." It was very similar to the ani which we were all searching for. What was it that made this small creek next to a highly austere neighborhood the perfect place for a Costa Rican bird to settle here in the middle of September? Was it lost or was it simply going a new direction looking for new places where other anis had dared not venture for food?

We joked and chatted. The three of us "zoo-people" (as my mother would call us) and Bruce, a man with a suiting name given his bulky appearance, who I had met before at the beginning of my quest. His friend had left and despite being the "ugly duckling" amongst us we accepted him into our flock and learned from his advanced knowledge in birding. Another man joined us who by another random coincidence had traveled before on the same trip with another one of my zoo mentors I had seen earlier in the day. It's almost as if by divine chance, all of us were in the same place looking for the same thing. Along the same path I had taken up, the young curly-haired birder approached our group. Hannah

punned at the coming stranger “Have ani luck?” We smirked at the pun’s cleverness. To our combined surprised, the lad responded: “Yes actually, I found him past the bridge about a quarter-mile.” Our new group was elated and decided collectively to venture on the direction the boy pointed us to. Having reached his quarry, the boy did not follow but instead showed me where he had spotted the bird and entrusted me to navigate the group.

We walked to the bridge and split up, the older members of the group taking the regular dirt path, leaving just me and my waterproof boots to cross a small stream. Upon doing this, I stopped and gazed at the creek once more with my binoculars. Now the binoculars were at my eyes and my camera was prepped and ready at my chest. An elderly woman joined me, also looking for the ani. As I was relaying the most recent sighting information to her a dark flash came into my peripheral vision. I quickly abandoned the conversation and swiveled my head. A black, medium-sized bird with a long tail flew onto a dead cottonwood branch. At first, I dismissed it as a great-tailed grackle (a beautiful yet annoyingly loud bird with an abnormally large tail as the name describes), however, I gazed at the old woman and suggested we double-check. I waded out onto a small concrete dam from which one stream flowed into another and raised the archaic binoculars to my face. I caught a small glimpse at the beak of the bird. As the binoculars focused, the view of the silver almond beak filled the frame. I ecstatically smiled and gave an enthusiastic thumbs-up to the rest of my “flock” as they hurried down a small hill to meet me. Sadly the sound of their hurried footsteps startled the bird and it flew to the other side of the stream. When they arrived I described what I had saw and pointed to where the bird was, making sure to make my experience as genuine as possible. My enthusiasm had distracted me from getting my camera out and taking a photo of the bird, leaving me with no proof of my sighting.

For the next hour, our group watched the bird slowly reveal itself, leave the tree it was in, and fly to different parts of the creek to conceal itself once more most likely wondering “why do these people keep following me?” Other birders joined us, sharing the same remarkable view of the rarity without doing the work of finding it. Despite these new additions we didn’t mind. We were not fishermen, leading others astray to keep the bounty to ourselves but instead partook in the past time together, a colony of oddballs of different backgrounds and skills yet united in the love of nature and birds. One elderly birder played the call of an ani on his phone which allowed us to hear the melodious shrill response of our new feathered friend. We discussed amongst ourselves, the nature of this odd community of the animal-loving world. The assorted hobbyists with their well-planned life lists, retirees finding new things to do with their lives, wildlife photographers with huge budgets and lenses, and zoo-people like myself, Katie and Hannah just trying to fill our lives with as many animals as possible. We alike were able to share this unusual find together. We worked together and cooperated hoping for the best for one another.

I like to think of what would have happened in different situations if something else would have happened and I'm thankful that for the act of serendipity that led me to my zoo-people when I was about to forsake the search. I sure do hope the ani finds its way home before the Colorado winter sets in. It's never good to be lost in the cold alone. Maybe he'll have to trailblaze a path of his own and others will follow him or perhaps there's other lost and misplaced birds nearby that he can join up with and conquer migration together.

Finding Your Passion

Stacie Barbarick
HNR 202 Honors Speaker Series February 2019

I want you to consider for just one minute, the traditional American branded "sequence to success". What does that look like? I'm guessing its some linear version of:

1. Graduate high school
2. Go to college
3. Find mythical path to self-discovery that incorporates personal passion/ global awareness/ financial success into a lucrative career that will allow for maximum life:work balance, marriage to your soul-mate….Oh and probably involves a startup.

To say that my life has followed a "non-linear" path, is a colossal understatement. In fact, I'd probably go with big, fat failure. So today I want to share my personal journey and my personal experiences and differentiate between passion and success because I think the lines get muddy. I'm going to warn you that this is not a candy-coated version of my story.

I started college, with the idea that I would become a world-renowned marine biologist-saving the world one plankton at a time. Financial success was trivial compared to ground-breaking research I'd conduct. I'd die a happy woman, knowing I had made a difference to the planet and mankind…..and if I won a Nobel prize in the meantime, well who am to argue with the committee?

So, I started college, my passion and career plan in hand, and I failed. And that failure was so devastating that I had to leave.

So I tried again. And failed.

In my first two years of college, I had attended four different universities. (Not a very fast learner for a Nobel Prize winner, huh?)

I didn't understand how my sincere passion for science was allowing me to fail at the one career path I was destined to do. So, maybe marine biology wasn't my passion?

My junior year I decided to really go out with a bang, and thinking perhaps my motivation had migrated to another continent, my student loans and I went backpacking across Europe..... twice.....ok, three times. You know, like a crime.

So, I passionately served drinks and tuned skis for a couple of years and it was amazing. But I always had this nagging inner voice that I was destined for something greater and by finding that direction and meaning, I would find happiness. Oh, and it would of course, require a college education. So, in order to finance that project, I enlisted in the Navy.

Where I passionately engaged in the service to my country by shooting a lot of guns and painting a lot of decks.
But, I met the first person I had ever wanted to marry, which was a pleasant surprise to my grandparents who believed my unwed status at the ripe ole age of 26 was the result of some curse. So, I got married, he got a promotion and I got out the Navy. We moved to Oregon so we could both finish our degrees and I felt like I had a fresh start, away from the desolate landscape of bad decisions and burned bridges. I decided my passion was medicine and like the majority of respectable biology-centric scientists, I decided to go to medical school. And I spent the next three years passionately filling my med school application with research, publications, clubs, work and destroying my marriage.

When my marriage fell apart, it was an all-time low in my life. I moved into this depressing basement apartment, because I couldn't afford to stay in our house. So, I spent the next 6 months, passionately drowning my sorrows in Pabst Blue Ribbon. Towards the end of my semester, the failure of my marriage and the seeming failure of my life (along with copious amounts of alcohol) culminated in a suicide attempt.

I woke up covered up half-digested sleeping pills and alcohol, with an apology note scrawled to my parents. And I would love to tell you that it was the colossal turn around in my life, but it wasn't.

I moved home, drifted, and started a PhD because they gave me money. But, it was getting harder to put on the passionate costume and pretend that my career was what my passion was. So, I quit graduate school, but with a little more intention this time. I moved home and got a respectable job as a pharmacologist at a biotech company in Boulder. On paper, it was as close to my dream job as I had ever gotten: good compensation, good medical coverage, working in science….but I had to kill mice. A lot of them.

So, my passion bank was running on dry at that point. I decided to join a gym, and I can't think of a more passionate workout facility/cult than Crossfit. Where I fractured my T8 Thoracic vertebrae. Three months later I contracted Salmonella which went septic and perforated the fracture, giving me osteomyelitis. I spend 9 days in the ICU and three months after getting antibiotics injected directly into my heart. I lost the mouse executioner job and was physically disabled. So, we moved to Steamboat where I spent the first six months passionately baking (and considering how I could market my startup) and then began managing a coffee shop. If something broke, I had to fix it. I spent nights alone, tech pubs in my lap, working to discover the mechanical failure, or power supply problem. And it was there, all alone, with no one to impress or answer to, when I realized I have a passion for engineering. And that thought wasn't a bright and shiny, self-sacrificing, facade; it was gritty and unformed; more self-serving than any other career path I had considered. And it was right.

Don't get me wrong, I sincerely felt passion for all those previous activities, but I realized a huge proportion of that passion originated from familial, societal, and marketed expectations of success and not my own.

Here is the problem:
Passion vs. success vs. reality

We live in an age when we rarely feel at peace with our educational and career decisions. Why? We define ourselves by what we do and what our achievements are. That's why I was trying so hard to find this career/passion amalgam, because I thought it had to define who I was. We live in an amazing time when the strongly held belief is, "anyone can achieve anything". But the danger in that belief, is that you are the sole creator of your success and you are also the sole owner of you failure, which elevates the successes to Nobel Prizes and the failures worthy of execution by firing squad. There are too many outside factors that can affect the outcomes of our decisions or from a scientific perspective, there are too many unknowns in the equation to accurately predict the outcome (I don't care how amazing your "k" value is). When we consider failure, we fear the judgement and ridicule. And when we consider success, we immediately conjure an idealized Hollywood version based on our "passion".

So here is my claim: Any definition of success needs to honestly assess that this idealized work:life balance for the end-all-B-all of happiness is a myth. And the construct we have of passion is typically not of our own creation, but of our parents, friends, social interactions and the media. Powerful forces that define what we want and how we view ourselves, because we are highly open to suggestion.

Why don't we follow through? Building grit is based on the concept that the ability to learn is not fixed but it can grow in response to effort. Psychologist Angela Duckworth explored this in her 2016 book, *Grit*. Students who understand this idea are much more likely to persevere after a failure, because they don't believe that failure is a permanent condition.

The more willing I was to risk failure, the more clear my passion became. It took a near-death experience and basically complete isolation to figure that out. I decided to take a path in engineering and found the Idea Lab. I found a place to start creating pieces using wood and metal and engineering and was able to pull in pieces of who I am and what's important to me.
I am an environmentalist and I worry about the amount of throw-away culture we're propagating, so I started creating pieces with reclaimed, reused, or thrown away items. Nothing that's going to change the course of humanity, but actual genuine reflections of who I am.
I created these lanterns from recycled tiles and wood, thrift store bamboo, donated solar lights and 3D printed flames. I rescued this beetle-kill log from the wood chipper out back. And the purpose of this log….Maybe a stool?

Now don't get me wrong, I have worked on a few projects that could alter the course of humanity:
Monster under the bed
Laser sounds diffusers
Dragon head

This decision has not been easy. I defend my current educational and career status, sometimes daily. My parents can't understand why I'm back in school when I already have a degree. My friends are bragging about vacations they're taking with their kids to Disneyland and I'm pretty sure if my dogs could talk, they'd be in therapy, explaining to their psychologist how neglected they are because their mom is always studying. Even within the student engineering population, I've been told within my groups, that I should "stay away from math and stick to organizing". I've been told that what they do is engineering and what I do is arts and crafts. And when I first started school, any one of those elements would have had me running towards the hills and a degree in underwater Basket-weaving. But when it's based in your authentic passion, there's really no option to quit.

What makes you get out of bed in the morning?

Things I know for sure:

Your passion shouldn't make you feel badly about yourself.

Passions, like everything worth having, take work and dedication but should leave you feeling energized not drained.

Passions evolve over time and that's ok.

Your career and your passion do not have to be the same thing.

I leave you with this:

If you were alone in a darkened, dusty bookstore—with no one around to judge, what would your passion be if you were never able to talk to another soul about what it was?

How Denver's Weather Impacts Bear Creek

Maeve Wilder

Field Journal
Physical Geography Weather and Climate Spring 2019

Introduction

For my field journal I chose to track how Denver's weather impacts water parameters in Bear Creek. I ordered an EarthEcho Water Challenge kit. It had 50 days worth of water testing equipment. From the creek I took samples for dissolved oxygen, pH, water temperature, turbidity, and flow rate. Next, I got the data for current temperature, max temperature, min temperature, average temperature, current dew point, average dew point, current wind speed, average wind speed, max wind gust speed, current humidity, average humidity, current pressure, and precipitation from the weather station. I also estimated the cloud cover percentage and made observations about the weather every day.

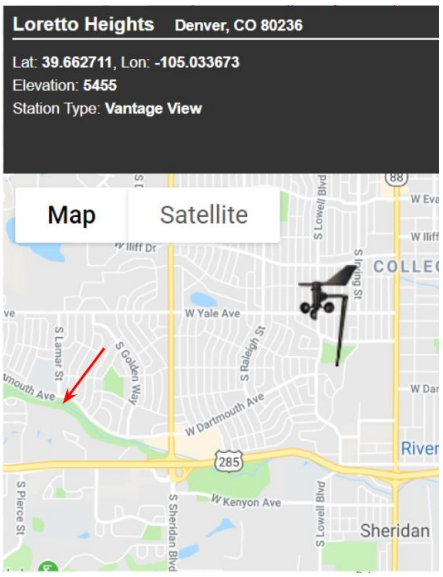

The map shows where the weather station I used for my weather data is. The red arrow indicates where I took my creek samples every day. It was interesting taking creek data every day. The first bomb cyclone was an adventure!

Harold was right there with me through it all.

Results

Date	Time (pm)	DO (ppm)	pH	Water Temp (°C)	Turb (JTU)	Flow Rate (cfm)	Curr Temp (°C)	Max Temp (°C)	Min Temp (°C)	Avg Temp (°C)	Curr Dew Point (	Avg Dew Point (°	Curr Wind (mph)	Avg Wind (mph)	Max Wind Gusts	Curr Hum (%)	Avg Hum (%)	Curr Bar (in)	Cloud Cover (%)	Precip (in)
2/16	2:30	1	7.5	4	40	12.2	-0.6	8.4	-5.8	-1.3	-2.17	-7.7	1	1	11	83	66	29.55	75	0.3
2/17	3:00	1	8	4	40	12.3	-1.1	4.9	-9.2	-4.2	-11.1	-12.1	5	0	7	59	57	29.9	75	0
2/18	3:30	1	7	2	50	12.7	-8.89	-6.4	-12.7	-9.3	-12.6	-13	1.9	1	7	68	75	30.3	100	0
2/19	3:30	4	7	2	70	12.4	-6.1	-5.8	-13.1	-8.7	-11.7	-11.9	1	0	5	65	77	30	100	0
2/20	5:25	2	7.5	2	40	13	-0.2	4.1	-14.7	-6.1	-13.8	-14.4	0.5	0	10	37	58	29.8	10	0
2/21	3:20	2	7.5	4	30	12.4	2.4	2.7	-11.9	-5.7	-10.2	-13.4	0	0.5	5	39	56	29.9	10	0
2/22	3:28	2	7.5	3	30	12.2	-5.8	0.9	-5.9	-3.9	-7.7	-6.4	0	0	7	87	84	30	75	0.6
2/23	4:50	2	7.5	4	75	19.8	1.9	5.3	-7.1	-1.2	-12.6	-6.9	1	0.8	4	33	71	30.1	10	0
2/24	6:45	2	7.5	3	40	14.9	0.5	9.7	-9.6	0.6	-8.2	-12.4	0	0.4	9	52	40	30	10	0
2/25	4:30	2	7.5	5	30	14.9	9.8	12.3	-7.9	0.7	-5.3	-7.8	0	0.3	1	34	58	29.9	20	0
2/26	5:00	2	8	7	30	15.5	12.6	13.9	-4.7	3.2	-0.3	-2.2	0	0.6	8	41	72	29.9	10	0
2/27	3:00	2	8	5	20	13.6	1.8	3.2	-7.4	-2.5	-3.4	-4.8	0	0	6	68	84	30	50	0
2/28	3:15	2	7.5	6	20	12.6	12.7	14.8	-3.7	4.4	-1.7	-2.8	1	0	7	37	66	29.9	50	0
3/1	4:00	2	8	6	20	12.4	4.2	11.8	-0.8	4.4	-3.1	-2.6	2	0.7	10	59	62	30	80	0
3/2	12:25	3	7.5	4	10	12.4	-15	0.6	-15.1	-5.4	-6.1	-7.9	3	1	7	71	83	30.1	100	0.45
3/3	3:25	2	7	1	60	14.1	-12.7	-10.3	-17.8	-14.9	-16.2	-17.8	0	0	4	75	78	30.5	100	0.37
3/4	4:00	2	7.5	2	40	16.9	-4.6	-2.2	-18.8	-10.6	-12.3	-15.8	0	0.4	6	55	68	30.4	0	0
3/5	4:45	3	7.5	3	40	16.2	0.9	2.9	-15.9	-6.9	-7.3	-12.3	1	0.4	4	54	69	30.4	25	0
3/6	2:45	3	7.5	5	30	14.9	5.1	7.2	-8.7	-2.4	-2.8	-7.3	0	0.4	4	57	72	30	90	0
3/7	4:30	1	7.5	7	50	14.9	11.6	16.2	-1.8	5.4	-2.6	-1.3	2	1	11	37	67	29.8	90	0.8
3/8	4:45	1	8	7	20	14.9	7.1	14	-2.5	4.9	-0.3	-1.8	3	1	10	59	65	29.3	75	0
3/9	12:30	2	7.5	7	20	12.4	11.6	12.3	2.2	6.1	-10.6	-9.5	4	2.2	13	20	34	29.6	10	0
3/10	3:30	4	7.5	8	20	12.4	9.4	12.1	-5.6	1.7	-3.5	-5.9	6	0.7	10	40	61	29.9	50	0
3/11	2:45	3	7.5	6	20	12.4	13.4	13.4	-4.7	0.9	-0.3	-3.8	1	0.2	5	39	73	30	50	0
3/12	3:15	1	8	9	10	12.4	16	16.8	0.2	10.7	2.1	0.5	1	0.5	6	39	77	29.4	50	0
3/13	11:50	2	7	3	>100	75.3	-0.11	11.00	-3.67	1.67	-0.83	-2.11	11	2	13	95	84	29	100	0.61
3/14	3:00	2	7.5	7	60	25.7	3.28	4.83	-6.78	-1.44	-5.39	-6.56	0	1	7	53	69	30.3		0.21
3/15	6:55	1	7	7	40	19.5	6.06	10.78	-8.89	0.00	-6.83	-8.44	0	0	8	39	59	30.3		0
3/16	6:45	2	7	8	30	12.2	7.33	11.67	-6.67	2.17	-3.83	-5.56	0	0	9	45	62	30.3		0
3/17	4:25	2	7.5	9	10	11.8	12.17	12.17	-5.39	0.06	-2.83	-4.89	1	0.3	5	35	73	30.3	0	0
3/18	3:50	2	7.5	9	10	13.6	11.39	12.06	-1.83	3.50	0.17	-2.39	1	0.4	6	46	67	30.1	50	0
3/19	3:30	2	7.5	9	10	20.5	9.39	10.22	-1.83	3.72	-4.56	-3.17	1	0.5	7	37	63	30.2	25	0
3/20	4:00	2	7	9	10	19													0	0
3/21	4:40	2	7	8	40	14.9													0	0
4/1	3:15	1	6.5	12	30	34.5	15.83	15.94	-2.50	4.67	-5.83	-4.17	3	0.8	12	22	62	29.9	75	0
4/2	5:35	1	7.5	10	30	24.5	11.50	12.83	1.39	6.06	0.89	-0.67	0	0.4	6	48	63	29.8	100	0
4/3	3:00	2	7.5	10	10	23.7	16.56	16.72	0.28	7.11	-0.22	1.22	2	0.3	6	32	70	29.7	75	0
4/4	3:15	2	8	12	20	23.7	20.56	20.83	0.94	8.78	-2.56	-0.56	3	0.5	9	21	60	29.9	25	0
4/5	4:35	2	7.5	13	10	22.1	21.61	23.89	4.56	12.06	-9.00	-1.67	1	0.6	10	12	46	29.6	90	0
4/6	4:15	2	7.5	13	10	22.9	19.44	21.50	4.78	13.44	-1.67	-1.61	1	0.6	10	24	39	29.6	50	0
4/7	5:15	2	7	14	20	22.1	20.61	23.78	3.17	14.22	-4.56	-4.06	4	0.9	12	18	31	29.8	25	0
4/8	4:10	3	7.5	14	10	22.1	22.50	24.83	5.72	14.67	-2.28	-2.83	1	0.5	6	19	33	29.8	50	0
4/9	4:40	4	7.5	14	5	19.8	24.06	28.28	8.44	16.89	-2.50	-1.39	0	0.6	6	17	32	29.3	75	0
4/10	1:05	2	7.5	9	30	24.5	2.11	15.83	-5.17	4.67	1.22	0.33	3	1.6	11	94	79	29.3	100	0.27
4/11	3:05	2	7.5	11	40	23.9	5.78	6.94	-7.67	-0.72	-3.06	-4.89	0	0	9	53	76	29.8	50	0.39
4/12	5:10	2	7.5	11	10	23.7	6.11	8.67	-3.06	1.22	-2.50	-3.22	0	0.5	6	54	74	29.9	95	0.02
4/13	3:00	2	7.5	9	10	24.5	6.28	8.39	-1.06	2.06	0.61	-0.78	1	0.5	7	67	83	30.02	80	0.07
4/14	5:15	3	7	13	5	23.7	16.83	20.61	-0.67	7.61	-2.28	-2.72	0	0.7	13	27	55	29.6	25	0
4/15	3:10	3	7.5	13	5	11.8	23.78	25.22	5.22	14.44	-1.22	-1.17	0	0.4	6	19	38	29.5	10	0
4/16	3:10	2	7.5	13	5	10.6	18.06	18.72	2.22	10.67	5.94	3.83	1	0.6	7	45	65	29.5	75	0

I know it's difficult to see but let me explain a few holes in the data. The blank section during 3/20 and 3/21 was where the weather station I was getting data from stopped working temporarily. Right after that my family left on vacation for spring break and by the time I got back the weather station was working again. There is a break in the data between 3/21 and 4/1 as I didn't collect data over spring break. There were also a few days when I was sick from 3/14 to 3/16 when my mom collected my creek data. I was able to go back and look at the temperatures, wind speeds, etc. for those days but my cloud cover data was just based on observation so I don't have percentages for those three days.

I'll just say right now that I'm not at all confident in my measurements of dissolved oxygen, pH, and turbidity. The kit that I had used little pills that would color the water based on its DO and pH levels, and I had to judge the levels using a colored charts. I also had to estimate the turbidity using a secchi disk, so these values could be way off.

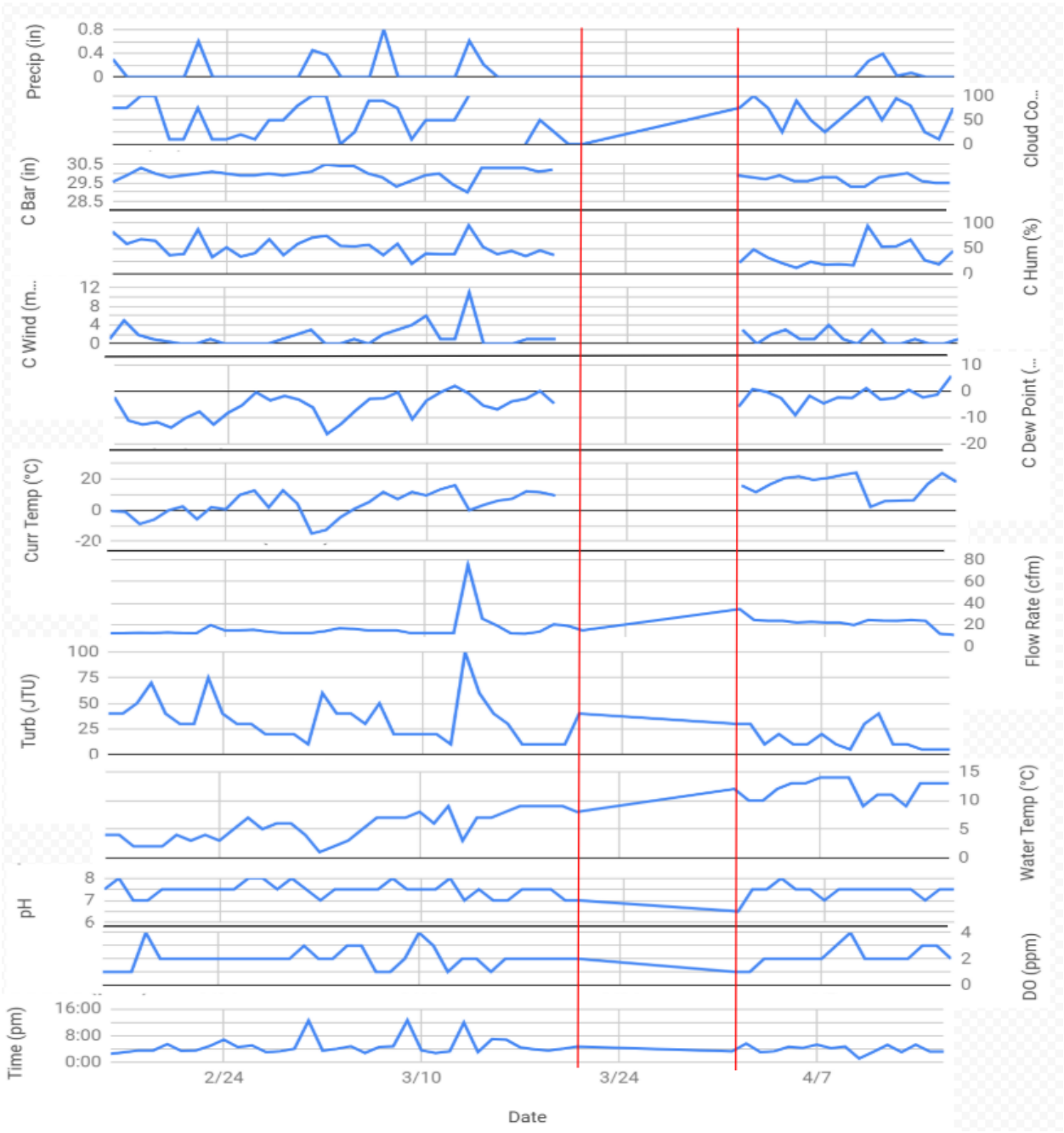

I decided to make a panel chart of all my data so I could look at correlations. I quickly realized that I needed to cut some of the data, and I only kept the essentials. Since google slides doesn't have a way to make panel charts I had to painstakingly piece it together on google drawings. Some things aren't lined up perfectly but that was the best I could do.
The red lines show where I was out of town and there is no data.

The two bomb cyclones on 3/13 and 4/9 were the most interesting correlations on my chart. I marked the two bomb cyclones with pink lines below. Clearly there was a bigger impact on nearly every parameter from the first bomb cyclone.

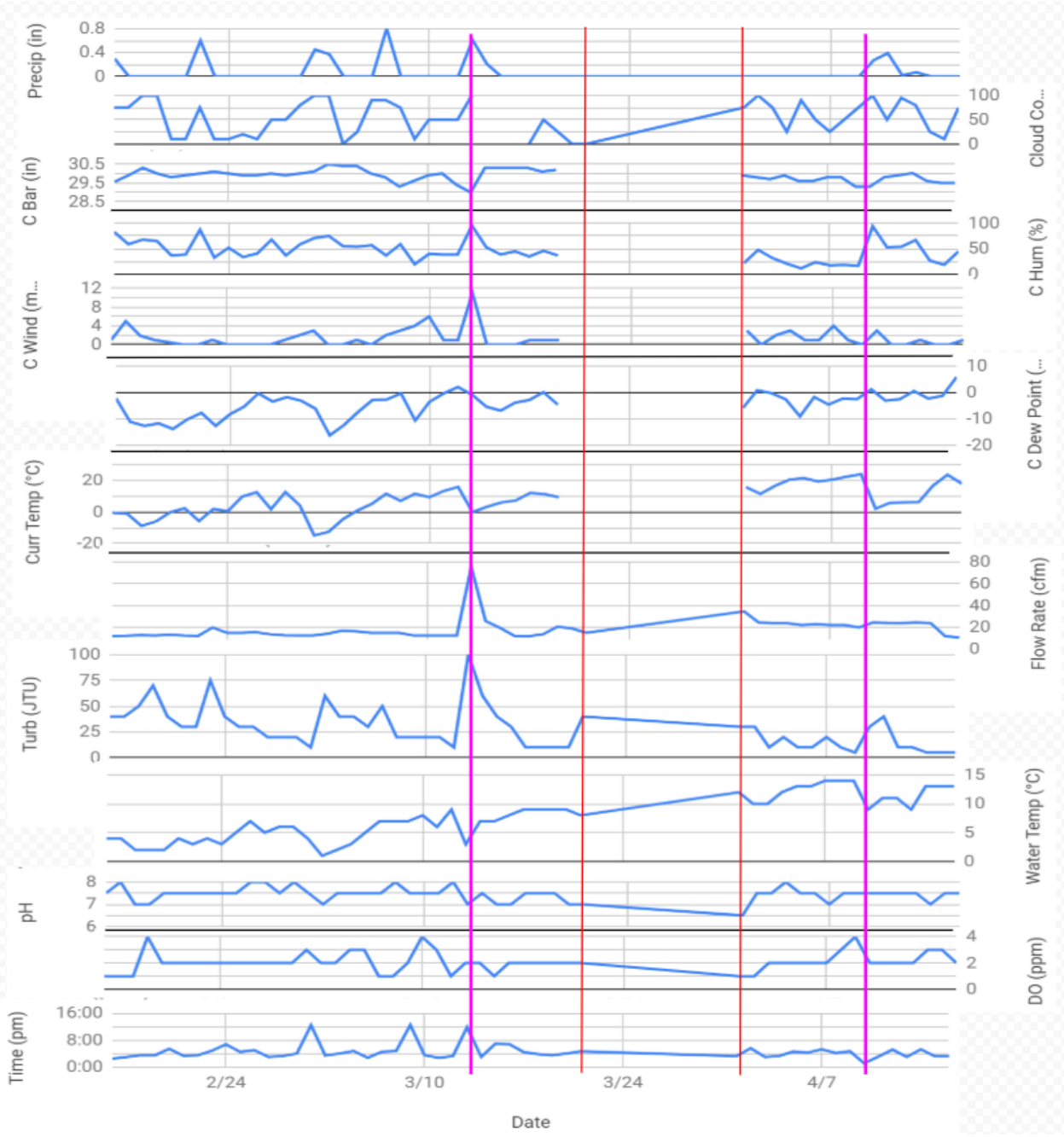

This was to be expected as the first cyclone was much more powerful than the second. It caused temps to drop and flow rates to go way, way up. The turbidity was so high that I couldn't even see the secchi disk.

I made a few more graphs just to look more closely at the some correlations.

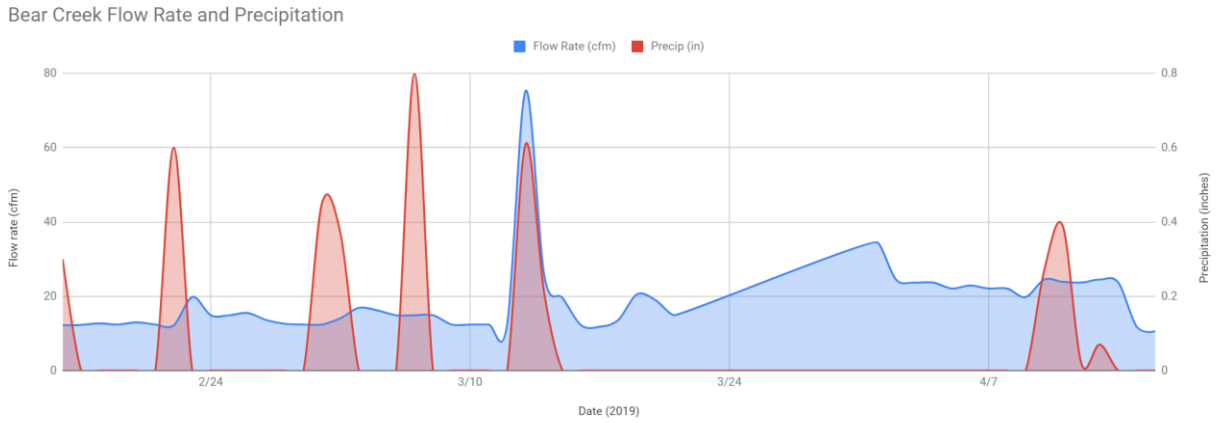

This chart clearly shows that the flow rate in Bear Creek is completely controlled by the Bear Creek dam. Whoever operates the dam knew the bomb cyclone would be a big one and let a bunch of water out on 3/13. It would have been good to find data on when the dam is opened and include that on my data sheet. Unless I know that they are keeping the dam closed I can't attribute any spikes in flow rate to Denver's weather.

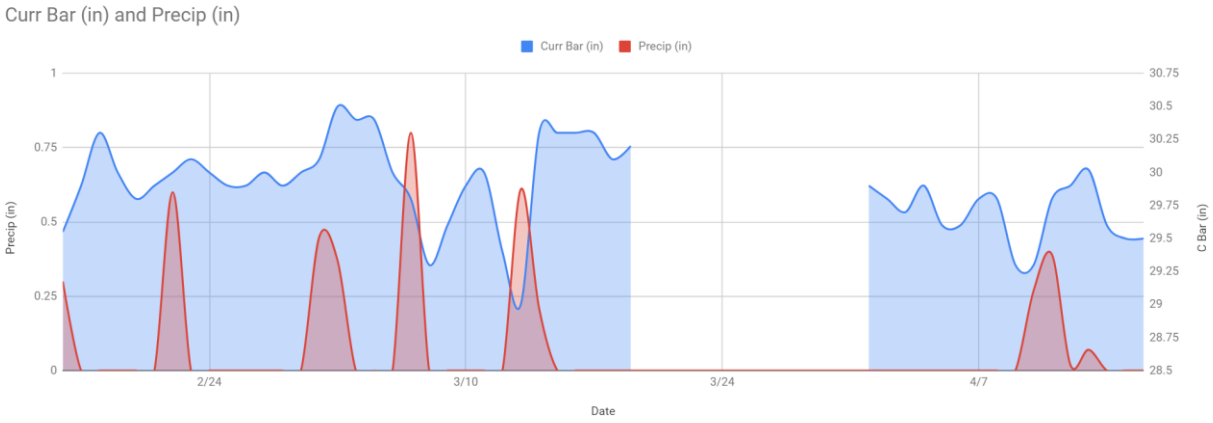

This chart shows strikingly the impact of the bomb cyclones, especially the first one. There was another steep drop in pressure on 3/8. My notes on that day say that the brown cloud was especially bad, but nothing else. I wonder why the pressure dropped that day?

Part II
Undergraduate Research

Effect of "The Miracle Tone," on Mycelial Growth of *Aspergillus niger*

Sarah Kidder

Dr. Darlynn Johnson, Dr. Lynne Albert and lab assistant D. Herrera

May 2017

Abstract

Aspergillus awamori has the ability to host and secrete a manufactured antibody fragment (scFv) that is invaluable to medical and biotechnical communities. *A. awamori* produced the protein by means of a fusion using shock waves, which proved to be much more efficient, less laborious, and more successful than previous fusion methods. The question raised is if the frequency of the shock wave played a large role in the success of genetic recombination. More specifically, could the frequencies produced by music stimulate the replication of DNA, causing an increase of mycelial growth in *Aspergillus awamori*?

A study on the effects of sound waves on mycelial growth of *Botrytis cinerea* found that a 5 kHz frequency was successful and significant inhibitor, whereas 1 kHz produced no effect. It's most likely that stimulating frequencies may be found in the range of 0.5Hz – 900Hz. Furthermore, some research has found that a specific frequency of 528Hz was able to repair damaged DNA, though these claims have been scarcely tested. Given the current evidence linking sound and biological processes, it is hypothesized that *Aspergillus niger* (sister species to *A. awamori* that is more accessible) exposed to music in the frequency of 528Hz will exhibit more mycelial growth than those exposed to music in frequencies between 0.5Hz – 500Hz and those exposed to no music at all.

1.0 Introduction

Fungi have extensive value to human economy and ecology, which is why it is beneficial to understand the conditions that affect their growth rate, toxicity, antibiotic properties, or production of certain biochemicals and heterologous proteins. Several types of filamentous fungi have been studied for their economic importance. Specifically, *Aspergillus awamori* has several commercial uses, such as a probiotic that could prevent and alleviate many dietary related diseases in humans, and as an organic food processor (Saleh et al., 2013). *A. awamori* also has the ability to host and secrete a manufactured antibody fragment (scFv) that is invaluable to medical and biotechnical communities (Joosten, et al., 2003). This ability to produce the heterologous protein was made possible by using fusion techniques that Magaña-Ortíz et al. (2013) criticize as being

"laborious" and "insufficient". Magaña-Ortíz et al. developed a fusion technique using shock waves, which proved to be much more efficient, less laborious, and more successful than the previous PEG-mediated protoplast fusion (2013). The question raised is if the frequency of the shock wave used by Magaña- Ortíz et al. played a role in the success of genetic recombination. More specifically, could the frequencies produced by music stimulate the replication of DNA, causing an increase of mycelial growth in *Aspergillus niger,* a close relative of *A. awamori*?

Jeong et al. (2013) studied the effects of sound waves on mycelial growth of *Botrytis cinerea*, and found that a 5 kHz frequency was successful and significant inhibitor, whereas 1 kHz produced no effect. They also mentioned that certain frequencies stimulate mycelial growth but did not cite any sources for this claim. Magaña-Ortíz et al. used shock waves produced at a rate of 0.5Hz, which is 1,000 times lower than those used by Jeong et al. Since the frequency of 0.5Hz did not damage the *A. awamori* cells in the recombination experiment, but the much higher frequency of 5kHz damaged the cells enough to inhibit the growth of *B. cinerea* in Jeong *et al.*'s experiment, it is possible that frequencies between 0.5Hz and 5kHz may stimulate mycelial growth. Music tends to fall in this range, such as the sound produced by a standard piano. A classic 88-key piano plays notes that range from A_0 - C_8, which translates to a frequency range of 27.5Hz – 4.2 kHz (Suits, 1998).

Jeong et al. found that a 1 kHz frequency produced no significant inhibiting effect on the mycelial growth of *B. cinerea*, so it's most likely that the stimulating frequencies they mention may be found in the range of 0.5Hz – 900Hz.

Furthermore, some research has found that the specific frequency of 528Hz could repair damaged DNA (Appelt, 2006). White noise contains all the audible frequency bands (Neal M., 2017). which includes the target frequency range for promoting growth as well as 20 kHz, which is well above the frequency that inhibits growth. Given these inductions of current evidence linking sound and biological processes, it is hypothesized that *Aspergillus niger* exposed to white noise will exhibit less growth than specimen exposed to music with a frequency of 528Hz.

2.0 Methods

To test the hypothesis, nine plates were isolated in three Igloo Boxes - two boxes with sound and one without. One sound was 528 Hz and another was to be between 27-100 Hz and was played until the power source ran out. Technical difficulties with the source of sound (an iPod) were not identified before the experiment took place, and trials were not run again after an unknown amount of hours with white noise instead of the intended 27-100 Hz. Therefore, the frequency of white noise was used as a negative control and the hypothesis altered to accommodate the

change. It was then hypothesized that *Aspergillus niger* exposed to white noise will exhibit less growth than specimen exposed to music with a frequency of 528Hz.

Figure 1: Top and bottom view of the "Mother Plate" after 9 days of growth. April 14, 2017

2.1 Materials

- Sample of *Aspergillus niger* from Carolina Biologicals
- 10 Potato Dextrose Agar Plates from Carolina Biologicals
- 1 Pack of Disposable Plastic Loops
- Plastic Wrap
- Roll of Parafilm
- Box of Latex-free Nitrile Gloves
- 2 Sterilized 10 x 75 mm borosilicate Test Tubes, modified to be Open-tube Tests
- 3 Igloo Cooler Boxes
  - 1 Large
  - 2 Mediums
- 1 iPod Touch
- 1 iPod Shuffle
- "528 Hz | Known as The Miracle Tone ➤ Love Frequency | Said To Heal DNA | Heart Chakra Activation" music from ZenLifeRelax (2016), set to repeat on an iPod Touch.
- "Gamma waves and binaural mix of 27Hz – 100Hz" music from Deep Wave Meditation (2015), set to repeat on an iPod shuffle.
- 2 Portable Speakers
  - 1 Battery Powered with Built-in Auxiliary Cord
  - 1 with a USB Compatible Charge Cord
  - 1 Auxiliary Cord
  - 1 USB Wall Plug

2.2 Procedure

2.2.1 Transfer of Original Sample

Aspergillus niger was provided to Red Rocks Community College by Carolina on March 9, 2017. On April 5, 2017, a swab was taken from the sample using a disposable plastic loop and transferred to a clean potato dextrose agar (PDA) plate. The transfer was done just outside of the school to limit student and faculty exposure to spores, and to reduce the risk of contamination. A board was wrapped in plastic wrap and secured to a metal frame, which provided a safe and sterile area to transfer spores and hyphae from the sample to one of the PDA plates. This "mother plate" was sealed with Parafilm,

and left to culture for nine days on a table in the Microbiology room. The average temperature was 18 °C, or room temperature, as is a normal environment for most fungi including *A. niger.* All tools were sterilized with bleach before being disposed of in the biological waste bin along with the original sample.

2.2.2 Transplantation

On April 14, 2017, after the "mother plate" had cultured long enough to nearly outgrow its substrate (about nine days), plugs were removed and transplanted into nine separate PDA plates. A 10 x 75 mm closed-tube test was modified to be open at both ends by Lynn Alberts, who then sterilized them in an autoclave. This allowed for a 9mm diameter plug to be removed from the center of the nine plates, then replaced with another plug of the same size from the mother plate. Sections from the 9-day-old colony were extracted by twisting and pushing down on the tube. Then the tube was placed in the voided area of each "daughter" plate, and the sample was pushed out of the tube with a small loop. The tube and loops were sterilized in bleach water and disposed of with the mother colony in the biological waste bin in the microbiology room.

Figure 2 April 14, 2017. Left, Open-test tube extraction of PDA substrate. Right, daughter plates with substitution plugs from the mother plate.

2.2.3 Experimental Groups

To expose the daughter colonies to sound, three plates were put in a plastic, medium size Igloo™ cooler with a small battery powered speaker box, and an iPod touch. The only song on the iPod was "528 Hz - Known as The Miracle Tone" (music from ZenLifeRelax, 2016). Another three plates were placed with a small portable speaker in different Igloo™ cooler of the same size, along with an iPod shuffle. The speaker was not battery powered, so a cord had to be ran through the cooler to an outlet on the bench preventing it from fully closing. The shuffle was wiped of all music except for the experimental song, "Gamma waves and binaural mix of 27Hz – 100Hz," and was set on repeat. However, technical difficulties prevented the music from playing and only white noise was produced at very low decibels (db). No sound from either experimental cooler could be heard when standing next to them but were barely audible when an ear was pressed against them. Based on information provided by AIC Acoustics (2017), this translates to about 10-20db. It is recommended that the experiment be ran again with consistent attention and maintenance over the three-day trail. However, as not to unnecessarily disturb the growth of mycelia, the source of music should be place outside of the boxes, and Bluetooth or wireless speakers should be used. The speakers could be charged at the same time each day, and the lids to each box - including the control- could be left open for the same length of time.

2.2.4 Controls

The last three daughter plates were used as the control group, which had no music playing in its Igloo™ cooler. The control cooler was the largest of the three and contained no MP3 player or speaker due to lack of resources, but these factors should have been controlled for. Each cooler was opened about 1/4th in. to control for external noise that the group whose lid could not fully close would have experienced. All the daughter plates were stacked on top of each other and labeled "top", "middle", or "bottom" and placed at bottom left corner (opposite of the speaker). This was done to account for possible differenced in growth caused by proximity to the speaker. All plates were positioned with the agar facing up to prevent condensation contamination.

3.0 Data Collection

The experiment began on Friday, April 14th at 4:45pm, and was terminated on Monday, April 17th at 9am. Data was collected at 12:15pm that same day in the General Biology Room. A small ruler and stereoscopic microscope were used to measure the total area of mycelial growth. Since several colonies grew incongruent from the mother plug, the parameters of the daughter colony had to be determined before measurement. If there was any space observed between the hyphae radiating from the mother plug under 30x magnification, then it was not considered part of the daughter colony. It is likely that the neighboring colonies were produced by contamination of spores during transplanting, so they were excluded from the measurements. Under 15x magnification, the longest span of growth was recorded to the nearest mm (D_1), and then the diameter perpendicular to that was recorded to the nearest mm (D_2). The diameter of each mother plug was also measured to be 9mm in all the daughter plates, so the area of which was found to be 63.62mm (A_2).

3.1 Statistical Analysis

To determine growth rate (G_r), the average diameter of each daughter colony (D_a) was first found by adding D_1 and D_2 and the sum was divided by two ($D_a = [(D_1 + D_2)/2]$). To find the gross area of growth (A), the quotient was divided by two, then multiplied by pi: ($A_1 = [D_a/2]\pi$). Then the difference of $A_1 - A_2$ provided the net area of growth, which was used to express the average growth in mm^2 of each plate (G). This number was divided by the time between the beginning of the experiment and data collection (55.5hr) to yield the growth rate;

$$G_r = [\ ^{G}/_{55.5hr}]$$

Finally, each expression (G_r and G) was run through a two-tailed student t-test assuming unequal variance in an Excel spreadsheet.

4.0 Results

The 528 Hz group had more total growth than the white n.0 oise group, and average growth rate was also higher. However, the control group had the highest overall growth rate of the three groups. All of the qualities of growth seemed to support the hypothesis, but

a t- test should have been ran between the groups to see if the results were significant. Because the growth rate of the control was greater than that of the 528Hz, frequencies between 0.5Hz – 500Hz should be tested for effectiveness. Also, the variance between plates in the white noise group was the highest of the three, so it is likely that lack of control for range of frequency contained in white noise affected the growth rate of this group and should be controlled for in future experiments.

4.1 Data

Table 1: Area of growth in mm^2 of each daughter plate after 55.5hr of cultivation, their averages, and the statistical data for each group

Table 1	528 Hz	White Noise	Control
Top	817.79	427.25	691.15
Middle	520.34	552.13	667.00
Bottom	574.32	791.68	982.73
Average	637.48	590.35	780.30
Standard Deviation	158.47	185.20	175.73
Variance	25111.33	34298.07	30881.26
P-value	0.35	0.27	N/A

Table 1 shows the growth of each plate found by averaging the perpendicular diameters. As illustrated in Figure 1, the bottom plates of each group had more growth than the top and middle plates except in the 528 Hz group. The average and total growth was lowest in the white noise group, and highest in the control group. Variance, and therefore standard deviation, was relatively high in all the groups, but lowest in the 528 Hz group, and highest in the control group.

Tables 1 and 2 also show p-values obtained from student t-tests that were greater than 0.05, meaning no significant difference was shown in either of the experimental groups.

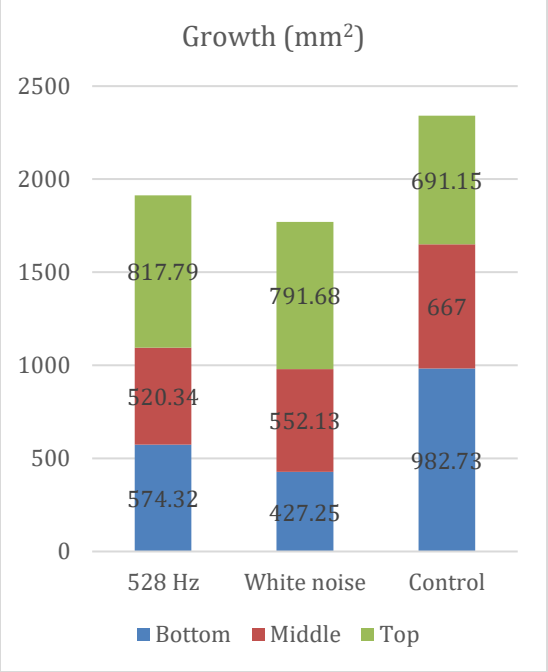

Figure 3 Area of Growth of each daughter plate and the total growth of each group

Table 2: Growth Rate and their averages of each plate (mm^2/hr), and the statistical data for each group

Table 2	528 Hz	White Noise	Control
Top	14.73	7.7	12.45
Middle	9.38	9.95	12.02
Bottom	10.35	14.26	17.71
Average	11.49	10.64	14.06
Standard Deviation	2.85	3.33	3.17
Variance	8.12	11.11	10.04
P-Value	0.35	0.27	N/A

The patterns of growth were intriguing but did not support the hypothesis that *Aspergillus niger* would grow better when exposed to music containing the "miracle tone" of 528 Hz. Instead the data would suggest that sound does not promote growth, as the control group seemed to do the best out of the three. However, student t-tests showed no significance of the experimental groups, which were ran against the control group. The control should have been run against an expected value from literature, or a group that was cultured under optimal conditions, which would have provided more accurate statistical analysis. It may have also given clues as to why there was no significance in growth between the two experimental groups and the control such as the igloo boxes themselves being variant in size. It is likely that not enough degrees of freedom, or sample sizes caused the high variation between plates in each group as seen in tables 1 and 2. Contamination of spores across the daughter plates during transplantation may have also created high variations and contributed to the lack significant results. Therefore, a more sterile method should be developed for the transplantation process, like covering each daughter plate with plastic wrap after removal of the agar and before replacement, cutting a 9mm diameter hole above the voided agar.

The hypothesis that *A. niger* would exhibit less mycelial growth when exposed to white noise than music predominantly containing the frequency of 528 Hz seems to be supported by the results, but a t-test should have been run between the groups to see if the results are significant. Figure 1 shows that the 528 Hz group had more total growth than the white noise group, table 1 shows that the total averages were also higher, and table 2 shows that the average growth rate was higher too. The variance in the white noise group was the highest of the three, so it is likely that lack of control for range of frequency contained in white noise affected the growth of each plate.

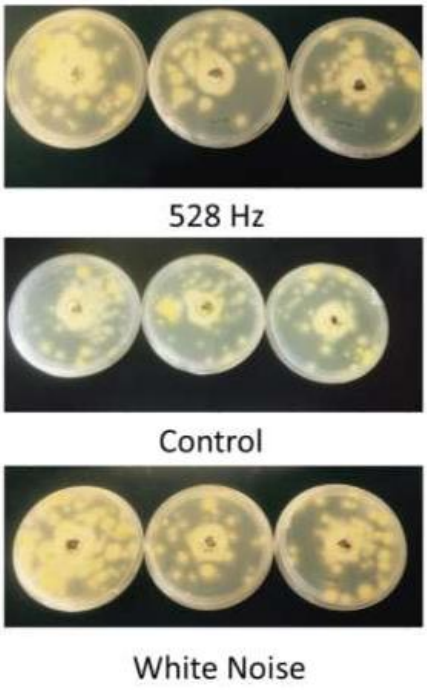

The control group was the highest in all overall growth except that it's top plate and less growth than the top plate of the 528 Hz group. It is interesting to mention the pattern of growth in each plate, as seen in figure 1. The 528 Hz group had more growth in the top plate, which was closest to the speaker, whereas the white noise

group experience the least amount of growth in the top plate (also closest to the speaker in proximity). This is more consistent with the pattern exhibited in the control group, whose bottom plate also had the most growth. The 528 Hz group had the opposite growth pattern suggesting that the close proximity to, or less interference of, exposure to the music could have had a positive effect on the mycelia growth. Again, the student t-test should have been run between the two groups and against an optimal value to confidently speculate on the correlational evidence. All of these qualities of growth do not support the hypothesis that *A. niger* exposed to music in the frequency of 528Hz will exhibit more mycelial growth than those exposed to no music. Future research should test the effect of music in the range of 0.5Hz – 500Hz against the 528Hz as well as using a pure 1000Hz negative control.

5.0 Works Cited

Appelt, C. (2006). Pulsed Biofeedback Clinic. *Pulsed Electromagnetic Field Therapy (PEMF): New Perspectives in Therapy*. http://pulsedbiofeedbackclinic.com/wp-content/pdfs/2006_Dec_A4M.pdf. Accessed February 24, 2017.

Comparative Examples of Noise Levels | Industrial Noise Control. (2017). *Industrialnoisecontrol.com*. Retrieved 26 April 2017, from http://www.industrialnoisecontrol.com/comparative-noise-examples.htm

Joosten V., Lokman C., van den Hondel C. A., and Punt J.P. 2013. Microbial Cell Factories2003 2:1. *The production of antibody fragments and antibody fusion proteins by yeasts and filamentous fungi.* http://microbialcellfactories.biomedcentral.com/articles/10.1186/1475-2859-2-1. Accessed February 17,2017.

Magaña-Ortíz D., Coconi-Linares N., Ortiz-Vazquez E., Fernández F., Loske, A. M., Gómez-Lim M. A. 2013. Fungal Genetics and Biology 56 (2013) 9–16. *A novel and highly efficient method for genetic transformation of fungi employing shock* waves. http://dx.doi.org/10.1016/j.fgb.2013.03.008. Accessed February 19, 2017

Mi-Jeong Jeong, Dong-Won Bae, Bae H., Lee S. I., Kim J. A., Shin S. C., Par, S. H., Soo-Chul Park. 2013. Journal of the Korean Society for Applied Biological Chemistry. *Inhibition of Botrytis cinerea Spore Germination and Mycelia Growth by Frequency-specific Sound.* https://www.researchgate.net/publication/271631915. Accessed February 17, 2017.

Neal, M. (2017). *The Many Colors of Sound*. *The Atlantic*. Retrieved 26 April 2017, from https://www.theatlantic.com/science/archive/2016/02/white-noise-sound-colors/462972/

Saleh A. A., Ohtsuka A., Yamamoto M., and Hayashi K. 2013. BioMed Research International. *Aspergillus awamori Feeding Modifies Lipid Metabolism in Rats.* http://dx.doi.org/10.1155/2013/594393. Accessed February 19, 2017.

Suits B. H. 1998-2015. Physics Department, Michigan Technological University. *Physics of Music – Notes.* http://www.phy.mtu.edu/~suits/notefreqs.html. Accessed February 24, 2017.

Change in Forest Composition with Change in Elevation in Colorado's Front Range

Ryan Reese
BIO 111 Fall 2019

Abstract

Forest stands can vary drastically from one another due to differing stand elevations. Stand characteristics such as tree species, species diversity, tree height, diameter at breast height, basal area, and other traits can vary significantly enough with only a slight change in elevation to create two juxtaposed types of stand. Such conditions are easily visible on Colorado's Front Range, where changes in elevation in excess of 3000 meters can be observed within a space of a few dozen kilometers. The species present at different elevations change according to a fairly uniform pattern across the Front Range: mixed ponderosa pine and Douglas fir stands transition to lodgepole stands, which slowly transition to mixed spruce and fir stands dominated by Engelmann spruce and subalpine fir. In order to see how stands transition from one type to another and gain additional information on stand type compositions, data was collected from semi-random forest plots at various elevations. This data better shows at which elevations and how forest composition changes in Colorado's Front Range.

Introduction and Concepts

Forest composition varies according to numerous environmental conditions. Moisture, temperature, sun exposure, soil conditions, competition from other plants, and numerous other conditions can impact the ability of different species to survive and thrive in different locations. These conditions can be heavily impacted by changes in elevation. Increasing elevation is associated with decreasing temperature and increasing precipitation in mountain ranges at middle latitudes such as those found in Colorado (Molles, 2010). As a result, different elevations can have very different forest compositions.

Trees generally favor specific temperature conditions. This is not unique; according to Molles (2010), "most species perform best in a fairly narrow range of temperatures." This is the result of numerous biological processes. Proteins from different species will be better suited to different temperatures, predisposing those species to locations within these temperature bounds. Different species may also develop different adaptations to regulate their temperature, either dissipating or retaining thermal energy from the environment by such means as improved radiation absorption (found in subalpine fir) or creation of a suitable microclimate (Molles, 2010). Each species, arboreal or otherwise, adapts in its own way to the unique temperature challenges found in its environment.

Tree species are generally found within very specific elevation bands where growing conditions are more favorable to that tree species. For instance, grand fir, a common tree in the Idaho panhandle and the Pacific Northwest, is generally found at elevations up to 1829m, while the western larch can be found in the same area up to 2134m (Little, 1992). These elevation bands also vary according to latitude and proximity to a coastal area. Subalpine fir can be found at sea level in Canada and Alaska but is generally found at elevations between 2400m and 3658m in the southern Rocky Mountains (Little, 1992). Taken together, this means that not only are trees adapted to specific elevation bands, but the boundaries of these bands are locally specific, with particular boundaries in particular locations.

Additionally, similar stands in different regions will have different species compositions. In central Idaho, ponderosa pine can frequently be found in the same area as Douglas fir, western larch, and grand fir, while similar stands in Colorado will only have ponderosa pine and Douglas fir, as the ranges of western larch and grand fir do not extend into the dryer, more continental southern Rocky Mountains (Little, 1992). Therefore, stand composition is also locally specific.

In order to better understand how elevation determines local forest structure, I collected data on forest composition at several sites in Colorado's Front Range. I hypothesized that there would be a transition from more drought and fire-resistant ponderosa pine and Douglas fir to a mixture of lodgepole monocultures and mixed spruce and fir stands. Additionally, I predicted to see indications that certain species create their own microclimates to assist in their adaptation to environmental conditions found at different elevations.

Methods

Data was collected from sixteen semi-random 10m by 10m forested plots in the area west of Evergreen, Colorado. Plots ranged in elevation from 2466m to 3358m, with most plots lying under 3000m in elevation. To avoid bias in the data set due to excessive slope or differences in aspect, slope was kept below 40 degrees for all surveyed plots, and only plots on east-facing aspects were used (aspect was kept between 45 degrees and 135 degrees). The aspect and slope were measured and recorded for each plot to retain the ability to identify potential bias in the data set. Plots were primarily located along a single east-west transect between 2400m and 3000m in elevation. Plots were generally 30m away from a water source or any form of human disturbance or development and were either 100m away from each other or 50m different in elevation.

Several tree species of interest were identified prior to data collection: ponderosa pine (*Pinus ponderosa*), Douglas fir (*Pseudotsuga menziesii*), lodgepole pine (*Pinus contorta*), subalpine fir (*Abies lasiocarpa*), Engelmann spruce (*Picea engelmannii*), blue spruce (*Picea pungens*), and bristlecone pine (*Pinus aristata*). The number of adults of each species was counted in each plot, along with each individual tree's circumference at breast height, from which diameter at

breast height, or DBH, could be calculated. For each species excluding lodgepole pine, trees with a circumference above 37cm (DBH of 12cm) were assumed to be adults. Due to the tendency of lodgepole pines to be tall and narrow, with most trees falling below this measure, all lodgepoles with a crown base above 2m in height were assumed to be adults. No data was collected from trees under this size or from snags (dead trees). Additionally, notes were taken on whether species of concern or auxiliary species were near each plot. Trees which split at the bole or below breast height were considered separate trees.

After data collection, plot data was entered into a database in Microsoft Excel. Metrics such as individual tree diameter at breast height, average diameter at breast height by species and plot, and basal area by individual, species and plot were calculated. Additionally, data at a sample level was used to calculate average elevation for each tree species and the percentage of the total sample from each tree species.

Data and Results

A total of 209 trees were surveyed across all plots. Of these, 131 were lodgepole pine (63%), 21 were ponderosa pine (10%), 18 were Douglas fir (9%), 18 were Engelmann spruce (9%), 20 were subalpine fir (10%), and 1 was a bristlecone pine (>1%). No blue spruce were observed in any of the plots. Due to the small sample size, bristlecone pine data was not analyzed.

The average DBH for the sample was 19.11cm, with an average elevation of 2830m with a standard deviation of 235m. Douglas fir had the lowest average elevation of 2513m (SD 42m), followed by ponderosa pine at 2565m (SD 100m). Lodgepole pine had a significantly higher average elevation of 2801m (SD 98m). Engelmann spruce and subalpine fir had significantly higher average elevations than any other observed tree species, 3139m (SD 100m) and 3304m (SD 97m) respectively. Average DBH ranged from 16cm (lodgepole pine) to 31cm (ponderosa pine).

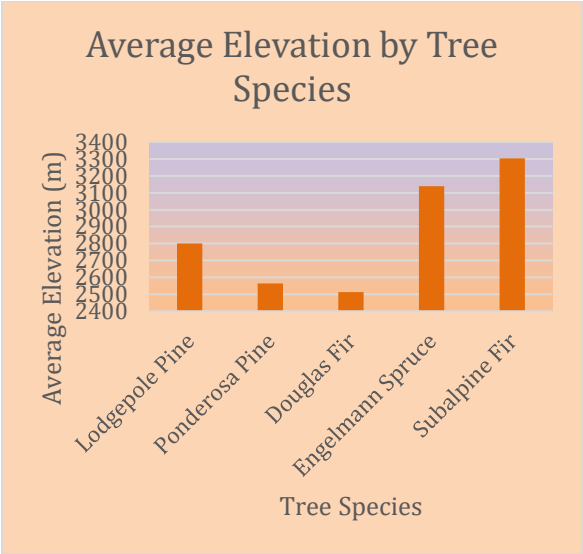

Table 1: Average Elevation by Tree Species

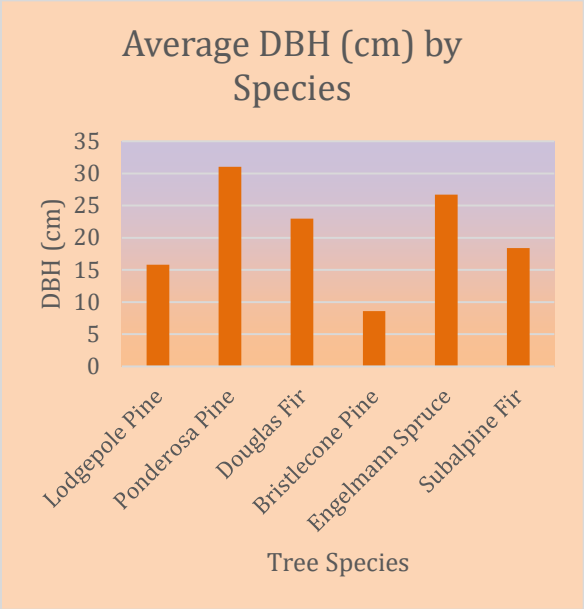

Table 2: Average DBH by Tree Species

Each plot was analyzed for each species' contribution to each plot's total basal. This was used as a proxy measure of each species' dominance and contribution to the surrounding stand type's biomass. Plots were arranged from lowest to highest elevation to show how successful each tree species is at each elevation.

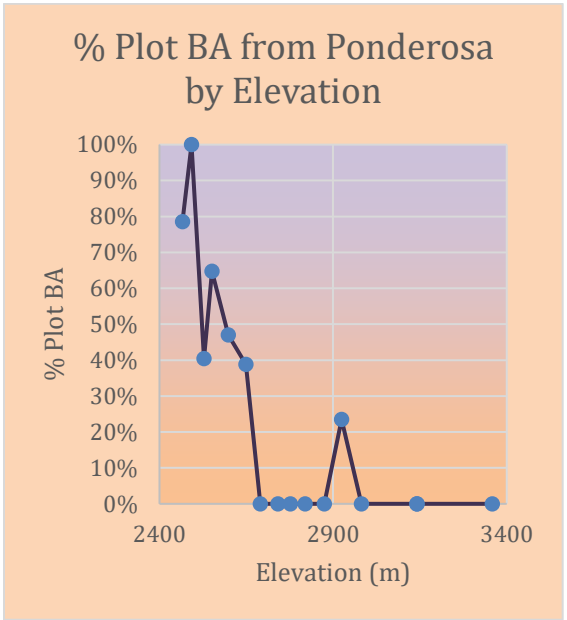

Table 3: Percent of Plot Basal Area from Ponderosa Pine

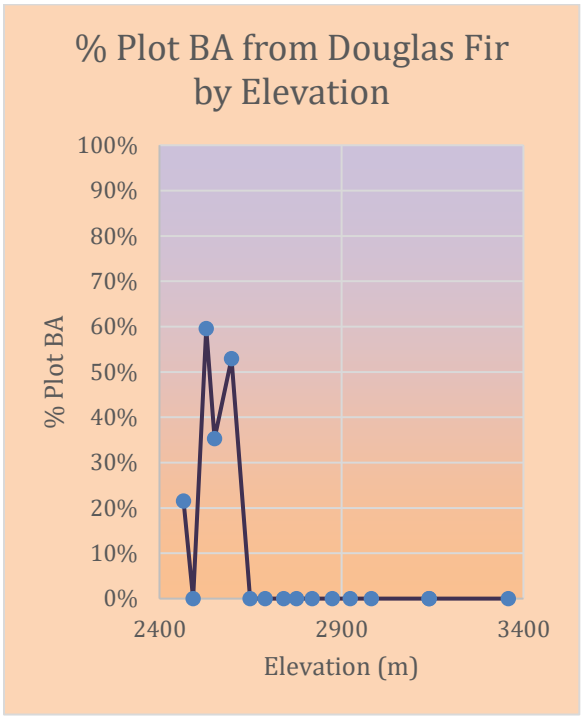

Table 4: Percent of Plot Basal Area from Douglas Fir

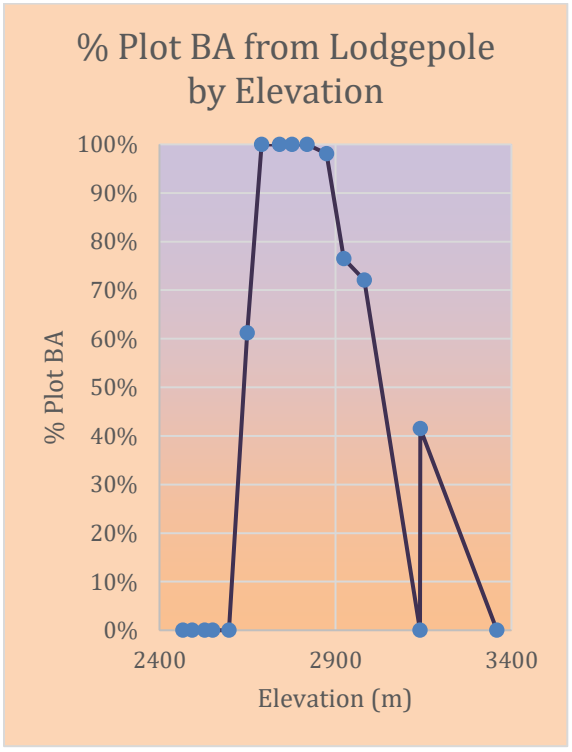

Table 5: Percent of Plot Basal Area from Lodgepole Pine

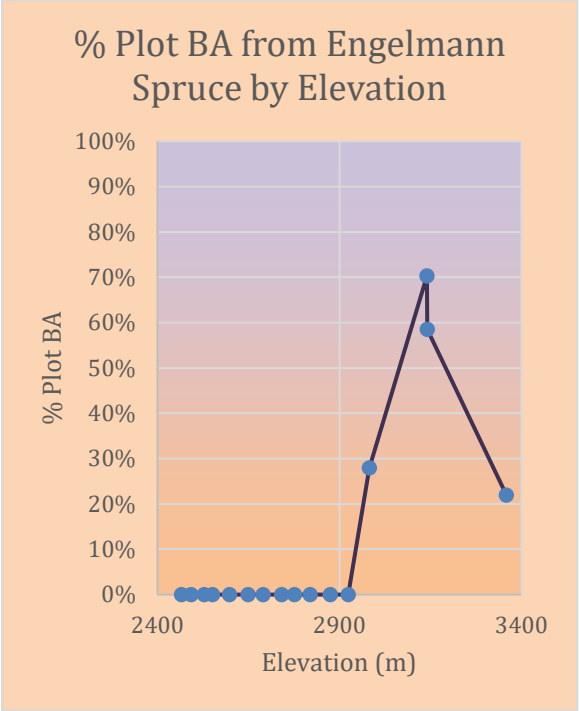

Table 6: Percent of Plot Basal Area from Engelmann Spruce

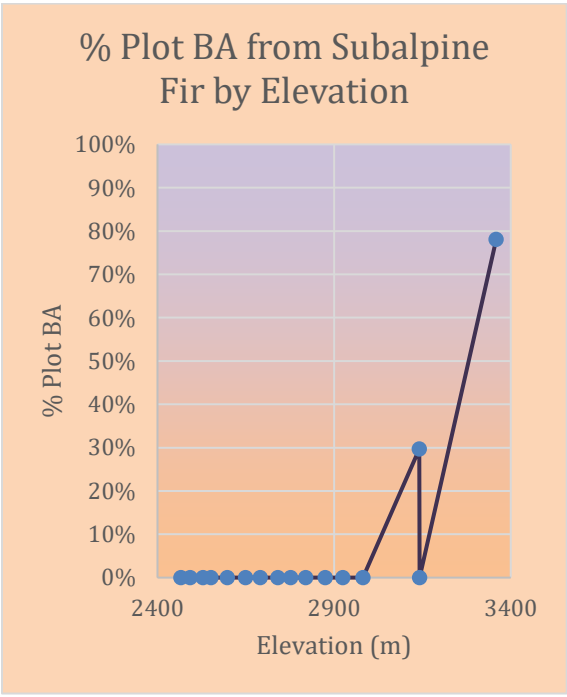

Table 7: Percent of Plot Basal Area from Subalpine Fir

Discussion

The collected data appears to support the hypothesis that there is a general transition from a Douglas fir-ponderosa pine stand type to a lodgepole stand type, followed by a slow transition from a lodgepole stand type to a mixed Engelmann spruce-subalpine fir stand type. As can be seen in Table 3 and Table 4, ponderosa pine and Douglas fir appear to be codominant at elevations below 2700m. Both ponderosa pine and Douglas fir are then replaced by lodgepole pine (see Table 5), which becomes the dominant tree species between 2700m and 3000m in elevation. While lodgepole pine continues to appear in the data set until 3100m in elevation, there appears to be a slow transition from lodgepole-dominated stands to mixed subalpine fir-Engelmann spruce stands starting around 3000m in elevation (see Table 6 and Table 7).

These observations correlate well with the observations of other researchers elsewhere in the Colorado Front Range. While researching stand regeneration in Rocky Mountain National Park, Perovich and Sibold (2016) found that Douglas fir did not show signs of encroachment in areas of high lodgepole pine mortality resulting from mountain pine beetle, while both Engelmann spruce and subalpine fir showed some level of encroachment. This suggests that the beginning of the optimal range for lodgepole pine begins above the upper elevation bound for Douglas fir, while the ceiling for lodgepole pine does not occur until well into the elevation range for subalpine fir and Engelmann spruce. This correlates well with the coexistence of Engelmann spruce with lodgepole pine at

the same elevation, as shown in Tables 5 and 6.

The hypothesis that trees can create their own microclimates is also somewhat supported, though more tenuously. Though not seen in either ponderosa pine-Douglas fir or subalpine fir-Engelmann spruce stand types, there appears to be a certain level of exclusion of other tree species from lodgepole stands. While studying morphological responses of aspen, lodgepole, and ponderosa pine to different environmental conditions, Carroll, Knapp, and Martin (2017) observed similar responses from ponderosa pine and lodgepole pine at similar elevations with some exceptions. This suggests that both species have a moderate level of overlap in elevation range. This correlates with the data collected, which shows ponderosa pine in the sample until 3000m in elevation. Between 2700m in elevation and 2900m in elevation, however, lodgepole pines made up more than 90% of the basal area in any one plot. This suggests that lodgepole pine either outcompete ponderosa pine at these elevations, or that lodgepole stands create an environment conducive to further lodgepole growth or detrimental to the growth of other trees such as ponderosa pines. Such an effect appears to have less of an impact upon Engelmann spruce, as evinced by their co-occurrence at higher elevations. I hypothesize that thick lodgepole stands create a shaded environment which is not favorable to less shade-tolerant ponderosa pines, but which has little effect upon shade-tolerant Engelmann spruce. Further research would be necessary to test this hypothesis.

It is also possible that a similar form of exclusion exists in Douglas fir-ponderosa pine stands. In their research on forest structure changes at lower elevations on the Front Range, Battaglia et al. (2018) speak extensively of how ponderosa pine and Douglas fir are fire resistant trees, having adapted to lower elevations where warmer conditions result in a more frequent wildfire schedule. The frequent occurrence of low-intensity fires in these areas may explain why the less fire-resistant lodgepole pine does not appear to coexist frequently with ponderosa pine and Douglas fir. Further research is necessary to test such a hypothesis.

The absence of any significant representation of either bristlecone pine or blue spruce in the data set is telling, as is the general silence of the academic community on their impact on stand-level changes in forest structure. The dearth of information on the role either play in their given ecosystems, along with their conspicuous absence from the data set, suggest strongly that neither tree is abundant enough to play a significant role in stand-level changes, and that neither tree is abundant enough to be considered a defining feature of a stand type in the same way as lodgepole pine, ponderosa pine, and subalpine fir.

Unfortunately, the data regarding subalpine fir and Engelman spruce is fairly weak, as is data on higher elevation lodgepole pine stands. The data collected from elevations above 3000m was collected from an area detached from the rest of the study area and was collected from sites close to human disturbance.

Additionally, this elevation range is not evenly represented, with large elevation gaps between plots. Furthermore, these plots were not chosen in a random manner; rather, they were "cherry picked" in an attempt to better represent the surrounding area, resulting in a greater level of diversity in tree species than would have resulted from truly random plots. These factors weaken the value of any analysis which can be made using data from the upper elevation range of the data set.

Conclusion

The data shown here supports the hypothesis that changes in elevation result in changes in environmental conditions significant enough to result in changes in stand type. These observations further suggest that tree species create environmental conditions which can be favorable to their own survival or competition with other species. Though the data from the upper elevation range of the data set can only be tenuously used to support a hypothesis, and though the data set is relatively small by academic standards, it adequately displays how changes in elevation correlate with changes in stand composition and forest structure in Colorado's Front Range.

Works Cited

Battaglia, M.A., Gannon, B., Brown, P.M., Fornwalt, P.J., Cheng, A.S., Huckaby, L.S. (2018). Changes in forest structure since 1860 in ponderosa pine dominated forests in the Colorado and Wyoming Front Range, USA. *Forest Ecology and Management, 422,* 147-160.

Carroll, C.J.W., Knapp, A.K., Martin, P.H. (2017). Dominant tree species of the Colorado Rockies have divergent physiological and morphological responses to warming. *Forest Ecology and Management, 402,* 234-240.

Little, E. L. (1992). *The Audubon society field guide to North American trees: western region.* New York, NY: Chanticleer Press.

Molles, M. C. (2010). *Ecology: concepts and applications.* New York, NY: McGraw-Hill.

Perovich, C., Sibold, S. (2016). Forest composition change after a mountain pine beetle outbreak, Rocky Mountain National Park, CO, USA. *Forest Ecology and Management, 366,* 184-192.

An assessment of the differences between the fungal endophyte communities in insect-affected and unaffected spruce trees

Kenya Gates[1], Carly Anderson Stewart[2], Mason James[2], Sarah Kidder[1]
[1]Red Rocks Community College, [2]University of Colorado, Boulder
Summer Internship 2019

Abstract

In light of the devastating tree mortality caused by recent bark beetle epidemics in the Rocky Mountain region, we sought to investigate the community differences between the fungal endophytes of insect-affected and healthy spruce trees (*Picea engelmannii)* to determine if a tree's ability to resist insect herbivory is related to the microbial community it harbours. Fungal isolates extracted from the needles of insect-affected and unaffected trees were sequenced and identified, yielding 19 probable and 39 possible species across multiple orders. Statistical analyses comparing the endophyte communities of the two experimental groups showed substantial dissimilarities, but more extensive sampling is required to reveal true patterns of community structure and species dominance.

1 | Introduction

Fungal endophytes are a ubiquitous, multi-phyletic assemblage of microorganisms defined as spending at least some part of their life cycle living as asymptomatic occupants of plant tissues (Petrini, 1991; Carroll & Carroll, 1978) In the past several decades, extensive work has been conducted to characterize the life cycles and ecosystem contributions of this diverse class of fungi (Arnold & Lutzoni, 2007; Tanney, 2016) especially concerning the potential benefits endophytes provide to the host as a means to increase plant survivability in periods of environmental and biological stress (Gennaro, Gonthier, & Nicolotti, 2003; Hata & Futai, 1995; Arachevalete et al., 1989) . In many instances (especially in graminoid species), the secondary metabolites produced by fungal endophytes have been demonstrated to possess fungicidal and insecticidal properties (Bills et al., 2012; Palaez-Angeles et al., 2000), deterring further infection by detrimental pathogens and decreasing insect herbivory (Rodriguez et al., 2009; Clay, 1988; Crawford, Land, & Rudgers, 2010). While fungal endophyte inventory of conifer trees has been conducted extensively in the Pacific Northwest and Canadian regions (Carroll & Carroll, 1978; Petrini & Carroll, 1981; Clark et al., 1989; Sumarah & Miller, 2009) the species of the Rocky Mountain region have yet to be comprehensively characterized -- an oversight, given that this region has been heavily impacted by insect herbivory throughout the last two decades (Chapman et al., 2012).

In North America, spruce beetle (*Dendroctonus rufipennis*) populations increased to epidemic levels in the twenty years between 1995-2015 (Hart et al., 2017; Hyde et al., 2016). While at typically observed levels this insect pest rarely causes tree mortality (Raffa et al., 2015), the most recent outbreak resulted in vast areas of standing dead forest, which have been correlated to secondary impacts on local hydrology and ecology (Brouillard et al., 2016; Morris et al, 2018). The primary means by which the beetle affects the spruce tree occurs during its early larval phase, when it hatches from its egg in the spring and consumes the cortex and primary phloem of the tree, effectively cutting off its circulation when larval populations reach reach high enough numbers. Such outbreaks are predicted to increase in frequency and severity as a result of decreasing winter temperatures and days of hard frost, which typically serve as population controls on bark beetles (Werner et al., 2006; Bent et al., 2010).

In beetle-affected forests, tree mortality is rarely 100%, even among homogeneous-aged stands (Hicke et al., 2016; Kayes & Tinker, 2011). While some theorize that genetic resistance may be a contributor to the survivability of certain trees (Yanchuk et al., 2007; Rosner & Hannrup, 2004), in this study we sought to investigate the endophytic communities of insect affected and unaffected trees to investigate the roles of a tree's microbial community in the individual's survival during periods of biological stress. We hypothesize that certain species of endophytes may contribute to host resistance through the production of insecticidal metabolites, and that trees with more diverse endophytic communities are more likely to harbor these specific species. In this study, we seek to investigate the community differences between affected and unaffected spruce trees, identify endophyte species that appear to be more commonly present in healthy trees than in insect-affected individuals, and provide a baseline study for the characterization of endophyte communities in the Rocky Mountain region.

In an era where anthropogenic factors have an ever-increasing impact on climatic and biological processes, it is imperative to understand the roles of species in an ecosystem in order to predict how critical habitats will be affected. The boreal forests of the taiga biome and beyond contribute a substantial amount of oxygen to the earth's atmosphere, and their preservation is of high importance. It is crucial to understand interspecies relationships and how they affect ecosystem health as we enter into an age of climatic unpredictability in order to implement effective conservation and remediation practices.

2 │ Materials & Methods

2.1 │ Site selection & sample collection

In this study, we selected sample sites on the West, East, and South-facing slopes of Tenderfoot Mountain in Summit County, Colorado, as well as an additional site in a meadow near the southern base of the mountain. This region was selected based on its proximity to areas of reported beetle kill. To the south of our sampling area, Colorado forests in the San Juan region of the state had been devastated by spruce beetle in the recent outbreak, and the region we sampled in has been heavily impacted by mountain pine beetle. While Spruce Beetle had been reported in the area, our sites have not yet experienced epidemic-level tree mortality. In all four of our sites, we observed both asymptomatic *Picea engelmannii* trees as well as individuals bearing sign of beetle infestation, but which did not yet exhibit the discolored foliage indicative

of tree mortality -- instead, they displayed indicators of bark beetle infestation such as sap runners from bore holes, woodpecker pitting, and wood dust at the base of the tree. Our sites included multiple aspects, elevations, and proximities to water sources, a measure we took in order to capture the most complete regional community possible.

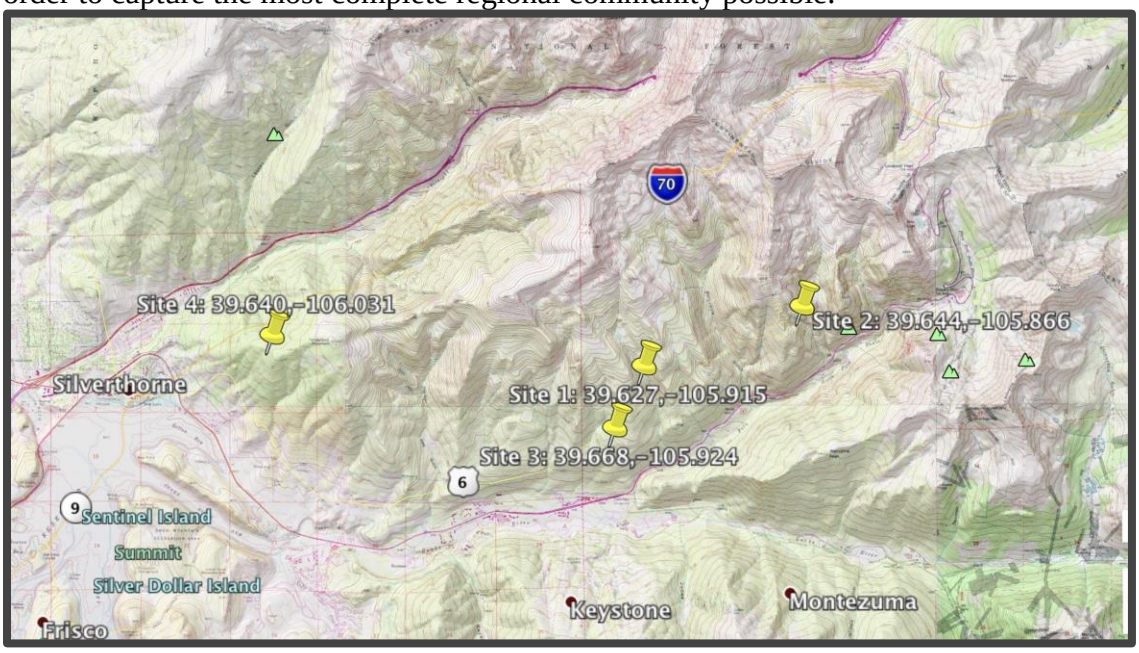

Figure 1: Sample site locations in Summit County, CO

In our experimental design, healthy trees displaying no signs of insect activity were included in our control group (henceforth called the "unaffected" group), and our experimental ("insect-affected") group was comprised of trees displaying the aforementioned indicators of insect activity. For sample collection, we selected a total of 10 individuals of each treatment group from each site for a total of 80 individuals, 40 in each treatment. From each tree, two sprigs of healthy needles were severed from the branches and bagged in plastic Ziploc bags for storage until processing. Healthy needles were selected from branches between 1.5 and 2 meters from the ground in most instances, and from sprigs between 2-5 years old.

2.2 │ Sample processing

Sample processing using sterile technique took place within 48 hours of collecting. From each sprig collected, three healthy needles were selected and surface sterilized using an ethanol-bleach-ethanol treatment, and then plated on Potato Dextrose Agar (PDA) plates with Streptomycin discs. Each plate was then labelled and sealed with Parafilm prior to the incubation period. In total, two plates for each individual tree were created, for a total of 160 plates prior to subplating. We then incubated the plates for a total of 6 weeks under ambient indoor conditions before subplating each appearing fungal colony. Subplating was conducted under a fume hood using a sterile razor to cut each colony from the agar to be replated individually on new PDA dishes. The subplates were then sealed and left to incubate for another 6 weeks under ambient conditions, after which the resulting colonies were divided into morphotype groups based on characteristics such as growth rate, coloration, mycelium depth and texture, and metabolite

coloration. Because none of our isolates sporulated, microscopy-based identification was not possible.

2.3 | Morphotyping & DNA extraction

Following morphotype grouping, approx. 1 square cm of mycelial tissue was removed from culture using a sterile razor and placed in specimen tubes. DNA extractions were performed using CTAB methodology. To lyse the specimen cells, we pulverized our samples with titanium beads included in the tubes using a Geno/Grinder (SPEX, 65 Liberty Street, Metuchen, NJ 08840). Following cell lysation, 500ul room temperature extraction buffer was added to each specimen tube, vortexed, and incubated for 75 minutes at 60C. The tubes were briefly cooled on ice before adding 500ul chloroform:isoamyl alcohol (24:1) under a fume hood, after which the contents of each tube were inverted multiple times to homogenize the contents thoroughly. The specimen tubes were then centrifuged at 15000 rpm for 5 minutes. The resulting aqueous top phase was transferred to a new tube. To each of the new tubes, 245ul of -20C 95% isopropanol was added, and the samples were placed in a -80C freezer for approx. 30 minutes. They were then centrifuged at 13000 rpm for 15 minutes, after which the supernatant was poured off, leaving the resulting pellet within the tube. Samples that did not separate into distinct phases were precipitated again with an additional volume of isopropanol and left in the -80C freezer overnight to be centrifuged the next day, at which point distinct phases formed. To each pellet, 100ul of 70% ethanol was added, and the contents of the tubes were swirled gently and then centrifuged for 5 minutes at 13000 rpm. The ethanol was poured off, and the tubes were inverted and left to dry overnight. The pellets were resuspended in 20ul TE buffer overnight at 4C. Nanodrop readings showing DNA concentrations for each sample revealed highly variable and values between 60-4000 ng/ul, but a Qubit showed that all samples did have high DNA concentrations between 8-16 ng/ul.

2.4 | Sequencing & identification

PCR and Sanger sequencing were conducted by Quintara Biosciences Inc. 96 of the 110 total isolates were selected randomly for sequencing. We selected the Internal Transcribed Spacer unit (ITS) and Large ribosomal Subunit (LSU) fungal regions for species identification and phylogeny construction. The ITS region was amplified using primers ITS1F (5'-CTTGGTCATTTAGAGGAAGTAA-3') and ITS4 (5'-TCCTCCGCTTATTGATATGC-3'). The primers LR0R (5'-ACCCGCTGAACTTAAGC-3') and LR5 (5'-TCCTGAGGGAAACTTCG-3') were used for the LSU region.

For species identification, sequences were run against NCBI GenBank as well as UNITE fungal database. Sequences with the highest base pair similarities and lowest expect values were used to determine the identities of our isolates.

2.5 | Genetic & community analysis

Phylogram visualization was conducted using FigTree version 1.4.4 with a Newick tree generated though EBI's Simple Phylogeny tree-generating service, with LSU sequences aligned with their Clustal Omega multiple sequence alignment tool.

Statistical analyses were performed in Microsoft Excel. Chi-squared values were calculated using the formula

$$x^2 = \sum \quad (\frac{(O-E)^2}{E})$$

The Jaccard distance was calculated using only sequences with high base pair similarities to sequences found in either GenBank or UNITE, with the formula

$$J(A,B) = \frac{|A \cap B|}{|A \cup B|}$$

The Bray-Curtis dissimilarity was calculated using the total isolation rates from both experimental and control groups, with the formula

$$BCd = \frac{\sum \quad |xi-xj|}{\sum \quad |xi+xj|}$$

Shannon diversity (*H*) was calculated using all distinct species with the formula

$$H = \sum_{i=1}^{s} \quad -(Pi \times lnPi)$$

Pairwise beta diversity (β) using the formula

$$\beta\beta = \frac{2xij}{xi+xj},$$

where *xij* is the total number of species shared between both groups, *xi* is the total species in the insect-affected group, and *xj* is the total species in the unaffected group.

3 | Results

3.1 | Species and phylogenetic analysis

In this survey, nineteen species with highly similar base pair similarities (greater than 98% match) were identified, with thirty-nine distinct species likely across sixteen families and thirteen orders, indicating a highly diverse community.

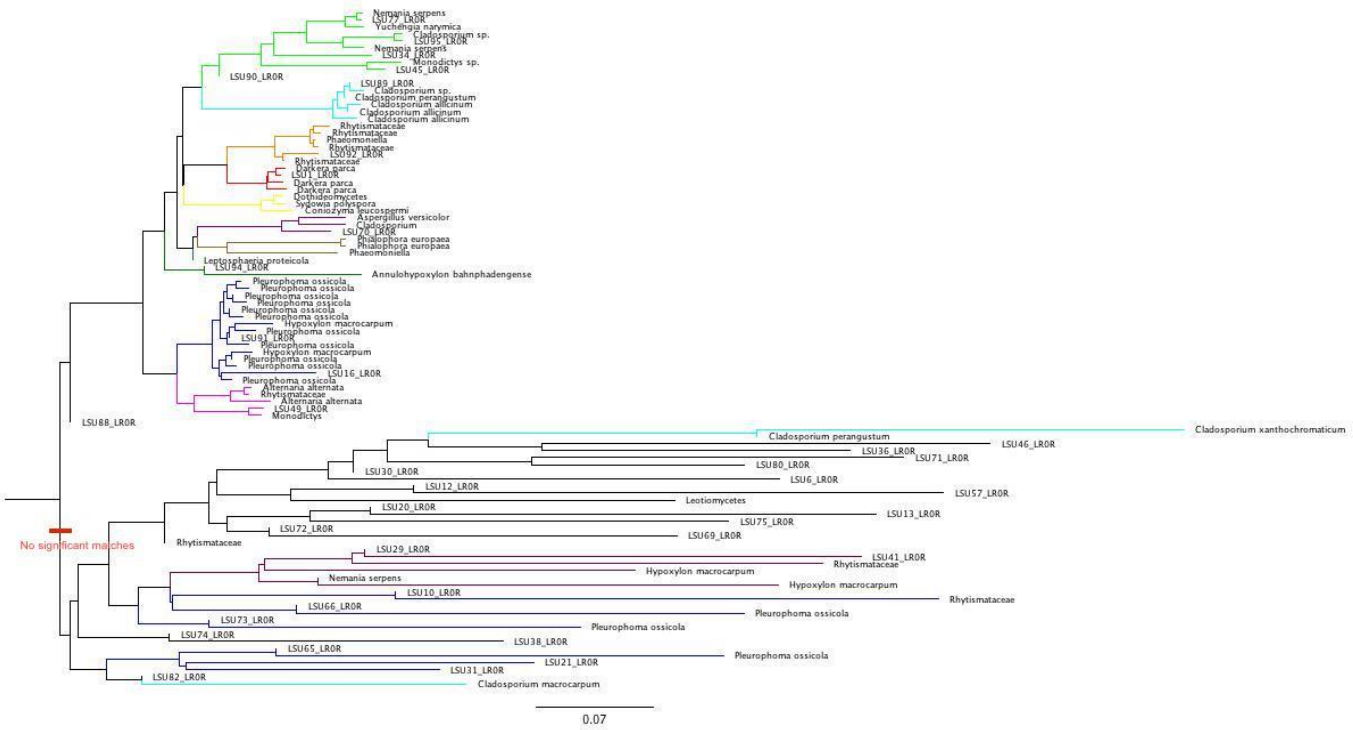

Figure 2: Phylogenetic tree constructed from aligned LSU sequences

Table 1: GenBank and UNITE species determinations based on bp identity matches of ITS sequences

Lab Number	Closest named GenBank match	bp identity match	E-value	Closest named UNITE match	bp identity match	E-value
5	*Alternaria alternata*	1042	0	*Alternaria alternata*	1012	0
47	*Alternaria alternata isolate*	1040	0	*Alternaria alternata*	1011	0
79	*Annulohypoxylon bahnphadengense*	948	0	No BLAST hits	-	-
50	*Aspergillus versicolor*	1022	0	*Aspergillus versicolor*	994	0
51	*Aspergillus versicolor*	845	0	*Pleurophoma ossicola*	987	0
14	*Cladosporium*	996	0	*Cladosporium*	969	0
67	*Cladosporium*	1005	0	*Cladosporium allicinum*	978	0
68	*Cladosporium*	1005	0	*Cladosporium allicinum*	976	0
35	*Cladosporium allicinum*	990	0	*Cyphellophora europaea*	1079	0

15	*Cladosporium perangustum*	996	0	*Cladosporium perangustum*	969	0
83	*Cladosporium perangustum*	994	0	*Cladosporium perangustum*	971	0
28	*Cladosporium xanthochromaticum*	983	0	*Cladosporium xanthochromaticum*	955	0
42	*Coniozyma leucospermi*	1070	0	*Dothideales*	1038	0
4	*Darkera parca*	950	0	*Darkera parca*	919	0
2	*Darkera parca*	922	0	*Darkera parca*	922	0
3	*Darkera parca*	923	0	*Pleurophoma ossicola*	62.6	4.00 E-08
10	*Dothideomycetes*	228	0	*Pleosporales*	-	-
27	*Dothideomycetes*	917	0	*Dothideomycetes*	904	0
62	*Hypoxylon macrocarpum*	1085	0	*Hypoxylon macrocarpum*	1036	0
63	*Hypoxylon macrocarpum*	-	-	*Hypoxylon macrocarpum*	1047	0
64	*Hypoxylon macrocarpum*	1074	0	No BLAST hits	-	-
11	*Leotiomycetes*	1155	0	*Leotiomycetes*	-	0
9	*Leptosphaeria proteicola*	885	0	*Leptosphaeria proteicola*	888	0
43	*Monodictys*	976	0	*Monodictys*	948	0
44	*Monodictys*	972	0	*Monodictys*	948	0
32	*Nemania serpens*	1068	0	*Nemania aenea*	1009	0
78	*Nemania serpens*	994	0	*Annulohypoxylon nitens*	933	0
33	NSSF	-	-	*Yuchengia narymica*	964	0
76	NSSF	-	-	*Nemania serpens*	980	0
59	*Phaeomoniella*	1014	0	*Fungi*	1260	0

37	*Phialophora europaea*	1109	0	*Cyphellophora europaea*	1025	0
39	*Phialophora europaea*	1046	0		-	-
8	*Pleurophoma ossicola*	1014	0	*Pleurophoma ossicola*	991	0
17	*Pleurophoma ossicola*	1007	0	*Pleurophoma ossicola*	984	0
18	*Pleurophoma ossicola*	1009	0	*Pleurophoma ossicola*	987	0
19	*Pleurophoma ossicola*	1007	0	*Pleurophoma ossicola*	984	0
22	*Pleurophoma ossicola*	1014	0	*Pleurophoma ossicola*	993	0
24	*Pleurophoma ossicola*	1020	0	*Pleurophoma ossicola*	1000	0
25	*Pleurophoma ossicola*	1007	0	*Pleurophoma ossicola*	984	0
40	*Pleurophoma ossicola*	745	0	*Pleurophoma ossicola*	758	0
52	*Pleurophoma ossicola*	1013	0	*Pleurophoma*	872	0
87	*Pleurophoma ossicola*	1003	931	*Pleurophoma ossicola*	980	0
53	*Rhytismataceae*	1210	0	*Pleurophoma ossicola*	989	0
54	*Rhytismataceae*	1210	0	*Fungi*	1193	0
55	*Rhytismataceae*	1218	0	*Rhytismataceae*	1243	0
58	*Rhytismataceae*	274	3.00E-69	*Phaeomoniella*	987	0
60	*Rhytismataceae*	1234	0	*Fungi*	1265	0
61	*Rhytismataceae*	1229	0	*Hypoxylon macrocarpum*	1058	0
84	*Rhytismataceae*	953	0	*Rhytismataceae*	949	0
85	*Rhytismataceae*	1212	0	*Rhytismataceae*	1193	0
86	*Rhytismataceae*	1232	0	*Rhytismataceae*	1207	0
93	*Rhytismataceae*	931	0	*Fungi*	926	0
48	*Sydowia polyspora*	1051	0	*Sydowia polyspora*	1023	0

3.2 | Community analysis

110 total specimens were isolated across both groups, 46 from the insect-affected (19.2% isolation rate) group and 64 from the unaffected group (26.7% isolation rate). The p-value between each of these isolation rates showed that this difference was not statistically significant. Across sites, isolation rates ranged between 20.0% and 27.5%, while *H* ranged between .89 and 2.34. Between the two experimental groups, the Bray-Curtis dissimilarity showed a 78.2% difference between the two communities, while the Jaccard distance showed a 75% dissimilarity, revealing distinct differences in both endophyte abundance and biodiversity in the affected and unaffected groups.

Table 2: Isolation rate, Shannon Diversity Index (H), and pairwise beta diversity (β) within sites 1-4

Site	# needles incubated	Isolates	Isolation rate in site (%)	Shannon diversity index (*H*)	Pairwise sites	Pairwise beta diversity (β)
1	120	25	20.8	2.09	1-2	0.4
2	120	24	20.0	2.31	1-3	0.29
3	120	31	25.8	2.34	1-4	0.17
4	120	33	27.5	0.89	2-3	0.26
					2-4	0.14
					3-4	0.22

Table 3: Isolation rate, p-value, Bray-Curtis dissimilarity, and Jaccard distance between experimental groups

Experimental group	# needles incubated	Isolates	Isolation rate in treatments (%)	Chi-squared (p-value) between treatments	Bray-Curtis Dissimilarity (%)	Jaccard Distance (%)
Insect-affected	240	46	19.2	0.086	78.2	75.0
Nonaffected	240	64	26.7			

4 | Discussion

When examining the statistical data for community abundance and biodiversity, we found distinct dissimilarities between the endophyte communities of our two treatments. We found that only 4 of the 39 potential species were shared between the two groups, resulting in a high Jaccard distance, and only 12 of the 110 total isolates belonged to those 4 species, resulting in

the high Bray-Curtis dissimilarity. While the p-value addressing abundance between these two groups (0.086) showed no statistically significant differences, we feel that the other measures were more comprehensive in assessing biodiversity as a function of community character.

These results contribute to our hypothesis that host resistance to beetle infestation may be related to the endophytic communities to which they play host, but we feel it is important to address some of the flaws in our experimental design. Many of the species we isolated were single-occurrence, and were likely artificially rarified due to inadequate sampling and species isolation methods. Because we only selected a total of 6 needles per tree samples for incubation, it is unlikely that we captured a complete snapshot of the community; therefore, inferences about species dominance and community structure would be extremely difficult to derive. It is also likely that culture-based isolation methods are inadequate for the capture of a complete community snapshot. Fungi are competitive organisms with varying growth rates. Isolates that appear in culture may outcompete other species present in the needle through the production of secondary metabolites. Many other factors may affect the ability of a species to grow in culture, including temperature, growth medium, and other climatic and biological variables. Despite these issues, we still feel that the data collected in this survey is evidence that the relationship between host trees and their fungal microbiomes should continue to be investigated in a more comprehensive study in order to further elucidate patterns in host resistance and endophyte species presence.

One of the most interesting pieces aspects of this study outside of the comparison between our affected and unaffected groups was the abundance of the species *Pleurophoma ossicola*, a species only recently described in 2015 by Crous et al., and which was originally isolated from bone near a pine plantation in Germany (Index Fungorum). No literature outside the original description currently exists for the species, and in this study it stood out as our most abundant species, comprising nearly 10% of our total isolates. This paper serves as the first and only description of *P. ossicola* in North America to date.

6 │ Conclusion

In summary, the spruce forest selected for this study was demonstrated to harbor a highly diverse assemblage of fungal endophytes, and analysis of our data showed distinct differences between the communities residing within the insect-affected and unaffected trees. Because so many of the species isolated appeared to have been artificially rarified by undersampling, in order to make a well-supported claim about the relationship between spruce trees and their resistance to insect herbivory, a more comprehensive survey of the area is required, including more needles selected for culture per tree and more individual trees included in the sample population. This study substantiates the need for such a survey and provides preliminary data indicating differences in these two communities.

5 │ Recommendations for future work

In addition to the necessity for a more comprehensive survey focusing on distinctions between the endophyte communities of insect-affected and unaffected trees, we also recommend the

establishment of baseline surveys in the region including multiple tree species and forest types. In the absence of these surveys, it is difficult to distinguish between normal and abnormal results in community and species-level data. Additionally, one of the focuses of subsequent studies should be on the description of new species that may be endemic to the Rocky Mountain region.

We also recommend conducting species-specific work on *P. ossicola* to investigate its ecological roles in host and forest health. Screening for secondary metabolites would be an important step in determining its contributions to the health of its host tree and how alters the structure of the endophyte community to which it belongs.

References

Arachevaleta, M., et al. "Effect of the Tall Fescue Endophyte on Plant Response to Environmental Stress." *Agronomy Journal*, vol. 81, no. 1, 1989, p. 83., doi:10.2134/agronj1989.00021962008100010015x.

Arnold, A. Elizabeth, and F. Lutzoni. "Diversity And Host Range Of Foliar Fungal Endophytes: Are Tropical Leaves Biodiversity Hotspots?" *Ecology*, vol. 88, no. 3, 2007, pp. 541–549., doi:10.1890/05-1459.

Bentz, Barbara J., et al. "Climate Change and Bark Beetles of the Western United States and Canada: Direct and Indirect Effects." *BioScience*, vol. 60, no. 8, 2010, pp. 602–613., doi:10.1525/bio.2010.60.8.6.

Bills, Gerald F., et al. "Hypoxylon Pulicicidum Sp. Nov. (Ascomycota, Xylariales), a Pantropical Insecticide-Producing Endophyte." *PLoS ONE*, vol. 7, no. 10, 2012, doi:10.1371/journal.pone.0046687.

Brouillard, Brent M., et al. "Water Quality Following Extensive Beetle-Induced Tree Mortality: Interplay of Aromatic Carbon Loading, Disinfection Byproducts, and Hydrologic Drivers." *Science of The Total Environment*, vol. 572, 2016, pp. 649–659., doi:10.1016/j.scitotenv.2016.06.106.

Carroll, George C., and Fanny E. Carroll. "Studies on the Incidence of Coniferous Needle Endophytes in the Pacific Northwest." *Canadian Journal of Botany*, vol. 56, no. 24, 1978, pp. 3034–3043., doi:10.1139/b78-367.

Chapman, Teresa B., et al. "Spatiotemporal Patterns of Mountain Pine Beetle Activity in the Southern Rocky Mountains." *Ecology*, vol. 93, no. 10, 2012, pp. 2175–2185., doi:10.1890/11-1055.1.

Clark, Catherine L., et al. "Toxicity of Conifer Needle Endophytes to Spruce Budworm." *Mycological Research*, vol. 93, no. 4, 1989, pp. 508–512., doi:10.1016/s0953-7562(89)80044-9.

Clay, Keith. “Fungal Endophytes of Grasses: A Defensive Mutualism between Plants and Fungi.” *Ecology*, vol. 69, no. 1, 1988, pp. 10–16., doi:10.2307/1943155.

Crawford, Kerri M., et al. “Fungal Endophytes of Native Grasses Decrease Insect Herbivore Preference and Performance.” *Oecologia*, vol. 164, no. 2, 2010, pp. 431–444., doi:10.1007/s00442-010-1685-2.

Gennaro, M., et al. “Fungal Endophytic Communities in Healthy and Declining Quercus Robur L. and Q. Cerris L. Trees in Northern Italy.” *Journal of Phytopathology*, vol. 151, no. 10, 2003, pp. 529–534., doi:10.1046/j.1439-0434.2003.00763.x.

Hart, Sarah J., et al. “Summer and Winter Drought Drive the Initiation and Spread of Spruce Beetle Outbreak.” *Ecology*, vol. 98, no. 10, 2017, pp. 2698–2707., doi:10.1002/ecy.1963.

Hata, Kunihiko, and Kazuyoshi Futai. “Endophytic Fungi Associated with Healthy Pine Needles and Needles Infested by the Pine Needle Gall Midge, Thecodiplosis Japonensis.” *Canadian Journal of Botany*, vol. 73, no. 3, 1995, pp. 384–390., doi:10.1139/b95-040.

Hicke, Jeffrey A., et al. “Recent Tree Mortality in the Western United States from Bark Beetles and Forest Fires.” *Forest Science*, vol. 62, no. 2, 2016, pp. 141–153., doi:10.5849/forsci.15-086.

Hyde, Kevin, et al. “Bark Beetle-Induced Forest Mortality in the North American Rocky Mountains.” *Biological and Environmental Hazards, Risks, and Disasters*, 2016, pp. 119–135., doi:10.1016/b978-0-12-394847-2.00009-7.

Kayes, Lori J., and Daniel B. Tinker. “Forest Structure and Regeneration Following a Mountain Pine Beetle Epidemic in Southeastern Wyoming.” *Forest Ecology and Management*, vol. 263, 2012, pp. 57–66., doi:10.1016/j.foreco.2011.09.035.

Morris, Jesse L, et al. “Bark Beetles as Agents of Change in Social-Ecological Systems.” *Frontiers in Ecology and the Environment*, vol. 16, no. S1, 2018, doi:10.1002/fee.1754.

Peláez, Fernando, et al. “The Discovery of Enfumafungin, a Novel Antifungal Compound Produced by an Endophytic Hormonema Species Biological Activity and Taxonomy of the Producing Organisms.” *Systematic and Applied Microbiology*, vol. 23, no. 3, 2000, pp. 333–343., doi:10.1016/s0723-2020(00)80062-4.

Petrini, Orlando, and George Carroll. “Endophytic Fungi in Foliage of Some Cupressaceae in Oregon.” *Canadian Journal of Botany*, vol. 59, no. 5, 1981, pp. 629–636., doi:10.1139/b81-089.

Petrini, Orlando. “Fungal Endophytes of Tree Leaves.” *Brock/Springer Series in Contemporary Bioscience Microbial Ecology of Leaves*, 1991, pp. 179–197., doi:10.1007/978-1-4612-3168-4_9.

Raffa, Kenneth F., et al. “Natural History and Ecology of Bark Beetles.” *Bark Beetles*, 2015, pp. 1–40., doi:10.1016/b978-0-12-417156-5.00001-0.

Rodriguez, R. J., et al. “Fungal Endophytes: Diversity and Functional Roles.” *New Phytologist*, vol. 182, no. 2, 2009, pp. 314–330., doi:10.1111/j.1469-8137.2009.02773.x.

Rosner, Sabine, and Björn Hannrup. “Resin Canal Traits Relevant for Constitutive Resistance of Norway Spruce against Bark Beetles: Environmental and Genetic Variability.” *Forest Ecology and Management*, vol. 200, no. 1-3, 2004, pp. 77–87., doi:10.1016/j.foreco.2004.06.025.

Sumarah, Mark W., and J. David Miller. “Anti-Insect Secondary Metabolites from Fungal Endophytes of Conifer Trees.” *Natural Product Communications*, vol. 4, no. 11, 2009, doi:10.1177/1934578x0900401112.

Werner, Richard A., et al. “Spruce Beetles and Forest Ecosystems in South-Central Alaska: A Review of 30 Years of Research.” *Forest Ecology and Management*, vol. 227, no. 3, 2006, pp. 195–206., doi:10.1016/j.foreco.2006.02.050.

Yanchuk, Alvin D., et al. “Evaluation of Genetic Variation of Attack and Resistance in Lodgepole Pine in the Early Stages of a Mountain Pine Beetle Outbreak.” *Tree Genetics & Genomes*, vol. 4, no. 2, 2007, pp. 171–180., doi:10.1007/s11295-007-0098-9.

Construction of a Spark Chamber for Cosmic Ray Detection at Red Rocks Community College

Stacie R. Barbarick, Katie R. Ammon, Bruce R. Bell, William R Brackney, John P. Edelen, Jacob D. Henningsen, Rhiannon R. Larsen, Marieke J. Spiegleman, Nicholas D. Vail, Benjamin Wartofsky, Audrey E. Whitesell

Red Rocks Community College Mathematics and Physics Departments

Physics Special Topics: Spark Chamber

Advisors:

Adam Forland, M.S., Carlos Medina-Hernandez, Ph.D., Shane Spivey, Ph.D.

Abstract

Galactic cosmic rays (GCRs) consisting of high energy nucleons (protons, neutrons and atomic nuclei) are constantly bombarding our solar system and planet. In the early 20th century, spark detectors were developed as a means of visualizing the pathways of these particles. In Spring, 2019, faculty from the Physics and Mathematics Departments were awarded a grant for the Red Rocks Community College Foundation Innovation Challenge to construct a student team and provide them the opportunity to participate in an exclusively project-based, interdisciplinary course resulting in a research apparatus that can be used by future cohorts. Students divided the project into four subsystem teams; chamber and gas delivery, logic, high voltage and detection systems. The team spent the Fall, 2019 semester designing, building, testing and troubleshooting a spark chamber particle detector. Future research will include particle detection in geographically distinct areas (such as the top of a fourteener, the bottom of a mine, etc.); observing differences in cosmic ray rates and trajectories; and building a long-term ray detection sensor and logging mechanism.

1. Introduction

1.1. Background

High energy particles emanating from deep in the galaxy are constantly bombarding our solar system and planet. Some galactic cosmic rays (GCRs) consist of high energy nucleon (protons neutrons) and atomic nuclei which have been ionized during their galactic voyage and collide with particles in the Earth's upper atmosphere that create detectable cosmic ray showers. Cosmic rays pass uniformly through our galaxy near the speed of light and provide one of the few direct samples of matter from outside the solar system, as graphically conceptualized in Figure 1 [1,2]. Unfortunately, magnetic fields of the Milky Way, the Solar System, and the Earth have rendered the origins of these particle sources a mystery. Detectors like spark chambers were developed to begin answering questions about these mystifying particles.

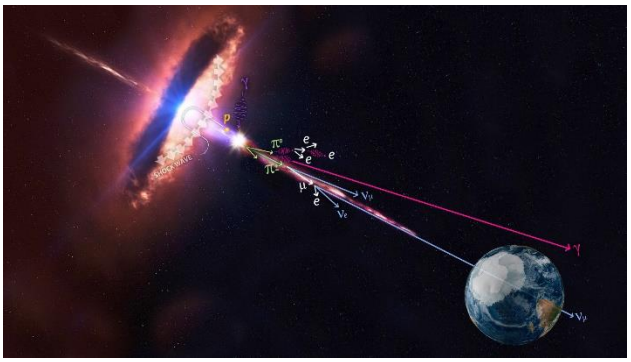

Figure 4: Neutrinos pelt the Earth every second. However, these uncharged, nearly massless particles can pass through whole galaxies without any interaction. When a neutrino is detected, its path leads right back to its origin [7]. (Photo credit: https://www.space.co)

1.2 History

The development of the spark chamber is credited to several scientists and a bringing together of varied technologies, beginning with the Geiger counter in 1910, which could detect an ionizing particle by triggering an electrical breakdown in a gas in a strong electric field. In 1948, Jack Warren Keuffel, used this technology to create the "spark counter" which employed a more uniform field provided by energized, parallel metal plates. His goal was to eventually build a timing device for detecting fast-moving particles [4].

In West Germany circa 1954, Paul-Gerhard Henning stacked three spark counters and took

photographic data of coincidences as charged particles passed through. In 1955, the concept was further developed by Marcello Conversi and Adriano Gozzini in Pisa, who built glass tubes filled with neon which when triggered by a microwave pulse, created a visible spark when charged particles passed. This work was reproduced in the following year by Shuji Fukui and Sigenori Miyamoto, where the team was able to visual the breakdown in proximity to the particle trajectory and allowed the creation of a detector which could display particle paths in 3D [4]. This ultimately prompted a surge of spark chamber fabrication across the globe as they were relatively easy and inexpensive to build, an example of which is shown in Figure 2. A chamber that utilized signaled particle detection and computer logging was the ancestor of most modern particle detectors.

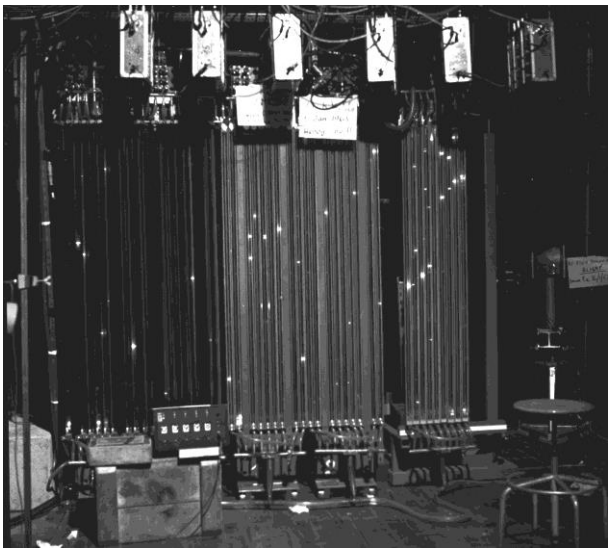

Figure 5: Photo of a cosmic muon track in the spark chambers of the neutrino experiment, CERN, 1963 (photo credit: http://cds.cern.ch/record/40299)

1.3 Mission Overview

The goal of the project was to design and assemble a functional spark chamber as a project-based learning tool for current students and an ongoing research device for future classes. It consists of an assembly of stacked aluminum plates enclosed in an acrylic box and sandwiched between scintillators that trigger a high-voltage pulse circuit. Argon gas fills the chamber, effectively lowering the breakdown voltage between the plates, and when a charged particle passes through, scintillators emit photons that are converted to electrical signals. Coincident signals (signals detected at the same time) produce a logic pulse, which when triggered and amplified, closes the circuit and energizes alternating plates. By applying high voltage to the plates before the ionized electrons can reassemble, the spark chamber allows visualization along the trajectory of the high-energy particle as pictured in Figure 3 [5,6].

2. Design and Functional Systems

The basic functionality of the spark chamber is as follows. A particle crossing the scintillator causes light to be emitted. A part of this light travels to the photomultiplier, where it is converted into an electronic signal. As a particle crosses the argon gas mixture inside the chamber, it causes ionization along its path, locally decreasing the electrical resistance. When the coincidence unit records signals arriving simultaneously, it triggers the momentary activation of the high-voltage supply. This generates large electric fields between aluminum plates and creates current flow along the paths of lowest electrical resistance, which is the particle trajectory. This is visualized as a "spark" through the chamber [8]. A graphical representation of this process is shown in Figure 3.

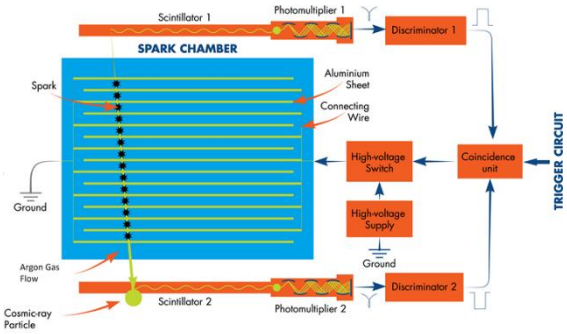

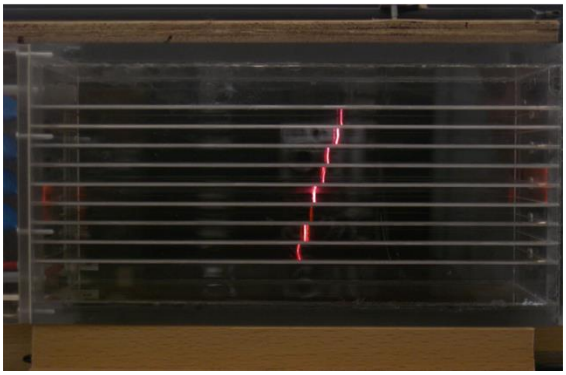

Figure 6: Functional diagram of entire spark chamber (above) and a photo of a spark event from "Cosmic Ray Spark Chambers at the University of Cambridge." (Diagram credit: The Royal Society and W. Brackney; Photo Credit: Jack Collins)

The design of the chamber was the result of mechanical, electrical, and software teams working in

concert at each stage of construction. Materials, electronic components, and process architecture were selected based on the requirements of the apparatus, previous construction, documentation, and budgetary constraints [5,6].

2.1 Detector System

The detector system's two scintillator paddles and silicone photomultipliers (SiPMs) were attached to Cosmic Watch boards for testing. The scintillator paddles provide a medium to decelerate particles that pass through the scintillator material and this slowing of the transiting particles results in the emission of photons. The scintillators are sealed from external light sources to ensure that all photon transmission occurs through the SiPM. When both SiPMs receive a photon within a target timeframe, this triggers the system that a cosmic particle event is occurring and the high voltage (HV) system is activated via the coincidence circuit. The goal was a target time for coincidence of 600 ns [5].

Coincidence within this timeframe will facilitate visualization of the ionization trail within the chamber. The paddles are placed on top of and below the chamber to ensure that the particle passes through the entire chamber before activating the HV system. This prevents unwanted arcing in the chamber which could result in acrylic burning.

Previous methodology to prepare the scintillators for the light-tight wrapping involved applying aluminum foil with minimal wrinkles. Initially, light isolation was not achieved around the SiPM mounting. This was remedied by fitting aluminum foil layers around the SiPM mounting, separate from the main wrapping of the paddles. Isolation was verified using an oscilloscope. It was found that wrapping the scintillators multiple times increased the effectiveness of the light-tight environment when testing with the oscilloscope.

The system was able to detect ambient radiation via testing with the oscilloscope using individual paddles. After the configuration for the scintillator paddles was stacked as opposed to back to back, t detection of a charged particle passing through both detectors in coincidence was achieved, as shown in Figure 4.

2.2 Logic System

The logic system is the bridge between the muon detectors and the high voltage. If a particle activates both the top and the bottom detectors, then the mutual detection will open the AND gate, sending the signal toward the spark gap, as shown in Figure 5 [12]. This AND gate allows voltage discharge only when a particle trajectory is entirely housed within the chamber.

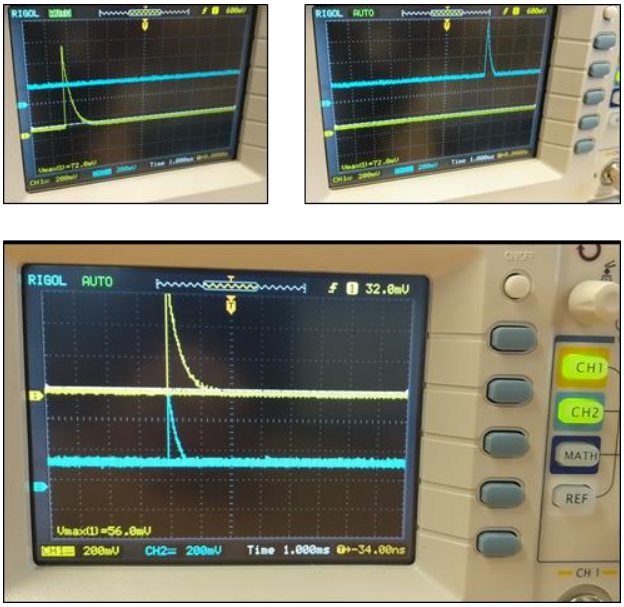

Figure 7: Signals from cosmic ray detection displayed from top and bottom scintillators (top left and right). When the scintillators were directly stacked, particle detection was simultaneous, which verified detection and coincidence. (Photo credit A. Forland)

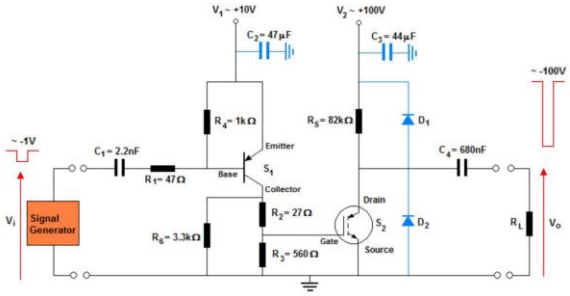

Figure 8: Circuit diagram for logic system of the spark chamber. (Circuit credit: P. de Grouchy, Construction and Evaluation of a Fast Switching Trigger Circuit for a Cosmic Ray Detection Spark Chamber)

The logic team built a functional version of the Cosmic Watch, a muon detector designed and shared as an open source project by MIT [9]. In their digital user's manual, MIT provided a comprehensive GitHub repository which included lists of components, schematics, populated circuit board (PCB) files and populating instructions. Each circuit required three PCBs: one for the logic, one for the SD card, and one for the photomultiplier, shown in Figure 6 [12]. Three complete particle-detecting circuits were successfully

built, although the SD card storage was omitted. The photomultiplier circuits were attached directly to the scintillator material, and an LED screen was connected to the logic circuit to verify muon detection. In addition, an oscilloscope was used to verify the detections and monitor the corresponding waveforms.

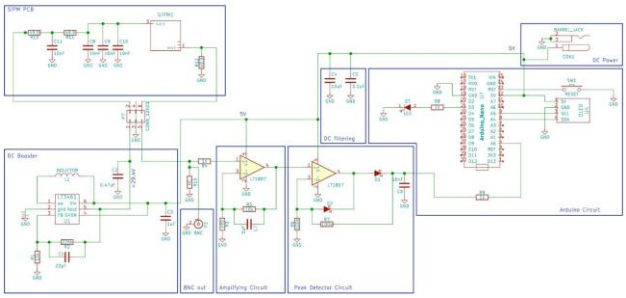

Figure 9: Circuit diagram for the Cosmic Watchbuilt to verify particle detection. (Circuit credit: P. de Grouchy)

One of the non-soldered PCBs was used to test surface-mount AND gates and a separate PCB was required for testing coincidence. Through-hole AND gates were selected but required a higher voltage than the Cosmic Watch circuit could output; it was necessary to sufficiently amplify the output signal using an op amp to trigger the spark gap. Successfully soldered AND gates and op amps produced too low a current to trigger the spark gap. The spark gap needed 12V in, with at least 0.3 amps of current. The AND gate op-amp circuit produced 9V and near to 0 amps of current.

2.3. High Voltage System

The high voltage team was responsible for connecting the logic system to the plate array and causing a timely discharge of a high voltage (HV) pulse. The system is comprised of three major components: a high voltage transformer, a spark gap, and a 10,000-volt DC power supply, as seen in Figure 8. The system is triggered after the logic system detects a particle and low voltage from the Logic Circuit is stepped through a DC to DC transformer. This voltage travels to the spark gap which acts as a switch for the chamber circuit. When high voltage is sent into the spark plug, it causes an arc between the plug and the rest of the system, as pictured in Figure 7. The spark gap ensures that the chamber will not activate unless the circuit is complete.

This voltage activates the fast-discharging capacitors attached to each plate in the chamber and the HVPS discharges. This allows a spark to jump from the positively charged plates to the negative plates, along the ionized path of the particle, illustrating the particles trajectory [5]. The biggest challenge for this team was meeting the time requirement to deliver the voltage. The time frame was extremely short (~600 ns max) to allow the chamber to accurately arc through the path of the muon.

Figure 10: Arc crossing from electrode to spark plug showed proof of concept for spark gap distance. (Photo credit: W. Brackney)

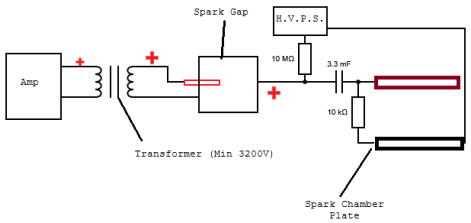

Figure 11: High Voltage Circuit diagram showing the connections from the computer system (The Amp) to the plates that are arranged inside the spark chamber. (CAD credit: J.P Edelen)

2.4. Chamber and Gas System

The external box was initially drawn in SolidWorks so purchase lists and build instructions could be verified. Once all materials were procured, the chamber was constructed of heavy acrylic milled with parallel rails for the square ¼ inch aluminum plates to rest upon. The acrylic faces of the chamber and aluminum plates were custom-machined and bonded with acrylic epoxy to ensure stability. Holes were drilled and tapped into the sidewalls of the aluminum and acrylic to serve as mounting points for easy connection to the high voltage system. Additional clearance was created at the front and back of each plate for uniform gas distribution, and all corners of the plates were rounded to prevent undesired arcing. Once the milling precision was verified, acrylic

cement was used to bond five of the six sides. The last plate acts as a back wall and will be held with a bead of silicone so the chamber can be opened if necessary. The CAD drawing and the finished product are shown in Figure 9 below.

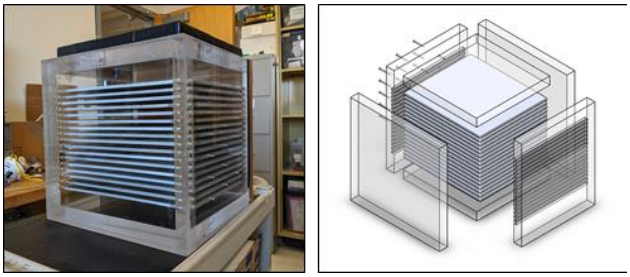

Figure 12: The final iteration of chamber constructed with acrylic and acrylic cement (left) and the CAD drawing of the completed chamber rendered in SolidWorks (right). (Photo credit: A. Forland, Drawing credit: B.Bell)

Figure 13: The first chamber prototype displaying an arc between two electrodes when filled with pure Argon gas. (photo credit: S. Barbarick)

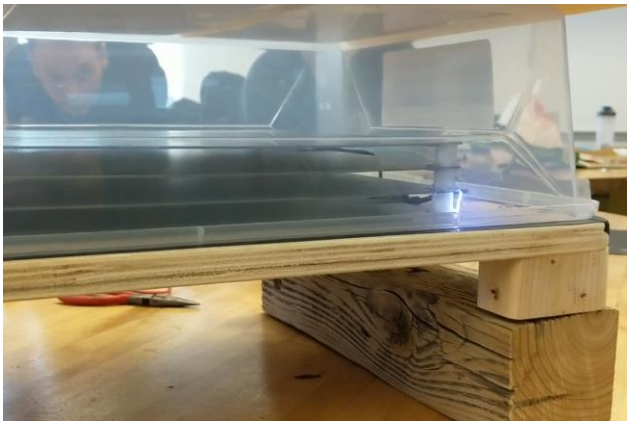

Figure 14: The second iteration of spark chamber used metal plates in an isolated Argon-rich environment, giving proof of concept that the plate and wire connections were robust enough to function with high voltage. (Photo Credit: A. Forland)

Two smaller chambers were prototyped to demonstrate that argon gas effectively lowers breakdown voltage and allows sparking and that soldered plate connectors were sufficiently insulated to prevent unwanted arcing as pictured in Figures 10 and 11. The gas delivery system was designed to allow precise control of the gas flow in, the pressure of the chamber and the vacuum system from the same valve, using the same port in the chamber.

3. Next Steps

For full spark chamber functionality and research purposes, the following recommendations were made:

3.1 Detector System

The detectors currently have no distance between them, which leads to an increased rate of false positive detections. A method to mount the detectors on the top and bottom of the chamber while still achieving coincidence needs to be engineered.

3.2 Logic System

The trigger circuit was prototyped on a breadboard and shorted when the input pulse (simulated muon) was applied to the system. The circuit needs to be rebuilt and tested with adequate wiring.

3.3 High Voltage System

The current high voltage DC to DC transformer used does not produce high voltage at the desired speed. A method of testing the time should be implemented for future testing to ensure the time delays are within the desired range.

3.4 Chamber and Gas System

While the gas system was successfully tested in every iteration of the chamber, the final, permanent gas fittings have not been installed. The back-facing, removeable face of the chamber is the ideal location to drill and tap threads of a permanent gas fitting.

The removeable face plate was left as way to make repairs within the chamber or for altering the testing environment. The acrylic manufacturer recommended using a small bead of silicone adhesive to secure the faceplate during future operations.

4. Conclusion

The spark chamber is of great scientific value to Red Rocks Community College, since it's relatively straightforward and inexpensive to build and it allows observers to directly view the paths of charged particles from cosmic rays. It is well-suited for lecture demonstration since it can be made visible to a large audience and there are multiple research opportunities that can be explored with a functioning chamber [11].

In addition, the project-based learning experience is invaluable to both students and staff since more robust, long-term projects have the potential to motivate students and help them better comprehend and internalize subject matter content [10].

5. References

[1] Smale, Alan. "Cosmic Rays." Cosmic Rays - Introduction, NASA-Astrophysics Science Division, 3 Feb. 2010, web.archive.org/web/20121028154200/http://imagine.gsfc.nasa.gov/docs/science/know_l1/cosmic_rays.html.

[2] Collins, Jack, and Christopher Lester. "Cosmic Ray Spark Chambers at the University of Cambridge." High Energy Physics Group - Department of Physics - University of Cambridge, University of Cambridge, 2011, www.hep.phy.cam.ac.uk/~lester/teaching/SparkChamber/Gallery.html.

[3] Davies, Bethan. "Cosmic Rays." AntarcticGlaciers.org, AntarcticGlaciers.org, 6 May 2016, www.antarcticglaciers.org/glacial-geology/dating-glacial-sediments-2/cosmic-rays/#:~:targetText=Cosmic%20rays%20(also%20called%20cosmic,electrons%20and%20so%20are%20ionised.

[4] Grozier, Jim. "A History of Early High Energy Physics Research at UCL: Spark Chambers." UCL HEP History, Department of Physics & Astronomy, University College London, www.hep.ucl.ac.uk/history/history_sparkchambers.shtml.

[5] Lin, Lisa, et al. "Design, Construction, and First Tests of a Demonstration Spark Chamber." Https://Indico.cern.ch/, The University of Chicago, Illinois, 21 Sept. 2018, indico.cern.ch/event/746023/contributions/3083406/attachments/1720811/2778056/Spark_Chamber_Paper.pdf.

[6] Merrill, Nicholas. "Conceptual Design Report For the Virginia Tech Senior Lab Spark Chamber." Https://Merrillphysics.weebly.com/, Virginia Tech, Jan. 2007, merrillphysics.weebly.com/uploads/1/0/7/7/10771802/conceptual_design_report.pdf.

[7] Tasoff, Harrison. "Discovery of a Cosmic-Ray Source Is a Triumph of 'Multimessenger Astronomy'." Space.com, Space, 12 July 2018, www.space.com/41156-cosmic-ray-source-multimessenger-astronomy.html.

[8] "Spark Chamber." Discovering Particles: Spark Chamber, www.ep.ph.bham.ac.uk/DiscoveringParticles/detection/spark-chamber/.

[9] Przewłocki, P., and K. Frankiewicz. "Catch Yourself a Muon." CosmicWatch, Massachusetts Institute of Technology , 2017, www.cosmicwatch.lns.mit.edu/about.

[10] Blumenfeld, P. C., Soloway, E., Marx, R. W., Krajcik, J. S., Guzdial, M., & Palincsar, A. (1991). Motivating Project-Based Learning: Sustaining the Doing, Supporting the Learning. Educational Psychologist, 26(3-4), 369–398. doi:10.1080/00461520.1991.9653139

[11] The Presidents and Fellows at Harvard College. "Cosmic Ray Spark Chamber." Cosmic Ray Spark Chamber, Harvard University Natural Science Demonstrations, 2019 sciencedemonstrations.fas.harvard.edu/presentations/cosmic-ray-spark-chamber.

[12] P. de Grouchy, Construction and Evaluation of a Fast Switching Trigger Circuit for a Cosmic Ray Detection Spark Chamber, (2009)

Review: The life cycle and secondary metabolites of *Lophodermium piceae*, a dominant spruce endophyte

Kenya N. Gates
CHE111 Fall 2019

Introduction

Lophodermium piceae, one of the most abundant species of endophytic fungi in coniferous forests throughout N. America and Eurasia (Sokolski et al., 2007; Muller et al., 2007; Solheim 1995) is a widely observed but poorly understood species. In early reports, *L. piceae* (Ascomycota) was classified as a weak to aggressive pathogen (Darker 1967; Butin 1986) and associated with needle cast in spruce trees, a disease in which affected needles exhibit dark brown spots prior to dying and falling from the tree. Since then, *L. piceae* has been isolated from apparently healthy needles in numerous endophyte studies (Suske & Acker, 1987, Muller et al., 2001) indicating that this species spends at least part of its life cycle in an endophytic stage as a latent saprophyte or symbiont (Darker, 1932). In this paper we seek to review the current literature on the species involving 1) the life cycle and physiology of this species at different stages, 2) its ecological significance, and 3) the bioactive compounds it produces.

In an era where anthropogenic factors have an ever-increasing impact on climatic and biological processes, it is imperative to understand the roles of species in an ecosystem in order to predict how critical habitats will be affected. The boreal forests of the taiga biome in particular contribute a massive amount of oxygen to the earth's atmosphere, and their preservation is of high importance. A significant portion of these forests are comprised of spruce (*Picea)* species (Esseen et al., 1997; Syrjanen et al, 1994), and *Lophodermium piceae* has been reported in species across the *Picea* genus (Livsey & Barklund, 1992; Stephani & Berubi, 2006). Due to its abundance and ubiquity, it is a good candidate for an in-depth analysis, and was thus selected as the subject of this review. Exploring the role of endophytes and fungal pathogens in the success and decline of coniferous forests is an important step forward in understanding the ecological functions of the taiga biome.

L. piceae life cycle and ecology

The life cycle of *L. piceae* has been described by Osario and Stephan (1991) in 6 stages: (1) spruce needles are infected with ascospores, (2) the fungus lives as an endophyte in the green needle for several years, (3) conidiomata and conidia form but are not relevant for further infection of needles, (4) ascomata form on retained and fallen needles, (5) ascomata ripen and release spores infecting more needles, and (6) empty fruit bodies and needles decompose in the forest litter.

Since Osario and Stephan's 1991 publication, several modifications to its life cycle have been proposed (Suske & Acker, 1987). First, the initial phase in the life cycle of *L. piceae*, an ascomycete in the

family Rhytismataceae, is contiguous with that of all endophytes of woody plants. In contrast with those of graminoids, woody endophytes are horizontally transmitted from host to host (Carroll, 1998). Fungal spores are carried by the wind, and infection occurs when these spores are deposited in perforations in the bark of a tree, at which point the spore undergoes germination and extends hyphae into the tissue of the tree. While occurrences of this fungi have been reported in the twigs of spruce trees (Seiber 1989), this species primarily occupies the needles and has been reported in higher abundance in shaded needles than in needles with full sun exposure (Barklund, 1987).

After establishing residence in the needle, *L. piceae* can exist asymptomatically for many years. It is during his phase that the fungus adheres to the traditional definition of an endophyte ─ an organism which forms inapparent infections within the leaves and stems of healthy plants (Carroll, 1988). In the vast majority of endophyte studies conducted on spruce species such as *Picea abies, P. glauca,* and *P. engelmannii, Lophodermium piceae* is demonstrated to be the dominant endophytic species present in healthy, green needles, regardless of needle age.

L. piceae exists in this stage until environmental stressors weaken the tree, at which point the fungus begins its reproductive stage. Conidiomata (asexual fruiting structures) are formed within the needle, becoming visible as concolorous vesicles on the needle's surface. It is at this stage that infection by *L. piceae* appears to manifest as spruce needle cast, and while the formation of conidiomata does not lead to further infection of the needle, it is associated with needle discoloration as the foliage turns from green to brown. Currently, *L. piceae* infection is not known to affect a significant enough portion of an individual tree to result in mortality. Following the maturation of the conidiomata, ascomata begin to form, presenting as dark, blister-like spots on the browning needle. Internal pressure exerted by the developing conidia results in perforations on the surface of the ascomata ─ a trait that makes *L. piceae* distinguishable from other *Lophodermium* species. Ascomata may form on both needles that are still attached to the tree, and on those that have already fallen to the ground. As they mature, the ascomata open by a longitudinal slit and release the ascospores.

Although *Lophodermium piceae* has been proposed as a pioneer decomposer in needle litter following needle senescence, a study by Muller et al. 2001 revealed a lower ratio of *L. piceae* in needle litter as compared to other species relative to its presence in green, healthy needles, when it is almost always the dominant species. Little is known about the life stage of *L. piceae* following ascospore release; it is possible that it returns to a hyphael phase and plays a role as a minor decomposer, but it is also likely that the fungus sceneses following sexual reproduction and *L. piceae* DNA isolated from needle litter may be from dead cells.

L. piceae pathogenicity

Spruce needle cast disease, attributed to members of the *Lophodermium* genus, is described as causing damage in ≤ 2-year-old infected needles without affecting the overall health of the tree. Climatic conditions influence spore dispersal and germination, and therefore the frequency and severity of infection. Needle cast diseases are more common following wet

springs, and lower branches and understory trees are frequently the most seriously affected as infections favor more humid conditions.

Generally, two types of fruiting bodies develop during the life cycle of fungi responsible for needle cast: asexual fruiting bodies, which occur as small dots (conidiomata) on the upper surface of the needles; and sexual fruiting bodies (producing the ascospores that transmit the disease), which are typically larger and occur along the mid-ribs of the lower needle surface. Most *Lophodermium* pathogens are conifer-associated, suggesting that pathogenicity may have evolved from endophytic relationships.

Initial reports of *Lophodermium piceae* described the fungus as a contributor to forest decline syndrome (Schutt, 1984), along with several other *Lophodermium* species (Rehfuess & Rodenkirchen, 1984). To date, none of the species mentioned in the Rehfuess publication have been conclusively proven to be true pathogens; in nearly all cases, the exhibition of needle cast correlates with reduced abundance of *L. piceae* as well as declining health of the host tree due to external factors. This relationship supports the characterization of *L. piceae* as a latent saprophyte, which exists in a near-dormant phase throughout most of its life cycle before opportunistically advancing to its reproductive stage when its host is weakened.

Beyond the initial miscatagorization of *L. piceae* as an aggressive pathogen, there may also be a case of mistaken identity between *L. piceae* and other species within the *Lophodermium* genus, which may actually act as pathogens in conifers. In a study conducted by Ortiz-Garcia et al. (2003), the authors attested this discrepancy to the practice of using ascomata and ascospores for visual identification, which has been shown to be a poor method for positively determining species and genus compared to sequencing methodology. In the same paper, *L. piceae* was shown to be in a phylogenetically distinct clade from all other *Lophodermium species*, and the bootstrap values relating the two clades was low, alluding to a lack of contiguity among sequences in the *L. piceae* pool.

Physiology and ecology

Despite its status as the dominant endophyte species within many spruce species, *Lophodermium piceae* has not been the focal species of any studies on secondary metabolite production. *L. piceae* was, however, one of several endophyte species investigated for their ability to convert Picein to P-hydroxyacetophenone (pHAP) in a study by Osswald et al. 1994. In this study, the fungi were subjected to pHAP to investigate the compound as a growth inhibitor of fungal mycelia. For two of the four endophyte species investigated (*Sirococcus strobilinus and Pecicula livida)* , pHAP inhibited mycial growth to a substantial degree. For *L. piceae*, however, mycelial growth was only inhibited by 30% at the highest pHAP concentrations. In the same study, the ability of the fungi to convert Picein to pHAP was investigated as well. For the two species that exhibited impaired mycelial growth when subjected to pHAP, complete synthesis of pHAP from Picein was observed. For *L. piceae* and the other uneffected species, however, synthesis of pHAP was observed, but time curves revealed the further degradation of pHAP into additional unknown compounds.

P-hydroxyacetophenone is a phenolic compound that has been demonstrated to

significantly increase the mortality and decrease the growth rates of spruce budworm larvae (Delvas et al., 2011), a significant spruce pest. Phenolic compounds, an important class of plant and fungal secondary metabolites, have been shown to conditionally promote or inhibit the survivability of insect pests. This difference originates out of the redox conditions of the intestinal cavity of insect larvae; the phenolics may be oxidized, forming protein-binding quinones and tissue-damaging oxygen compounds (Felton et al, 1991), or they may remain unoxidized under low O2 concentrations, when they can act as beneficial antioxidants (Laranjinha et al., 1994; Johnson & Felton, 2001). It is hypothesized that through the accumulation of these secondary metabolites in the needles in their host trees, fungal endophytes can help to deter insect activity within the tree, thus increasing the survivability of individual trees and stands in times of herbivory-induced stress.

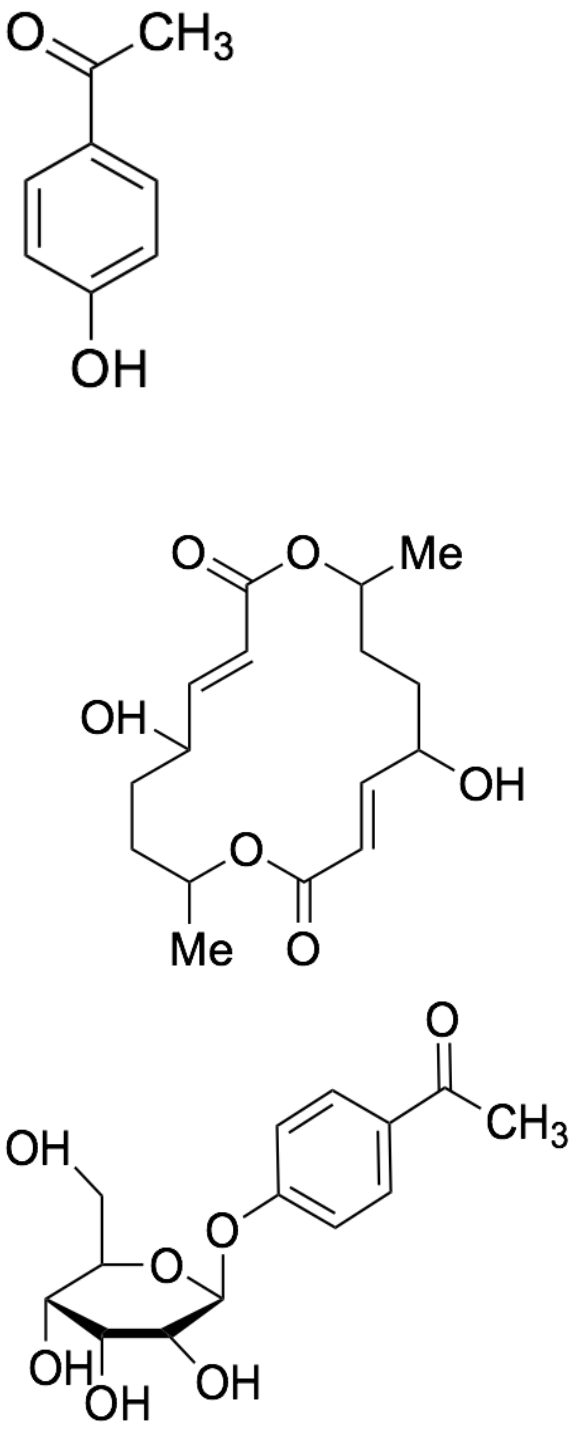

P-hydroxyacetophenone (left), a product of Picien (right) found in spruce needles (Osswald et al., 1994)

In addition, *L. piceae*, as well as many other species within the *Lophodermium* genus, have been shown to produce pyrenophorol (Sumarah et al., 2015), an antifungal and anthelmintic agent. Sumarah et al (2015) studied the sensitivity of *Cronartium ribicola*, the fungus responsible for white pine blister rust, to pyrenophorol and concluded that the compound did show toxinogenic effects, significantly reducing cell density in both *C. ribicola* and *Saccharomyces cerevisae*, a representative ascomycete species.

Pyrenophorol (C16H24O6), a fungicidal metabolite produced by L. piceae

Further work by Sumarah (2015) has demonstrated that the production of pyrenophorol by *Lophodermium* has likely contributed to its dominance in infected trees due to the antifungal properties of the secondary metabolite. This has the subsequent benefit of protecting host trees to *Lophodermium* from fungal pathogens, thus further increasing the tree's survivability under pathogenic stressors.

The production of pyrenophorol appears to be a trait shared by multiple members of the *Lophodermium* genus (Sumarah et al., 2011), including *L. nitens*, another dominant *Lophodermium* species isolated from spruce and pine trees.

Discussion

The story of *L. piceae* is complex and convoluted by protocol error. Inaccurate early assessments of tree disease, paired with outdated sampling methods using spore morphology, have painted a contradictory and highly variable picture of the species in terms of its ecological roles and individual physiology. After accounting for phylogenetic uncertainty, the difficulty in drawing accurate conclusions is further increased. Even with all this in account, there is a substantial amount of literature assessing the life stages of *L. piceae*, which serves a significant role in revealing the physiology and ecological contributions of the species at different stages. As an asymptomatic endophyte, the fungi appears to serve as a symbiont, contributing to its host tree's ability to resist insect pathogens such as spruce budworm, with low resource tradoff. When its host enters into a weakened state, however, the fungus is better categorized as as an opportunistic saprophyte, developing reproductive structures and appearing as spruce needle cast, the reason for its original categorization as a pathogen. Following reproduction, the fungus settles into its role as a decomposer, with bioactive properties lasting for years after needle desiccation. While in most spruce endophyte studies *L piceae* is revealed as a dominant species, it is unclear how directly the fungus influences the health of its host tree, and what would change in the case of its absence. It is possible that other endophyte species would simply fill the niche that was previously occupied by the more competitive species, but it is difficult to predict changes in host-symbiont physiology as a result. For more conclusive evidence, *in vitro* studies on inoculated and sterile trees subjected to various environmental and biological stressor may be beneficial in assessing how the species influences the resistance ability of its host. Studies focusing on the fungus's production of secondary metabolites would also be useful in elucidating the physiological pathways that affect the health of the fungus and its host, rather than depending on genus-wide trends to make predictions about its behaviour.

L. piceae, while fairly well-described in literature, offers a case study of the many issues with the field of mycology as a whole. Possibly the foremost issue is the inconsistency of early phylogenies, which are used to identify fungal species in later literature, leading to erroneous conclusions about the character of different taxa. The massive biodiversity of Fungi as a kingdom is also problematic in attempting to derive patterns in ecological and physiological functions. This, paired with the fact that fungi spend the majority of their life cycle invisible to the human eye, has resulted in low interest in these organisms from a historical perspective

In spite of all this, there has been a growing awareness in the last century of the critical roles fungi play in all of earth's ecosystems. It is imperative that we gain a strong understanding of the functions of major species in critical habitats and how anthropogenic factors influence them in order to assess how best to direct conservation strategies.

Recommendations for future work

Some of the primary issues with the literature on *L. piceae* to date are due to inconsistencies in species identification protocols. Particularly in older studies, visual morphotype identification using fungal spores was a common technique, one which is now well known to be inaccurate due to the tendency of fungi to change physical traits depending on their growth media and environmental conditions. In the studies that did use sequencing, often only one region (typically the internal transcribed spacer (ITS) region) was sequenced, yielding low taxonomic certainty at the species level. The large subunit (LSU) region is now accepted as the standard for species identification, and it is practical to use both the ITS and LSU regions for accurate identification and phylogeny construction. In future studies concerning the isolation of novel compound from fungi or other samples, it is pertinent to conduct proper DNA extraction and sequencing in order to ensure accuracy in the attributed source of the compounds.

Another area that came up in our review of literature concerning Picein and pHAP is the redundancy in the production of pHAP, as it is apparently derived from host-produced Picein by both the fungus and the tree itself (Mendez-Espinoza et al., 2018). While pHAP has been repeatedly shown to be an effective agent in herbivory reduction, the metabolite has also been identified as a phytotoxin by Hoque, 1985, causing needle yellowing, foliage loss, and inhibiting needle development in young trees. From the perspective of resource allocation, it would be interesting to test the efficiency of fungal vs. host metabolite synthesis in order to derive the basis for the formation of the plant-fungi symbiosis in regard to pHAP production. Another possible explanation for this, especially as it relates to *L. piceae*, is if the unknown compounds observed in the Osswald et. al. study serve functionally distinct roles compared to Picein and Piceol. Further studies on these secondary metabolites may yield a more complete understanding of the relationship between the tree and the fungus. *In vitro* studies on the molecular contents of spruce foliage without possible endophytic occupancy may also be beneficial in distinguishing between the molecular characteristics of the species and those of interacting species within the microbiome.

Experimentation on the effects of pyrenophorol on the mycelial growth of blue stain fungus (*Grosmannia clavigera*) may also be productive in assessing the ability of *L. piceae* to mitigate the impacts of the pathogen, which is responsible for massive forest decline in Pinus species throughout North America. Likewise, an investigation into the effects on pHAP on bark beetle larvae, including *Dendroctonus rufipennis* (spruce beetle) and *Dendroctonus ponderosae* (pine beetle), may be beneficial in contributing to our understanding of the factors that make a forest susceptible to bark beetle outbreaks. It may also be necessary to determine the presence of these metabolites in the tree outside its photosynthetic tissues, such as in its phloem, which is heavily impacted in a variety of herbivore activities.

Works Cited

Barklund, Pia. "Occurrence and Pathogenicity of Lophodermium Piceae Appearing as an Endophyte in Needles of Picea Abies." *Transactions of the British Mycological Society*, vol. 89, no. 3, 1987, pp. 307–313., doi:10.1016/s0007-1536(87)80111-0.

Butin, H. "Endophytische Pilze in Griinen Nadeln Der Fichte (Picea Abies Karst.)." *Zeitschrift Fur Mykologie*, vol. 52, 1986, pp. 335–345., www.dgfm-ev.de/publikationen/artikelarchiv/endophytische-pilze-in-gruenen-nadeln-der-fichte/download.

Carroll, George. "Fungal Endophytes in Stems and Leaves: From Latent Pathogen to Mutualistic Symbiont." *Ecology*, vol. 69, no. 1, 1988, pp. 2–9., doi:10.2307/1943154.

Darker, Grant Dooks. "The Hypodermataceae of Conifers /." 1932, doi:10.5962/bhl.title.152928.

Darker, Grant D. "A Revision Of The Genera Of The Hypodermataceae." *Canadian Journal of Botany*, vol. 45, no. 8, 1967, pp. 1399–1444., doi:10.1139/b67-145.

Delvas, Nathalie, et al. "Phenolic Compounds That Confer Resistance to Spruce Budworm." *Entomologia Experimentalis Et Applicata*, vol. 141, no. 1, 2011, pp. 35–44., doi:10.1111/j.1570-7458.2011.01161.x.

Esseen, Per-Anders, et al. "Boreal Forests—The Focal Habitats of Fennoscandia." *Ecological Principles of Nature Conservation*, 1992, pp. 252–325., doi:10.1007/978-1-4615-3524-9_7.

Felton, G.w., et al. "Impact of Oxidized Plant Phenolics on the Nutritional Quality of Dietar Protein to a Noctuid Herbivore, Spodoptera Exigua." *Journal of Insect Physiology*, vol. 38, no. 4, 1992, pp. 277–285., doi:10.1016/0022-1910(92)90128-z.

Hoque, E. "Norway Spruce Dieback: Occurrence, Isolation and Biological Activity of p-Hydroxy Acetophenone and p-Hydroxy Acetophenone-O-Glucoside and Their Possible Roles during Stress Phenomena." *Forest Pathology*, vol. 15, no. 3, 1985, pp. 129–145.,

doi:10.1111/j.1439-0329.1985.tb00877.x.

Johnson, Kelly, and Gary Felton. “Plant Phenolics as Dietary Antioxidants for Herbivorous Insects: A Test with Genetically Modified Tobacco.” *Journal of Chemical Ecology* , vol. 27, no. 12, Dec. 2001, pp. 2579–2597., doi:https://doi.org/10.1023/A:1013691802028.

Laranjinha, João A.n., et al. “Reactivity of Dietary Phenolic Acids with Peroxyl Radicals: Antioxidant Activity upon Low Density Lipoprotein Peroxidation.” *Biochemical Pharmacology*, vol. 48, no. 3, 1994, pp. 487–494., doi:10.1016/0006-2952(94)90278-x.

Liedeker, H., et al. “Symptoms of Forest Decline (Waldsterben) on Norway and Red Spruce.” *Forest Pathology*, vol. 18, no. 1, 1988, pp. 13–25., doi:10.1111/j.1439-0329.1988.tb00749.x.

Livsey, Susan, and Pia Barklund. “Lophodermium Piceae and Rhizosphaera Kalkhoffii in Fallen Needles of Norway Spruce (Picea Abies).” *Forest Pathology*, vol. 22, no. 4, 1992, pp. 204–216., doi:10.1111/j.1439-0329.1992.tb00785.x.

Livsey, Susan, and Pia Barklund. “Lophodermium Piceae and Rhizosphaera Kalkhoffii in Fallen Needles of Norway Spruce (Picea Abies).” *Forest Pathology*, vol. 22, no. 4, 1992, pp. 204–216., doi:10.1111/j.1439-0329.1992.tb00785.x.

Mcmullin, David R., et al. “Antifungal Sesquiterpenoids and Macrolides from an Endophytic Lophodermium Species of Pinus Strobus.” *Phytochemistry Letters*, vol. 14, 2015, pp. 148–152., doi:10.1016/j.phytol.2015.10.006.

Méndez-Espinoza, Claudia, et al. “Genetic Control and Evolutionary Potential of a Constitutive Resistance Mechanism against the Spruce Budworm (Choristoneura Fumiferana) in White Spruce (Picea Glauca).” *Heredity*, vol. 121, no. 2, 2018, pp. 142–154., doi:10.1038/s41437-018-0061-6.

Müller, M. M., et al. “Genetic Diversity of Lophodermium Piceae in South Finland.” *Forest Pathology*, vol. 37, no. 5, 2007, pp. 329–337., doi:10.1111/j.1439-0329.2007.00504.x.

Müller, Michael M., et al. “Diversity of Endophytic Fungi of Single Norway Spruce Needles and Their Role as Pioneer Decomposers.” *Molecular Ecology*, vol. 10, no. 7, 2001, pp. 1801–1810., doi:10.1046/j.1365-294x.2001.01304.x.

Müller, Michael M., et al. “Diversity of Endophytic Fungi of Single Norway Spruce Needles and Their Role as Pioneer Decomposers.” *Molecular Ecology*, vol. 10, no. 7, 2001, pp. 1801–1810., doi:10.1046/j.1365-294x.2001.01304.x.

Ortiz-García, Sol, et al. “Phylogenetics of Lophodermium from Pine.” *Mycologia*, vol. 95, no. 5, 2003, pp. 846–859., doi:10.1080/15572536.2004.11833044.

Ortiz-García, Sol, et al. “Phylogenetics of Lophodermium from Pine.” *Mycologia*, vol. 95, no. 5, 2003, pp. 846–859., doi:10.1080/15572536.2004.11833044.

Osorio, M., and B. R. Stephan. “Life Cycle of Lophodermium Piceae in Norway Spruce Needles.” *Forest Pathology*, vol. 21, no. 3, 1991, pp. 152–163., doi:10.1111/j.1439-0329.1991.tb01419.x.

Osswald, W.f., et al. “The Occurrence Of Picein And P-Hydroxyacetophenone In Spruce Needles And The Effect Of The Monophenol On The Growth Of Different Forest Pathogens.” *Acta Horticulturae*, no. 381, 1994, pp. 548–556., doi:10.17660/actahortic.1994.381.73.

Rehfuess, K. E., and H. Rodenkirchen. “Über Die Nadelröte-Erkrankung Der Fichte (Picea Abies Karst.) in Süddeutschland.” *Forstwissenschaftliches Centralblatt*, vol. 103, no. 1, 1984, pp. 248–262., doi:10.1007/bf02744236.

Sieber, Thomas N. “Endophytic Fungi in Twigs of Healthy and Diseased Norway Spruce and White Fir.” *Mycological Research*, vol. 92, no. 3, 1989, pp. 322–326., doi:10.1016/s0953-7562(89)80073-5.

Sokolski, Serge, et al. “Black Spruce (Picea Mariana) Foliage Hosts Numerous and Potentially Endemic Fungal Endophytes.” *Canadian Journal of Forest Research*, vol. 37, no. 9, 2007, pp. 1737–1747., doi:10.1139/x07-037.

Stefani, F.o.p., and J.a. Bérubé. “Biodiversity of Foliar Fungal Endophytes in White Spruce (Picea Glauca) from Southern Québec.” *Canadian Journal of Botany*, vol. 84, no. 5, 2006, pp. 777–790., doi:10.1139/b06-022.

Sumarah, Mark W., et al. “Screening of Fungal Endophytes Isolated from Eastern White Pine Needles.” *The Formation, Structure and Activity of Phytochemicals*, 2015, pp. 195–206., doi:10.1007/978-3-319-20397-3_8.

Suske, Jurgen, and Georg Acker. “Internal Hyphae in Young, Symptomless Needles of Picea Abies: Electron Microscopic and Cultural Investigation.” *Canadian Journal of Botany*, vol. 65, no. 10, 1987, pp. 2098–2103., doi:https://doi.org/10.1139/b87-288.

Syrjanen, Kimmo, and Risto Kalliola. “Landscape Structure and Forest Dynamics in Subcontinental Russian European Taiga.” *Ann. Zool. Finnici* , vol. 31, 31 Jan. 1994, pp. 19–34.

Orbital Debris Redirection and Thermal Reentry D.O.T.T.S. (Debris Orbital Tumbler and Thermal Sensor)

Stacie Barbarick[3], Bruce Bell[2], Cassidy Bliss[1,3], James Cook[3], Jack Dryden[3], Ethan Ford[1], Ruby Martinez Gomez[2], Joseph Harrell[2], Rhiannon Larsen[3], Ian McComas[3], Dallas McKeough[3], Henry Reyes[2], Nick Vail[1,3], Ryan Wade[2], Audrey Whitesell[1,3]

Advisors

Victor Andersen[2], Jennifer Jones[1], Barbra Sobhani[3]

Arapahoe Community College[1], Community College of Aurora[2], and Red Rocks Community College[3]

09/30/2019

Abstract

Our mission is to develop a concept toward a cost-effective method for de-orbiting space debris that is too small to be tracked from Earth. Our secondary experiment's mission is to find more cost-effective materials for future experiments/projects in space that can sustain the effects of re-entry into Earth's atmosphere.

1.0 Mission Statement

We have designed a sounding rocket payload which contains two experiments. 1) Implementation and use of a static electric field to meaningfully impact the trajectory of a simulated space fragments. 2) Testing and documentation of key characteristic material properties on the effects of thermal reentry on multiple 3D printed structures of various filaments.

The 2017-18 Colorado Community Colleges RockSAT-X project demonstrated the influence of an electrostatic field on charged debris particles in microgravity. We will expand on this concept, with our primary experiment. The primary experiment will use an apparatus covered in rabbit fur attached to a mounted worm-drive motor to impart static charge on an adjacent polycarbonate plate. Using a linear sequence of specific timer events, four servos mounted within an ABS printed launcher will then propel a series of four small (6mm, 26 g) aluminum balls across the charged sheet at a muzzle velocity of less than one-inch per second. The first trial servo will launch the debris with no charge induced on the plate to serve as a control. A camera augmented with image processing code, mounted to the launcher and the payload

deck will record changes to particle trajectory with video over-plotting onto a grid system. Limited data will be sent back via telemetry to confirm functionality and all image capture data will be stored on a secure digital (SD) card for analysis after payload retrieval. This will provide a proof of concept for a space cleanup method where the orbital velocity of space debris could be reduced, resulting in a decaying orbit where debris burns up in the atmosphere before reaching earth.

The use of additive manufacturing in aerospace applications is revolutionizing the industry and there is limited data on the thermal effects of reentry on additive manufactured materials, it is the focus of our secondary experiment [8]. Distinct filament structures, composed of either acrylonitrile butadiene styrene (ABS) or polyethylene terephthalate with a glycol modification (PETG) will be printed, measured and affixed to mounts installed on the payload deck. The vertical orientation of this deck allows for full exposure of all printed materials. Each design has a centered cavity containing resistance temperature detector (RTD) probes to measure internal temperature. The base of each shape has an interlocking design and screw holes to accommodate hardware attachment to the payload. Temperature data prior to launch will be collected as an internal baseline and temperature probes will continue to collect data through launch until splash down. Temperature data will be sent via telemetry to verify functionality and all temperature data will be stored on an SD card. Upon retrieval of the deck, printed structures will be analyzed qualitatively and compared to pre-launch, any deformation and change in shear strength will be analyzed and reported.

2.0 Mission Requirements and Description

According to the requirements established by the team, RockSAT, and Wallops, the following is a description of the general guidelines that were obeyed. Firstly, the mission parameters for the primary experiment were; can any significant change in the trajectory of non-ferrous materials passing through the field be observed using the tribo-electric effect. To do this, a charge generation needed to be established to create the static-electric field. A non-ferrous material would need to be used for the testing subject. The material would need to be a consistent and simple shape to evaluate. A launching mechanism would need to be designed to consistently launch the material at the same velocity and in the same trajectory. Wallops Flight Facility (WFF) also required that any deployable object have a max velocity of one-inch per second. A measurement system would need to be applied to track the progress of the material as it moves through the field. WFF requested that telemetry be used for the payload in the case that the rocket was not recoverable. As a convenience requirement, remove before flight software inhibitors were installed so that the material would not be ejected during testing procedures.

Secondly, the mission parameters for the secondary experiments were to receive qualitative and quantitative data on how well additive manufacturing materials (AMM) would survive

reentry and how viable these materials would be as an inexpensive resource to use for payloads such as these. In order to accomplish this, the following parameters were set. Two different high temperature and widely available materials would be tested and chosen. The tests would consist of heating the materials in a forge, placing them in a vacuum, and simulate flash cooling by moving the forged materials quickly into an ice bath. Two simple shapes would be chosen for simple evaluation of the material. Accurate temperature data would need to be taken consistently throughout flight both inside the materials and outside as a control.

Thirdly, the payload has specified design and power requirements before being integrated into the rocket. The payload's center of mass would need to be within one-inch of the measured center of the plate deck. A height limit of 5 inches and weight limit of 15.0 +/- 0.5 lbs including the plate deck, and any other provided components such as the power and telemetry harnesses. In order to make sure there was no difficulty fitting into the skirt or messing with the stacking of the plates in the rocket a framed keep out zone on the edge of the plate was given as well. For power, the payload was given a limit of 28 Volts and 1 Amp Hour unless otherwise requested. The telemetry that was requested (Asynchronous, using RS232 protocols) was also limited to 19,200 bps baud rate. Any chemicals or biological materials would need to be approved by WFF before being allowed for flight.

Lastly, due to the nature of the experiment, an establishment of the effects of static electricity would need to be thoroughly explored and documented in order to understand or expect any desired or undesired results of the experiment. To do this the general concept of attraction for non-ferrous materials to a static charge, as well as if this property is maintained in a vacuum environment.

3.0 Payload Design

The Community Colleges of Colorado payload designed to fly on the August 2019 RockSAT-X sounding rocket from Wallops Launch Facility, functions as a platform to begin the research in sub-orbital debris cleanup technologies which utilize electrostatic charges to interfere with small non-ferromagnetic materials in a vacuum, as well as the thermal capabilities of different 3D printed plastics during reentry into the atmosphere. These objectives are separated into two main experiments: primary and secondary experiment.

3.1 Full Assembly

The plate layout consists of five main regions, these are depicted in figures 5.1.1 through 5.1.4.

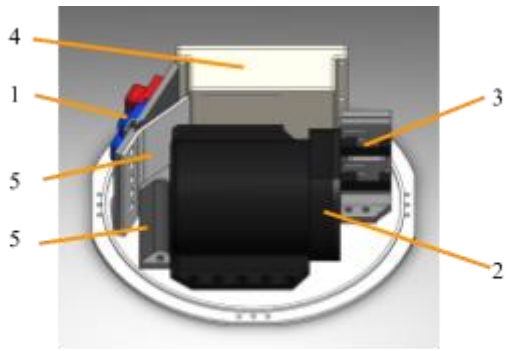

Figure 5.1.2 Front view of payload

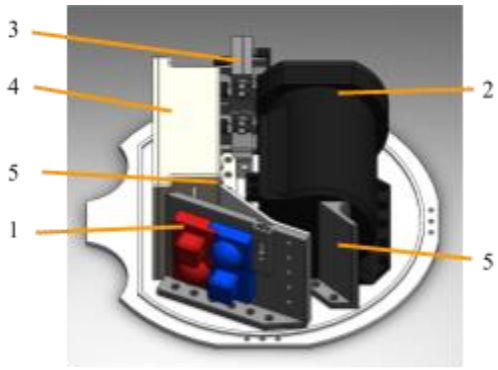

Figure 5.1.1 Right view of payload

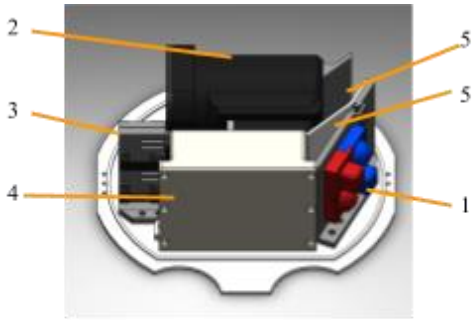

Figure 5.1.3 Back view of payload

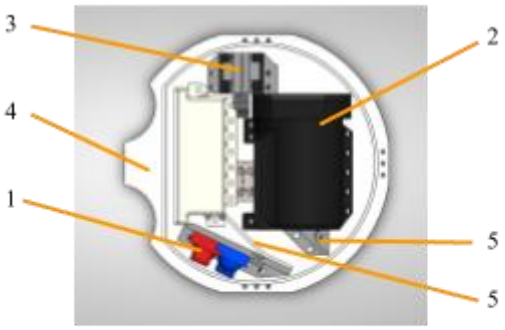

Figure 5.1.3 Top view of payload

Region 1 contains the secondary experiment; 3D printed structures, temperature probes, and surface mounts. Cubic and hemispherical structures will be printed in ABS and PETG to compare properties.

Region 2 is the earth atmospheric chamber (EAC) which houses the charging apparatus and polycarbonate charged plate. This chamber is to ensure static generation and is constructed primarily with 3D printed ABS. The lid is sealed with a rubber gasket and RTV silicone sealant.

Region 3 is the launcher tower made of ABS which houses the servos to launch the aluminum particles. This is also where one of two cameras will be mounted.

Region 4 is the location of the sealed electronics box, which will house the printed circuit boards (PCB), microprocessors, and SD cards. The box is constructed of 3D printed ABS. The lid is sealed with a gasket and RTV silicone sealant. The wires connected to the sides of the box and were sealed with RTV silicone sealant to waterproof.

Regions 5 are the deflector plates A and B, both made of ABS, to deflect particles launched and prevent them from continuing to register by the cameras.

3.2 Primary Experiment

The design for the primary experiment is broken down into three major components. The first being the electrostatic generator with a charge plate that produces an electrostatic field which is emitted from a flat plate (Figure 1).

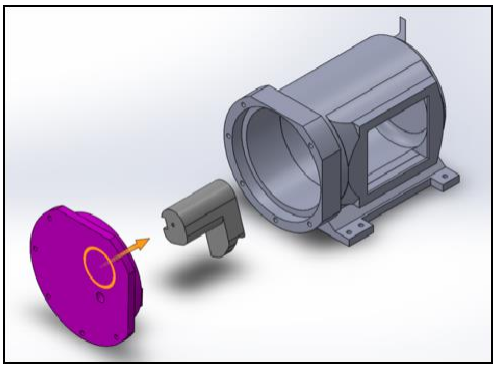

Figure 1: Exploded View of the EAC

The second component is the launcher which ejects the simulated debris samples at a rate of one-inch per second, with a straight trajectory parallel to the electrostatically charged flat plate (Figure 2). The launcher tower houses the test particles and the servos that will launch the debris. The servos will be held in place with a 3D printed plate that is screwed into the tower itself. Figure 3 shows an exploded front view of the launcher tower to highlight the plates.

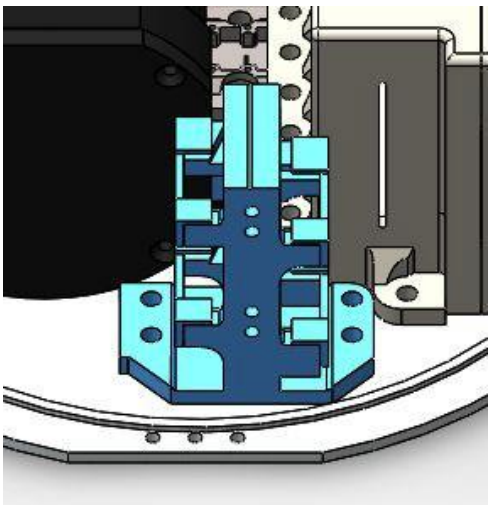

Figure 2: Assembled Launcher

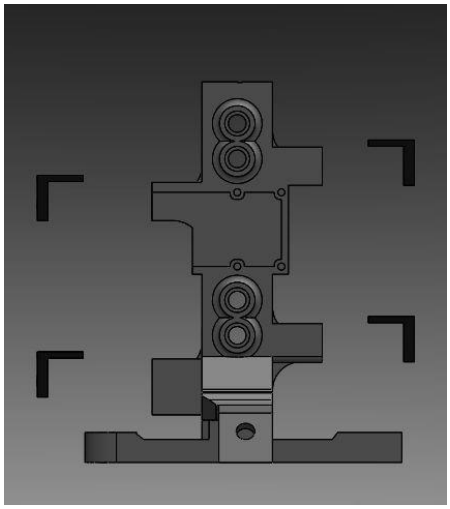

Figure 3: Exploded Front View of Launcher

The third component to support the primary experiment is the data collection method. The experiment's focus is to observe the trajectory of the debris samples as they enter the electrostatic field, this data must be stored and transmitted for post-flight analysis. This data collection is conducted through the utilization of two cameras whose field of view run perpendicular to each other, covering the are that the samples will travel (Figure 4).

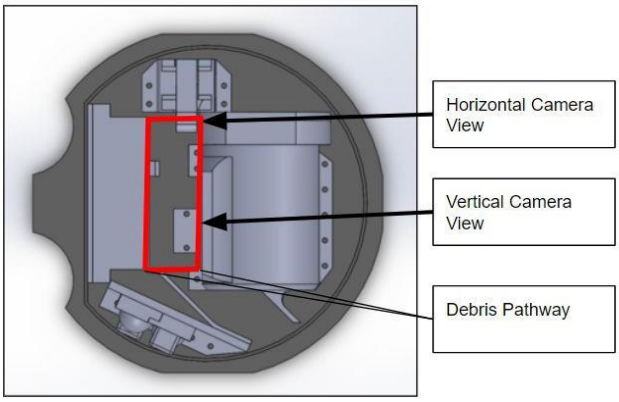

Figure 4: Top View of Payload

The primary experiment is designed to run three test trials, in addition to a fourth control trial. In figure 5, these four launches are illustrated in conjunction with the other operations in sequence. To ensure the best execution of the control data, it will be conducted first prior to any static charge generation on our payload.

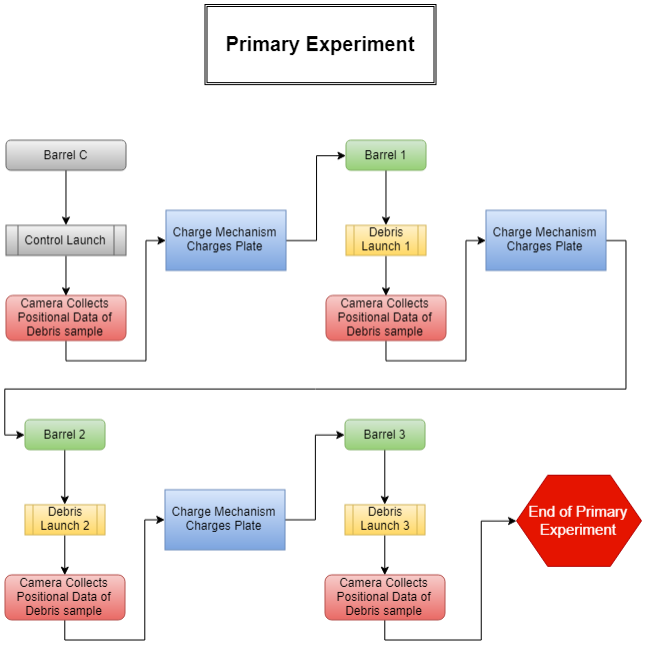

Figure 5: Primary Experiment System Block Diagram

3.3 Secondary Experiment

The secondary experiment is composed of three main components (Figure 6). 1) The deflector plate. 2) The secondary mount wall. 3) The 4 test subjects.

The deflector plate mounts to the secondary mount wall and ensures that the BBs ejected from the primary experiment is cleared from the cameras view point.

The secondary wall mount is mounted directly to the payload deck and holds the control probe as well as the 4 test subjects. The control probe is exposed to the external environments to compare external temperatures to the internal temperatures inside the shapes.

The final component of the secondary experiment is the test subjects. There are two shapes and two filaments. One cubical shape and one half sphere shape.
There are two of each shape, one printed in PETG and one in ABS. The shapes have a wall thickness of 5 millimeters, and each contain a temperature probe on the inside to measure how heat resistive the printed material and shape is. In order to prevent the shapes from melting off of the payload, the base of each shape was covered with an external fiberglass sheet (Figure 7). This ensured that the measured internal temperatures would be just from the exposed subjects and that upon splash down we could measure qualitative data.

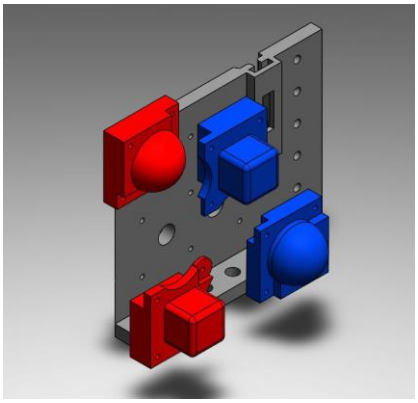

Figure 6.1: Exploded ISO View of Secondary Secondary

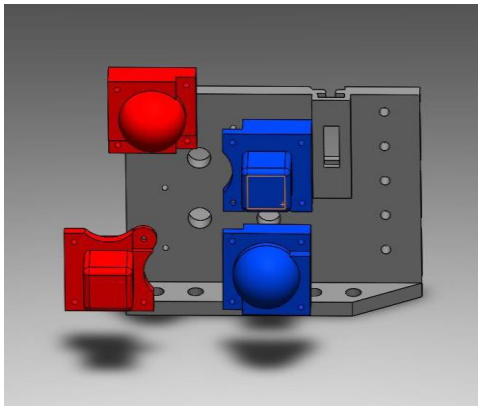

Figure 6.2: Exploded Angle View of

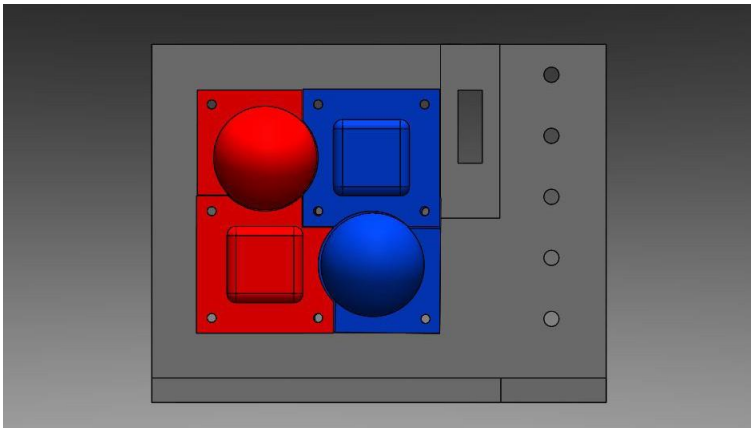

Figure 6.3: Assembled Front View of Secondary

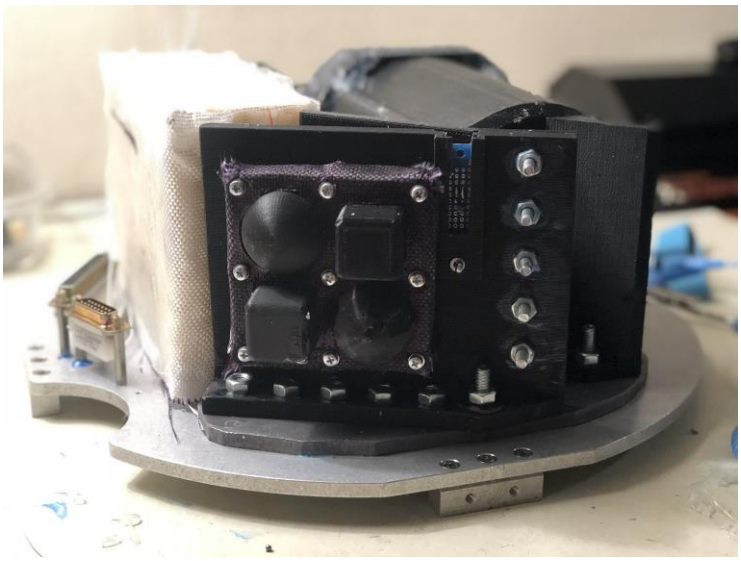

Figure 7: Assembled Flight Version of Secondary

4.0 Student Involvement

Sub-Team: Management

Ruby Martinez, Project Manager

Ruby is now studying Aerospace Engineering at the University of Colorado - Boulder. Ruby served as lead for management and made sure that the progress of the payload was continued as well as ensuring all documentation was completed.

Stacie Barbarick, Assistant Project Manager

Stacie is now studying Materials Engineering at Minnesota State University - Mankato in a new cooperative and integrated program through Iron Range Engineering. She was involved in multiple aspects of the project. This ranged from management, to developing new concepts to the project, and being highly involved with design and mechanical components.

Sub-Team: Mechanical Design and Manufacturing

Bruce Bell, CCA - Mechanical Design Engineer

Bruce is now studying at Metropolitan State University of Denver to obtain a Bachelor's degree in Mechanical Engineering and will then pursue a graduate degree at the University of Colorado Boulder. Bruce heavily supported the mechanical design team for both the primary and secondary experiment. Bruce was responsible for assembly, manufacturing testing, and 3D CAD.

Cassidy Bliss, ACC - Mechanical Design Engineer

Cass is studying at Red Rocks Community College transferring to CU Boulder to pursue a degree in Engineering Physics. She was a vital engineer within the primary experiment mechanical design team, as she was responsible for designing and

testing multiple solutions for the payload. Cass also assisted in other sub-team objectives to help push this rapidly developing project along.

Dallas McKeough, RRCC - Mechanical Design Engineer

Dallas is studying to transfer from RRCC to Metropolitan State University to study Mechanical Engineering and hoping to pursue a graduate degree in space resources at Colorado School of Mines. During the project, Dallas was responsible for the organization and cohesiveness of the overall design for the payload, as well as the 3D CAD used for presentation, analysis, and construction of the payload.

Henry Reyes, CCA - Mechanical Design Engineer

Henry is studying at Community College of Aurora to transfer to University of Colorado at Boulder to study engineering physics. He assumed the secondary experiment and oversaw testing operations at CCA.

Nick Vail, ACC - Mechanical Design Engineer

Nick is studying at Red Rocks Community College to transfer to University of Colorado at Boulder studying astrophysics. Nick supported both primary and secondary designs and ensured the scientific quality was optimal.

Sub-Team: Electrical Design

Rhiannon Larson, RRCC - Electrical Design Engineer

Rhiannon will complete her Associates of Science with transfer designation in Physics from RRCC in Fall 2019 and transfer to Colorado School of Mines in Spring 2020. She worked on soldering and harnesses.

Ryan Wade, CCA - Electrical Design Engineer Lead

Ryan is studying at CCA to transfer to University of Colorado at Boulder to study electrical engineering. Ryan was heavily responsible for the design and manufacturing of the specialized PCBs accompanied with the multitude of other electrical components.

Audrey Whitesell, ACC - Electrical Design Engineer

Audrey is studying Physics at RRCC and is planning to transfer to the Colorado School of Mines to study Mechanical Engineering. She was part of our electrical team and contributed to the testing and integration of the project. She also helped with the mechanical team.

Sub-Team: Software Design

James Cook, RRCC - Software Design Engineer

James is studying Aerospace Engineering and will be transferring to the University of Colorado - Boulder in the Spring 2020. He was on the software team and was part of writing the code for data transfer and communication between the Raspberry Pis and Arduino micro controllers.

Joseph Harrel, CCA - Software Design Engineer

Joseph is studying Aerospace Engineering at the University of Colorado - Boulder. Joseph was the essential for software production for the secondary experiment and conducted multiple tests.

Ethan Ford, ACC - Software Design Engineer

Ethan is studying Computer Science and is still unsure of where he will be transferring. He contributed to the software team and became a resource for things that need to be completed.

Ian McComas, RRCC - Software Design Lead

Ian is now studying Aerospace Engineering and Applied Mathematics at the University of Colorado - Boulder. Ian lead code production and testing throughout the project.

5.0 Testing Results

5.1.1 Mechanical Design: Primary Experiment

Once the debris launcher was chosen as the testing methodology for static repulsion, several mechanical design factors had to be accounted for. The NASA Wallops Flight Facility requires any projectile shot from the sounding rocket to be at a velocity of less than one-inch/sec. To achieve this goal, the team was required to design and implement a mechanical gate, testing apparatus, and procedure.

After several iterations of design, a simple spoke mechanism was found to be the most effective and energetically inexpensive way to hold the debris in place until testing and to launch the debris with a controlled speed (Figure 8).

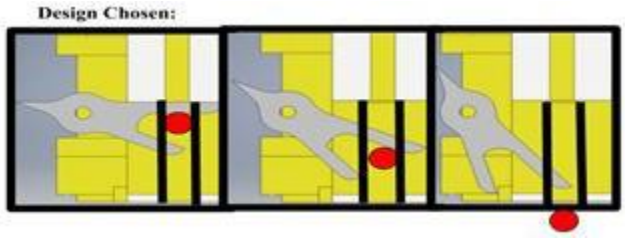

Figure 8: Mechanical launcher spoke design

The spoke was mounted to a servo which was programmed with a simple Arduino delayed step servo code. Measurements were initially taken with slow motion video and a meter stick along a track. Delays in the return of the servo arm were increased systematically the data collected is graphed below. A strong correlation between increased servo step delay and decreased velocity of the debris was observed (Figure 9).

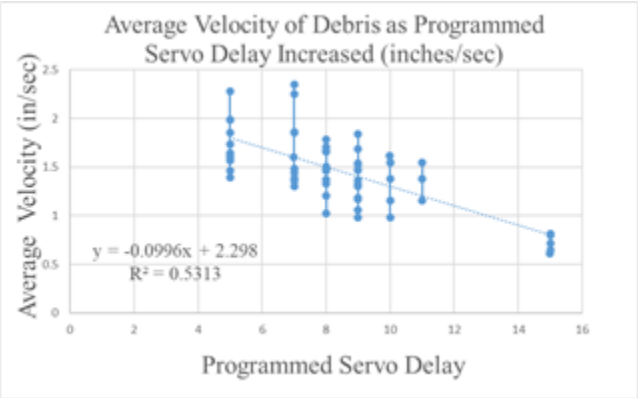

Figure 9: Testing Velocity of Debris

To increase trial speed and accuracy, a photogate was constructed with SparkFun photo resistors and a 3D printed launch tube with apertures for LEDs and sensors. To calibrate the ideal setting for photogate sensitivity, 30 trials at each of the sensitivity settings were conducted and graphed (Figure 10). We assumed the setting with the smallest average deviation within a data set was the most accurate and selected 910 as the setting to move forward with .

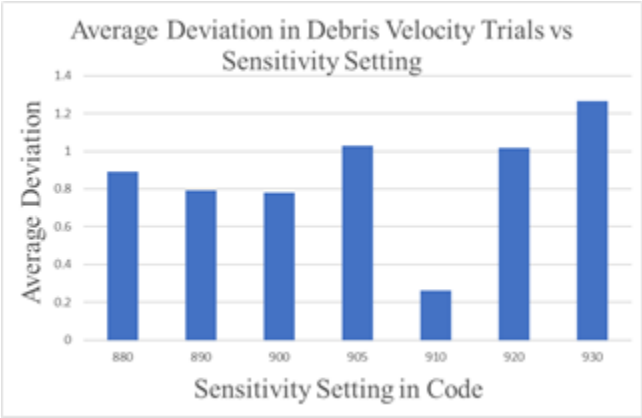

Figure 10: Testing Servo Sensitivity

To reduce variables in the calibration, we removed the servo and positioned the tube at a 20° incline. We then took 30 data points per sensitivity setting and graphed average deviation within each data set, in addition to the percent error found from calculating the ideal velocity we could expect with our parameters (Figure 11).

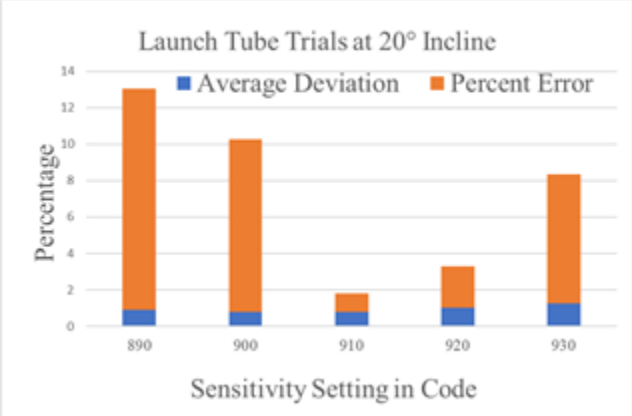

Figure 11: Decreasing Percent Error of Debris Speed

Again, we found the coded sensitivity setting at 910 to produce the lowest average deviation in addition to the lowest percent error. This allows us to use the settings of our test apparatus with confidence.

We determined the speed of the delay of the servo using our first plotted graph. Since we are required to have any deployments be one-inch per second or less, we used the delay setting of 15 milli-Seconds which gave us 100% of values well below the prescribed limit (Figure 12).

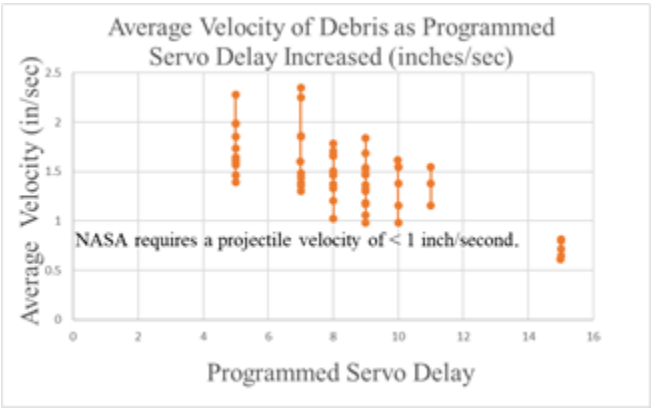

Figure 12: Average Deviation within trial sets vs sensitivity settings

As a result of testing regarding the charge imparted on the polycarbonate plate, we acquired instrumentation that measures electrostatic charge and will immediately begin testing charge generation, duration of charge, and radius of maximum influence on our debris particles.

Shake testing showed no visible fractures or defects; however, charging apparatus appeared to move during vibration and was moved further away from plate in order to prevent premature static charging during launch.

5.1.2 Mechanical Design: Secondary Experiment

The limited data on thermal effects of reentry on affordable 3D printed materials allowed for more design freedom in the secondary experiment. Our goal is to test and record the effects of thermal build up on the rocket and its payloads during reentry in order to determine the viability of common 3D printed materials in future space flights. To this end, we compiled a list of potential filaments types and began elimination based on inherent material properties, limitations to equipment, and testing results.

We printed a variety of prototypes with varied parameters, such as wall thickness, material usage, and theoretical deterioration of melted filament and subjected them to high heat in a lab-built forge (Figure 13).

Figure 13: Lab Created Forge for Thermal Testing

Filament selections were based on access and availability with the intent to reduce research and development costs. Our initial tests included ABS and HIPS printed structures, exposed to heat in the forge for two minutes.

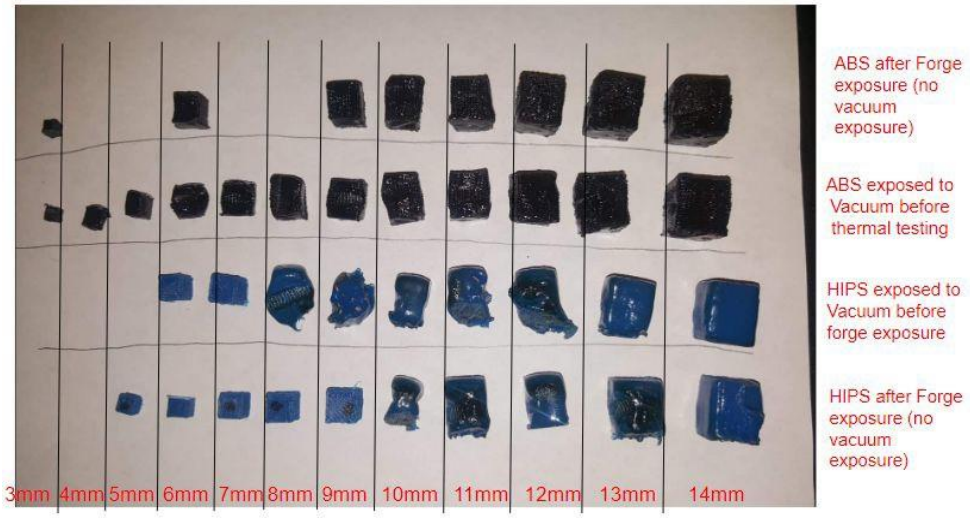

Figure 14: Qualitative data for ABS and HIPS materials exposed for two minutes.

The results of this testing seen in Figure 14, are as follows:

HIPS

Qualitative Results: The 13mm cube withheld its shape the best but high temperatures clearly penetrated through the cube. A different high temperature filament will be used for flight.

Quantitative Results: The 14mm cube lost the least amount of mass (0.027g) compared to the average (0.054g).

ABS

Qualitative Results: The ABS material held its shape both inside and out, suggesting less internal penetration.

Quantitative Results: Compared to HIPS, the ABS material lost less mass when exposed to the forge. The 14mm cube lost 0.004g compared to the average (0.0105g).

Variations that performed the best were then tested both in and out of a vacuum chamber. This was done to ensure the filaments used were porous enough to avoid explosion under extreme variations in atmospheric pressure. In order to replicate flight, the filaments were then exposed to the forge. Results are shown in Table 1 and Table 2.

AFTER-VACUUM												
Trial 1 (BLUE) HIPS												
Wall Thickness (mm)	Weight Before(g) (+- 0.001g)	Weight After(g) (+- 0.001g)	Temp. When Weighed (Degrees F)	Change in Weight	Time	Stone Stand Temp. Degrees (F)	Stone Stand Temp. Degrees (C)	Inside Temp. (F)	Inside Temp. End of Trail (F)	Object Temp. (40 sec before take out) (F)	Object Temp. End (10 sec before take out) (F)	Qualitative / Comments
9	1.426	1.41	74.1	0.016	1 min 10 sec	874	467.777 7778	624	590	788.5	798.3	Very gooey. If squeezed easily deformation...
10	1.825	1.787	75.2	0.038	1 min 10 sec	890.8	477.111 1111	628		819.1	826.3	Seems like the heat made it through
11	-			-	1 min 10 sec		0					
12	2.331	2.221	74.8	0.11	1 min 10 sec	943.9	506.611 1111	620	645	999	HI	Very Gooey while Taking out despite maintaining structure
13	2.874	2.845	74.8	0.029	1 min 10 sec	996.1	535.611 1111	618	610	820.9	887.4	
14	3.556	3.529	75	0.027	1 min 10 sec	979.5	526.388 8889	608	600	929.1	919	

Table 1: Trial data for HIPS after exposure to a vacuum chamber

AFTER-VACUUM													
Trial 1 [GRAY] ABS													
Wall Thickness (mm)	Weight Before(g) (+- 0.001g)	Weight After(g) (+- 0.001g)	Temp. When Weighed (Degrees F)	Change in Weight	Time	Stone Stand Temperature Degrees (F)	Stone Stand Temperature Degrees (C)	Inside Temp. (F)	Inside Temp. End of Trail (F)	Object Temp. (40 sec before take out) (F)	Object Temp. End (10 sec before take out)(F)		Comments
9	1.079	1.071	77.7	0.008	1 min 10 sec	817.3	436.3	611		758.5	732.9		Losing stiffness, easier to...
10	1.46	1.45	77.2	0.01	1 min 10 sec	835.3	446.3	617	590	763.5	789.8		Still has some stiffness not deformed at all...
11	1.847	1.84	77.7	0.007	1 min 10 sec	817.9	436.6	603	605	760.6	758.5		A little bit gooey but still maintained structure
12	2.381	2.378	77.9	0.003	1 min 10 sec	828.7	442.6	609	598	821.8	772.3		No real damage
13	3.007	2.976	77.9	0.031	1 min 10 sec	844.9	451.6	612	600	852.1	847.8		A little bit gooey however no real damage
14	3.641	3.637	78.6	0.004	1 min 10 sec	852.4	455.8	621	600	750	695		

Table 2: Trial data for ABS after exposure to a vacuum chamber

One concern we had was mounting 3D printed structures to the payload. The high (above 600°F) temperatures anticipated upon reentry, could cause 3D printed structures to dislodge. Since fiberglass is highly heat-resistant, we decided to use it to create a base cover that will allow exposure of the structure but with added protection to the base. This protective layer will help eliminate inaccurate data and ensure the experiment survives reentry.

The fiberglass cover was constructed out of molded, 5in x 5 in lightweight fiberglass solid mat. We tested the fiberglass cover by inserting it into the forge, forming a barrier between the torch and the RTD-100 temperature probes. The temperature probes printed numerical temperature data to the computer and the induced heat was read with a temperature gun. A temperature reading was taken every 30 seconds up to 3 minutes, to approximate anticipated reentry time. The results of this testing is summarized in figure 15.

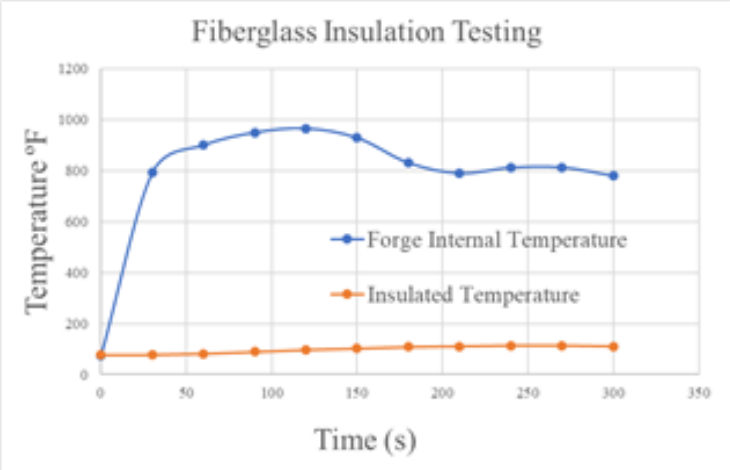

Figure 15: Testing fiberglass Insulative Properties

5.2 Electrical Design

The electrical design team was tasked with meeting the power needs of each experiment as it developed, while maintaining a strict power budget for the team to adhere to. We made decisions to accommodate the payload's restricted size and extreme environmental conditions, while adapting to design changes as the project progressed. We wanted to optimize payload deck space and make connection points accessible and reliable. We eliminated the use of multiple bulky buck converters and sizeable components with unnecessary utilities, by minimizing step down points and incorporating I2C components directly into our PCB design. Solid-state relays replaced mechanical relays for actuator activation, ensuring voltage reduction and reliability. All harness points and pin connection points were equipped with crimp pin sockets as opposed to solder joints, making boards and harnesses easier to access and change out during troubleshooting. A solid-state relay system was designed to switch the secondary experiment's power from the Wallop's timer event line to a self-contained LiPo battery, powering the thermal sensors for secondary experiment during descent. Detailed schematics were created using customized CAD libraries and 2D trace components which were edited to include specific order number details written into their code descriptions. An ever-evolving functional block diagram was referenced to assist the rest of the team as the payload was readied for subsystem integration (Figure 16).

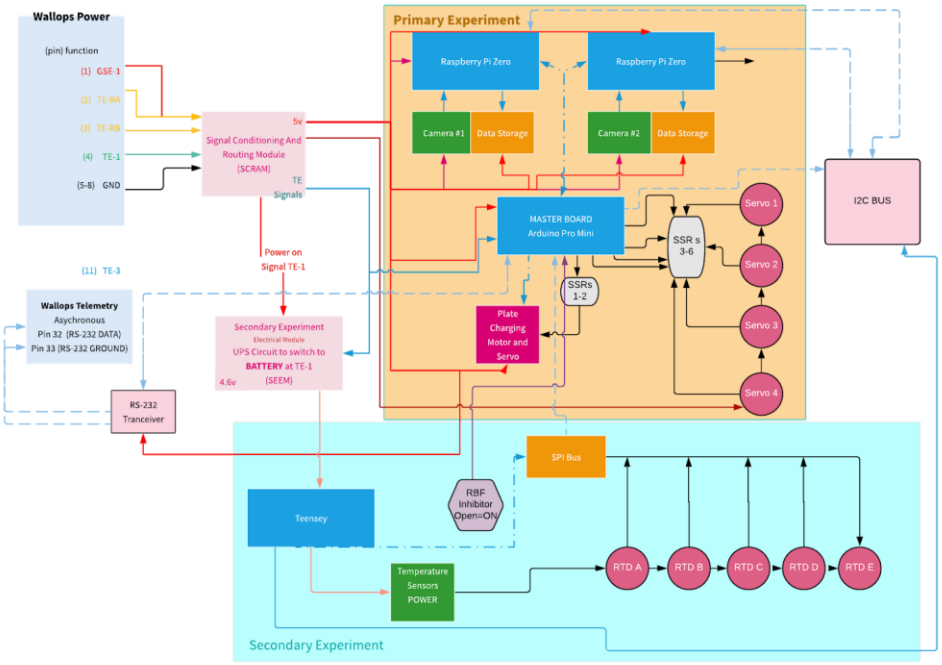

Figure 16: Electrical Functional Block Diagram

5.2.1 Electrical Design: Primary Experiment

The main electrical considerations for the primary experiment were pin availability and power budget. This experiment requires five servos and a motor which runs in sequence. Since each component requires several pins for power, data, and grounds, we decided to design and print customized printed circuit boards (Figure 17).

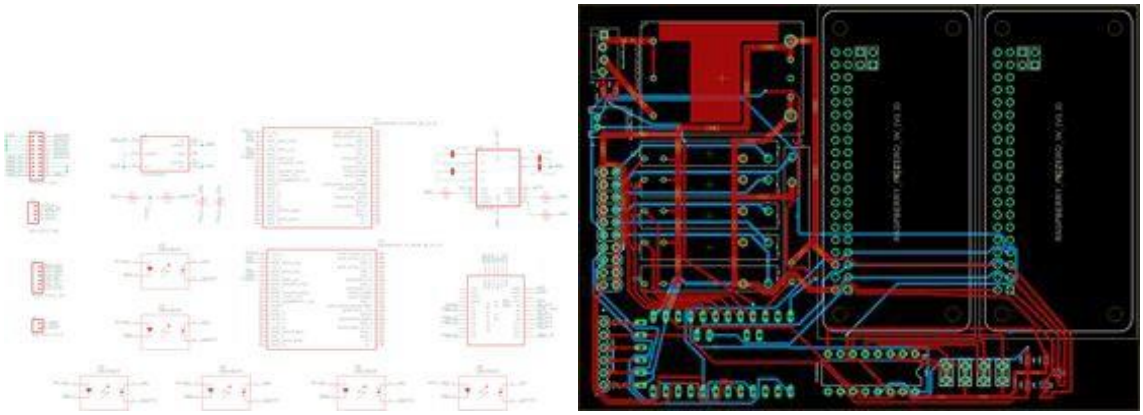

Figure 17: Autodesk Eagle Schematics for Primary Experiment PCBs

5.2.2 Electrical Design: Secondary Experiment

In order to record secondary data upon reentry, the electrical team designed an internal power supply and switch over circuitry because rocket power shuts off before reentry. The secondary experiment requires the use of five thermal probes and thus also requires

increased access to power and input pins. Therefore, PCBs were also designed and implemented (Figure 18).

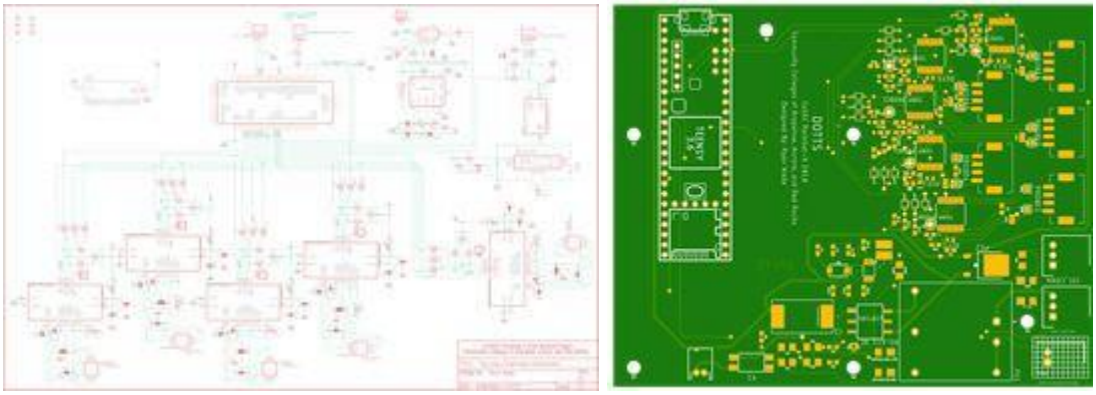

Figure 18. Autodesk Eagle Schematics for Secondary Experiment PCBs

All electronic components were closely inspected and individually tested to ensure there was no bridging or thermal damage from soldering. To further ensure protection from arcing or contamination, all electronic boards were conformally coated. In addition, all wiring insulation were tested to ensure safety and reliability of signal transfers.

5.3 Software Design

Software design required creative coding solutions to meet our unique data capture and storage needs, especially for our photo-recognition telemetry. We chose to code in Python because it has superior data processing, is open-source, and has access to high-level code libraries. Raspberry Pi Zero microprocessors and camera modules were chosen because of size and weight, but also processing capabilities. The Arduino platform is an ideal choice for designating events, so it was chosen as the master microprocessor and the Raspberry Pi's were designated slave microprocessors (Figure 19). Since there is no Linux driver that allows for this setup, the software team developed a work-around that allows the Pi's to function in this manner.

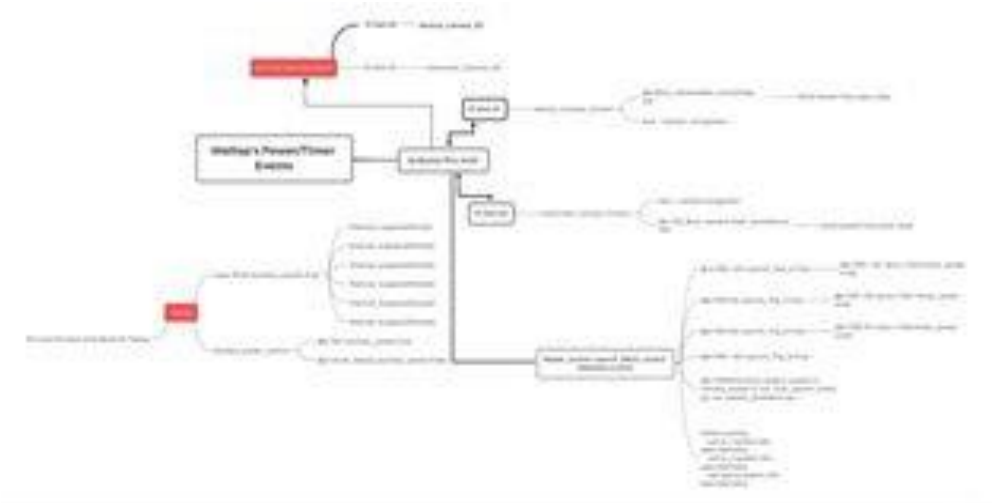

Figure 19: Software Functional Block Diagram

5.3.1 Software Design: Primary Experiment

The primary experiment required extensive programming for photo recognition software that will allow us to use a simplified matrix to track debris vector changes via telemetry (Figure 20).

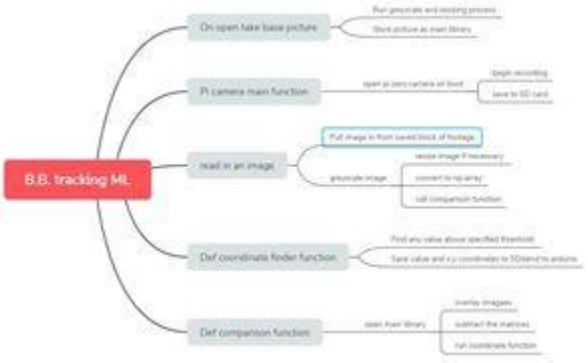

Figure 20: Photo Recognition Functional Block Diagram

An RGB sensor is a three-dimensional numerical space that combines red, green, and blue weights into numerical values that make up pixels. We can convert these values to grayscale by multiplying by a scalar and taking an average value to create a new two-dimensional image. Now the image is scaled from a 500 x 500 matrix via max pooling to a 100 x 100 matrix to lower processing time. A background image of a precisely created grid system will be stored as a library and all other images will overlay this background and comparisons made to x, yand pixel values. These comparisons allow us to determine distance in terms of pixels and create a 3D mapping of how the debris is moving through the field. The reduced data size allows for telemetry to be sent in addition to the video and array set data stored on a SD card. Figure 21 demonstrates the photo recognition process.

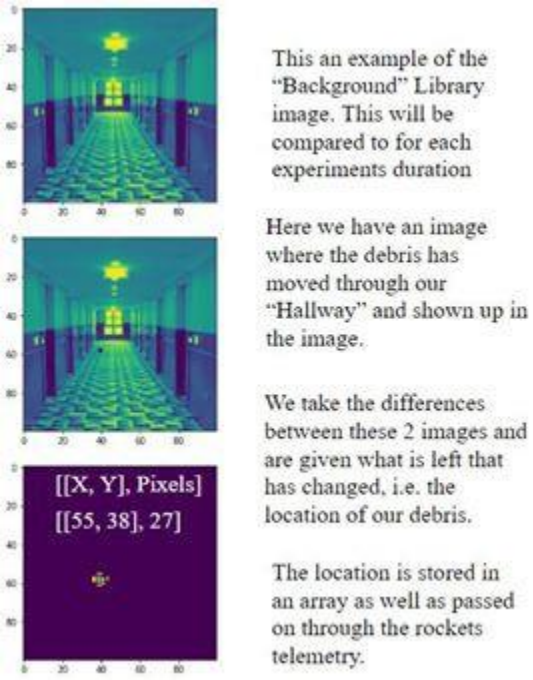

Figure 21: Photo Recognition Process

The two Raspberry Pi Zeros and an Arduino Pro Mini will be powered off the rocket's power, with a kill command assigned to preserve SD card data during splash down.

Major components:

- Raspberry Pi Zero #1 controls camera 1 to monitor debris vertically and saves data to SD card 1.
- Raspberry Pi Zero #2 controls camera 2 to monitor debris horizontally and saves data to SD card 2.
- Arduino Pro Mini controls all the servos and the motors and communication between our data processors and rocket telemetry.

Data will then be saved to its own SD card. It will also control timer events for the main systems.

6.0 Mission Results

Primary Experiment Analysis

Both the EAC and Electronics Chamber exterior of the primary experiment exterior survived reentry well, with minimum damage from reentry and splashdown. There was evidence, however, that both of the chambers leaked water in upon the ocean splash or shortly thereafter.

The Launching System was severely damaged. The launching tower had broken in half. Three out of the four servos that were attached to the launching tower were lost, as well as the camera attached to the front of the launcher. We hypothesise that most of the damage was done to the launching system because of the heat from reentry and the impact upon splashdown, not prior to descend. The BB's were not inside what was remaining of the launch system and there was physical evidence from the servo that had remained had in fact turned as instructed in order to launch the BB. This was determined because of the angle of the lever mounted on the top of the servo.

The interior of the EAC had a substantial amount of water inside when taken apart. The charging plate itself had evidence of heat damage, and what appeared to be dust and small particles melted into the surface. This may have been indicative that the plate had attracted dust and small particles during the charging sequence of the primary experiment.

Aside from the qualitative data collected upon inspection of the payload after retrieval, we had two primary sources of data to analyze. The first was the telemetry data collected, which gave matrix values indicating position of the objects within the launching hallway after each launch. Within the telemetry data was also pixel values indicating the distance of the object being observed in relation to the camera. A "control" image was taken shortly before the launching of each test subject, this acted as a zero or a reference frame so when the BB is

within the view of the camera it could accurately determine the position in the x-, y-, and z-direction

The second form of data collected was video footage taken during each launching sequence. Unfortunately, none of our footage of the launches showed evidence of the simulated debris moving in the view of the camera. There was also evidence of a crack on the camera that was attached to the launch tower (Figure 22). In test footage prior to the launch we found evidence that the crack had started before the launch and existed at least during our check-in at Wallops Island.

Our telemetry data showed matrix and pixel values indicating that objects were moving across the camera at the time the footage took place (during the launches). However, this was not consistent with the footage taken of the launches as there is no evidence of movement in the camera frame during this time.

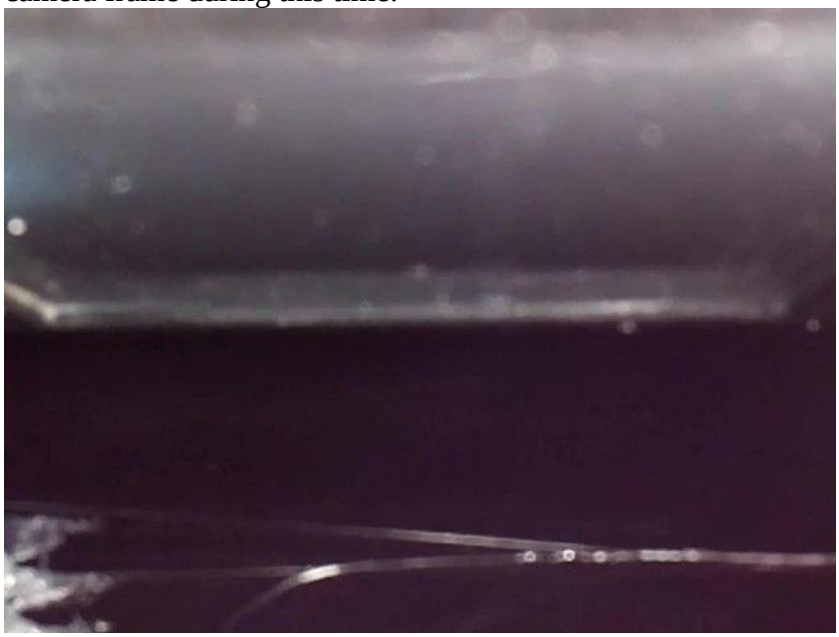

Figure 22: Visual Crack in Camera Lense

Secondary Experiment Analysis

Upon retrieval of the payload, one of the first things that was observed was the state that the 3D printed shape components were in. The structure of the 3D parts showed extremely promising results as from the outside view the shapes were not warped and barely had any considerable damage on them. From this first glance the hypothesis, that alternative low cost materials can be used in space and can resist the intense heat of reentry, was indicating promising results.

As seen in graph 1 there is a total of five lines, each corresponding to the indicated probes. The horizontal axis represents time in seconds ranging all the way from -300 seconds (GSE Start Up) through 0 seconds (time of launch) to after splash down and ending at approximately 2500 seconds. There is a clear distinction between the temperature collected

from the control probe and the rest of the test probes. The maximum recorded temperature gathered by our control probe was 230°C, the minimum 0℃.

With regards to the PETG filament, the maximum temperature recorded was 49°C for both the cube and the spherical shapes, the minimum being 20°C and 19°C, respectively (Graph 3). This temperature data along with our qualitative analysis of the 3D parts was a very clear indication that the PETG filament is a very viable option as a low cost material for low earth orbit space flight. It also has the ability to shield about 181°C of heat, with only 5 millimeters of shell thickness.

For the ABS filament, the maximum temperature recorded was 48°C for the sphere and 38°C for the cube, while the minimum temperatures were 19 °C and 20°C, respectively (Graph 4). The ABS filament maintained its shape and integrity, it also shielded about 182°C of heat, with only 5 millimeters of shell thickness.

As noted, the ability for both ABS and PETG to withstand reentry in both heat insulation and structural integrity cannot be denied. However, another question that needed to be answered is: Which material and shape resisted better?

Graph 2 shows a pretty big distinction in temperature detected. When analyzing the cubic structure, ABS shows that it did a better job at shielding the internal probe from heat compared to the PETG. The maximum temperature experienced by PETG was 11°C greater than the temperature experienced by ABS. Unlike the cubic structure, the sphere structures did not show any significant differences in temperature; both filaments experienced around 49°C.

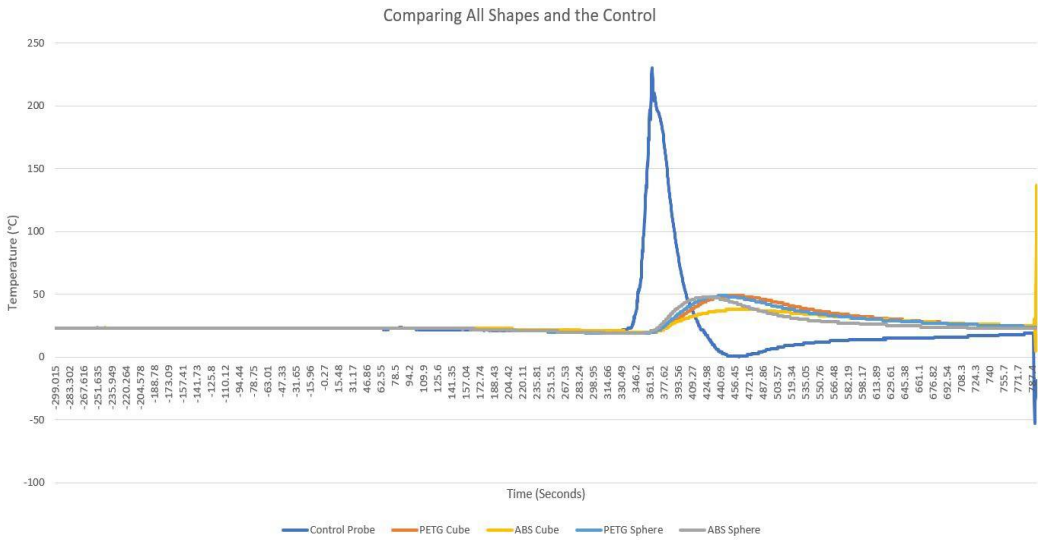

Graph 1: Comparing Internal Temperatures of All Shapes with the Control

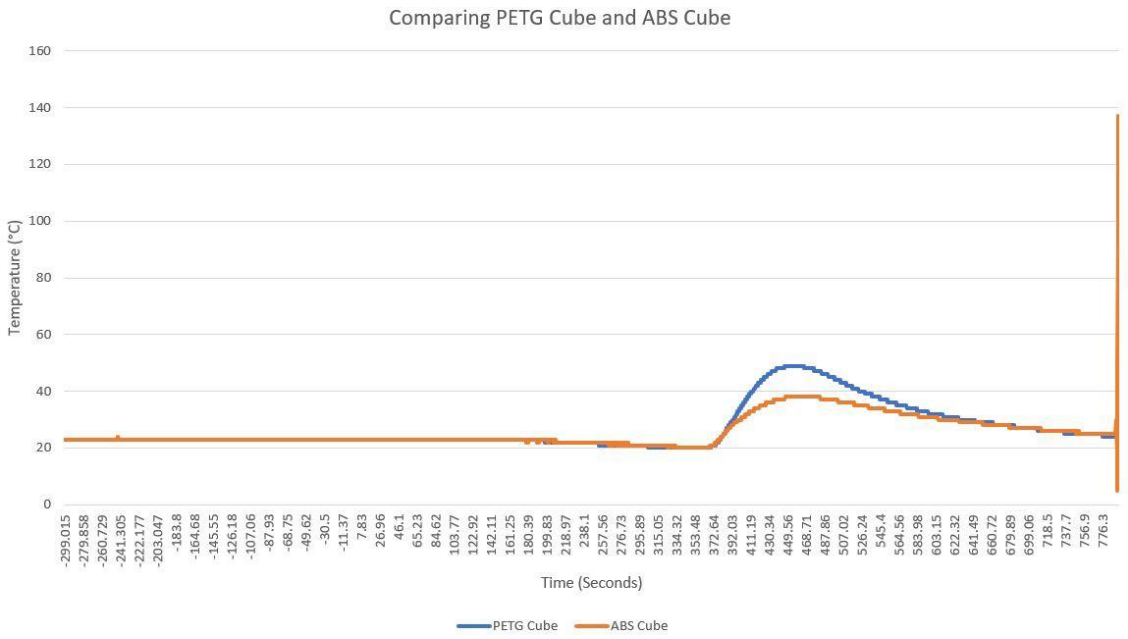

Graph 2: Comparing Internal Temperatures of PETG and ABS Cubical Shapes

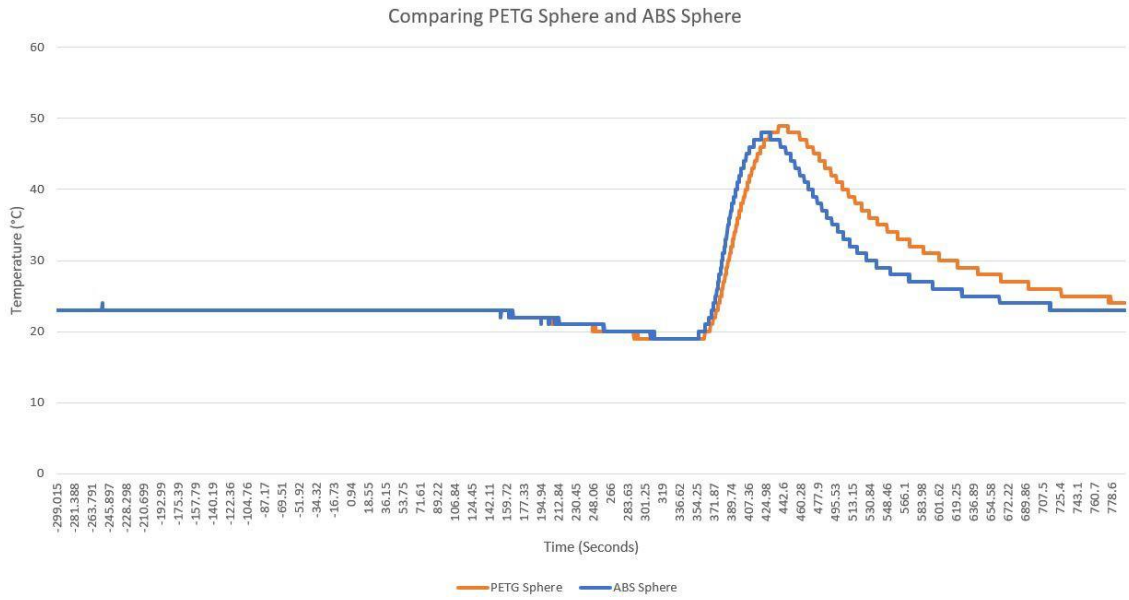

Graph 3: Comparing Internal Temperatures of PETG and ABS Spherical Shapes

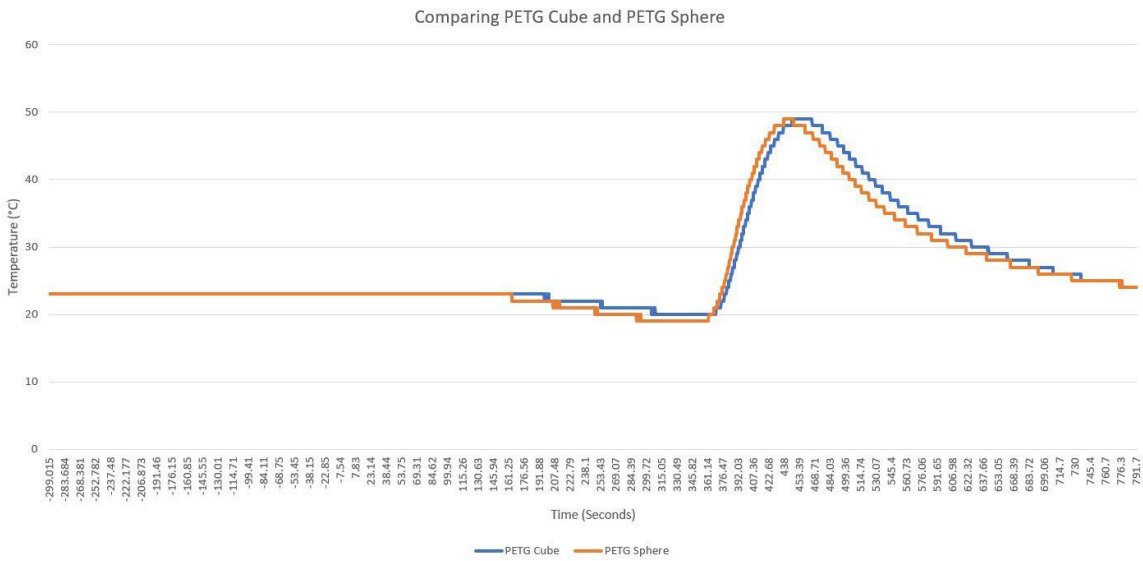

Graph 4: Comparing Internal Temperatures of PETG Cubical and Spherical Shapes

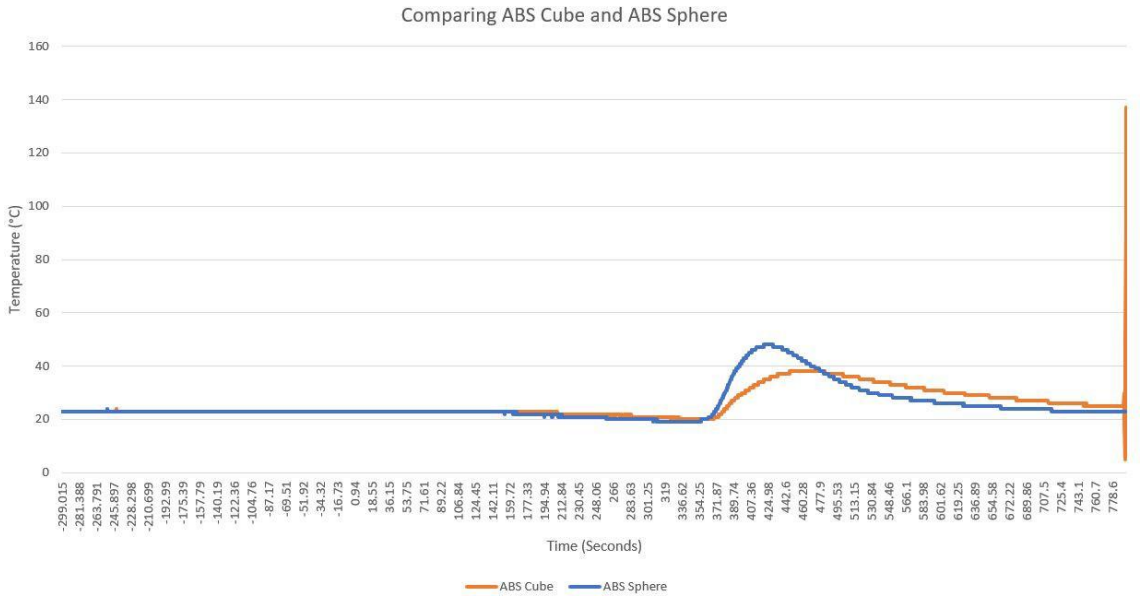

Graph 5: Comparing Internal Temperatures of ABS Cubical and Spherical Shapes

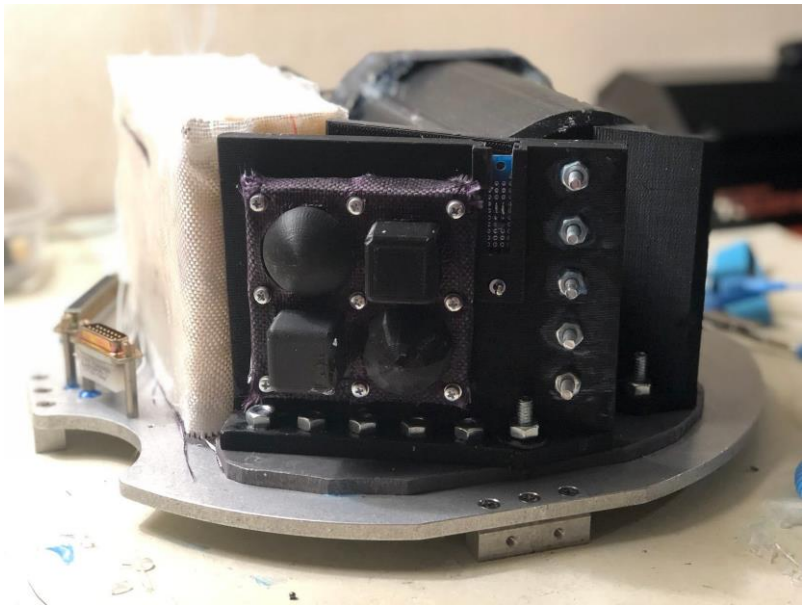

Figure 23:Secondary View Before Flight

7.0 Conclusions

7.1 Primary Experiment Conclusions

After reviewing the camera footage and the data gathered from telemetry, no conclusions could be made from our primary experiment. Pixel values gathered from the telemetry show that there were objects moving, however the data does not correlate with what we would expect. The values stored are essentially an x, y, z coordinates indicating the depth of the BB and it's position. The values that were collected are inconsistent and do not match with the values gathered during our testing. This could be due to the sensitivity of the camera, the camera could have picked up a light source or a different object. These inconsistencies in both the cameras, along with the lack of footage, our primary experiment is inconclusive.

We can however make predictions on what we would have expected to see had the data been accurate. During ground testing, we saw a strong attracting from the BB to the charged polycarbonate plate. When these same test conditions were conducted in a vacuum, the attraction was no longer present, hence the creation of the EAC. When repeating the same test conditions but now with the EAC, the attraction of the free hanging BB and the charge plate were seen once again. The BB and the charged plates behaved like magnets, once close enough the forces between them rapidly grew, this shows that the theoretical math of electrical fields supports our experiment. The EAC was carefully sealed and tested in numerous conditions until we found the perfect procedure to obtain a sealed container. Assuming that the EAC stayed sealed during flight and that the attraction between the BB and the charged plate remained present, the primary experiment would be proved successful; static electricity is a viable way to change the trajectory of non-

ferrous space debris. The experiment should be reconducted with improved data measuring methods to ensure that this statement is accurate.

7.2 Secondary Experiment Conclusions

The secondary experiment collected thermal data upon reentry. The experiment contained two spherical and cubic shapes printed from PETG and ABS 3D filament. Housed inside a hollow section of these shapes was an RTD temperature probe to measure the internal temperature. Aside these printed shapes sat another RTD temperature probe which served as a control. The secondary experiment began upon GSE start up which was approximately T-minus 300 seconds and continued to record temperature data until after splashdown. When analyzing the numerical data of the secondary experiment the control probe gives a clear indication when launch occurred, when apogee was met, when reentry heat was at its peak and when splashdown occurred (Graph 1). A few seconds before shoot deployment the temperature experienced on the payload was 230°C. At this same time the internal temperatures of our test subjects only read 20°C. 56 seconds after the peak of the control, the ABS sphere reached its maximum temperature of 48°C. 74 seconds after the peak temperature of the control, the PETG sphere reached its maximum temperature of 48°C. 86 seconds after the peak of the control the PETG cube and the ABS cube reached their highest internal temperature of 49°C and 38°C respectively. It can be assumed that the shapes didn't report their highest temperature at the same time as the control because the shapes were on fire. The high external temperature was likely burning through the material and did not stop until after shoot deployment and splashdown. Given that there was no notable differences in the shapes appearance, the quantitative data shows that the ABS cubic structure withheld the best from the high temperatures on reentry. Not only did it report the lowest internal temperature but it also took the longest for the heat to penetrate through the structure.

8.0 Potential Follow-on Work

There is a lot that the team has learned from the results of our experiments and there is still a lot to discover. It is important to better understand the effects of reentry and to determine reliable, cost effective materials for future space flight. We received very reliable data from our secondary experiment, the next steps would be to take the experiment to new heights and expand the concept. The sounding rocket only reached an apogee of about 100 miles thus its reentry energy is not as great as a full descend from outside of Earth's atmosphere. Given the opportunity and funding the next steps to expand the testing of this experiment would be to test and catalog the effects of reentry from a higher descend. The printed structures will likely be exposed to a higher wind velocity and temperature which will affect their strength, insulative properties, and deformation. The secondary experiment can go as far as testing 3D printed material while in space for a certain duration to measure the effects of radiation, extreme cold, and the rate of decay of the filaments.

As space travel continues, the number of space debris will continue to grow. It is imperative that the necessary steps are taken to deorbit the debris. The primary experiment showed promise during our pre-flight testing and while the flight data did not fully capture or prove

the concept, we strongly believe that the use of static electricity is a viable option to change the trajectory of small low earth orbital debris. The team plans to continue testing and exploring this concept. The next steps for this project are to determine how we can get better data in the future. We will then explore static charge in a vacuum state, determine more efficient ways to generate an electric field, and redesign our parts to accommodate our findings.

9.0 Benefits to the Scientific Community

As participants in a global effort to prevent harmful repercussions associated with increasing space debris, our project mission was to design, implement and fly a sounding rocket payload that will collect robust, foundational data to develop passive, cost-effective methodology for de-orbiting small, fragmented space debris using a platform of electrostatic repulsion and incorporating material properties of 3D printed components. Arapahoe Community College, Community College of Aurora, and Red Rocks Community College working in collaboration have developed D.O.T.T.S. (Debris Orbital Tumbler and Thermal Sensors), an experimental payload which contains two experiments: 1. Implementation and use of a static electric field to meaningfully impact the trajectory of simulated space debris fragments. 2. Testing and documentation of key characteristic material properties (internal temperature, shear strength, and deformation) on the effects of thermal reentry on multiple 3D printed structures and varied filaments. Our hope is to contribute meaningful data to the research and development of space remediation and gain a foundational understanding of systems engineering and integration.

The aggregate of space debris orbiting the earth has grown exponentially over the past two decades, an alarming trend with potentially catastrophic impacts on global aerospace activity [1,2]. According to Holger Krag, head of the European Space Agency's (ESA) Space Debris Office, approximately 60 percent of missions follow the International guidelines for removal of spacecraft from low-Earth orbit (LEO) within 25 years of mission completion [1]. The current debris load will require the removal of more than 100 objects from LEO at aminimum rate of five per year to “stop the proliferation of fragments resulting from in-orbit collisions and explosions,” says Satomi Kawamoto, of the Japan Aerospace Exploration Agency (JAXA) [1]. Currently, the U.S. Space Surveillance Network tracks 1,200 intact, operational satellites, and 18,000 objects larger than 4 inches (~10 centimeters) but estimates that about 750,000 "flying bullets” (~1 centimeter) and roughly 150 million fragments (~1 millimeter) are orbiting earth, which could damage operational satellites [3]. In 1978, Donald J Kessler, a scientist at NASA, predicted the finite area in LEO available to satellites coupled with the growing number of satellites, would lead to an inevitable, self-sustaining cascade of collisions which has far-reaching negative impacts on space exploration [4].

As participants in a global effort to prevent these consequences, our project mission was to design, implement and fly a sounding rocket payload that will collect robust, foundational data to develop passive, cost-effective methodology for de-orbiting small, fragmented space debris using a platform of electrostatic repulsion and additive manufacturing.

10.0 Lessons Learned

Being part of a team that was geographically segregated amongst three community colleges that composed our 15 team member team, there were many things that were learned from this experience. When referring back to our mission statement and while analyzing the data obtained, our team noticed that sometimes even the most precise planning can come with flaws. Our primary experiment experienced vital issues which vandalized our desired results. This caused our team to not meet this part of our mission fully since we were not able to prove nor deny that a static electric charge can change the trajectory of space debris fragments. It could be inferred that components of this particular part of the experiment might have been affected by the force of launch which caused our deployables to not be able to be tracked by our cameras. This taught us what to expect in microgravity being that this was the only thing that was not able to be tested on earth. Our experiment was very successful; we received our temperature data and were able to physically inspect the experiment upon its retrieval.

Aside from these learning components, it could also be said that all the team members grew as individuals. All of the team members were involved in one way or another without putting a main focus to our previous strengths. Some of us wanted to improve our skills in different sectors which allowed us to split accordingly in order to learn new concepts while making positive contributions to the team. Communication was another skill that played a huge part in understanding meetings, payload development, part manufacturing and team dynamics. Good communication helped a lot of team members work through problems that were causing friction between themselves, and helped lead to a more harmonious outcome. Time management is another thing a lot of us learned quickly. Balancing a project that was so demanding and in need of such attention, with heavy class loads and homework assignments, was something we had to figure out quickly in the beginning. If this payload were to be flown again, something that would not be allowed would be using lower quality manufacturing materials for vital components to the experiment such as the launcher tower or using higher quality printers to ensure consistent design prints. Our team would manufacture a stronger and better developed launcher since this was the only component that was completely destroyed from our payload.

As per our secondary experiment, we had set out to see which of two 3D printer material would withstand the transfer of heat from re-entry the best. As per the data above, the ABS was much better in dissipating the heat and keeping the probe at a cooler level. This shows that in the future, if we were to fly again, ABS would be best to hold up against the harsh conditions of reentry. Along with another, more durable design, if we were to 3D print the launch tower, it would definitely be printed out of ABS material.

11.0 References

[1] Pultarova, Tereza. “Meet the Space Custodians: Debris Cleanup Plans Emerge.” Space.com, Future US

Inc, 26 Apr. 2017, www.space.com/36602-space-junk-cleanup-concepts.html.

[2] Popova, Rada, and Volker Schaus. “The Legal Framework for Space Debris Remediation as a Tool for Sustainability in Outer Space.” Aerospace, vol. 5, no. 2, 2018, p. 55., doi:10.3390/aerospace5020055.

[3] ESA. “Space Surveillance and Tracking - SST Segment.” European Space Agency, Http://Www.esa.int, 11 Nov. 2017, www.esa.int/Our_Activities/Operations/Space_Situational_Awareness/Space_Surveillance_and_Tracking_-_SST_Segment.

[4] Kessler, Donald J., and Burton G. Cour-Palais. “Collision Frequency of Artificial Satellites: The Creation of a Debris Belt.” Journal of Geophysical Research, vol. 83, no. A6, 1 June 1978, pp. 2637–2646., doi:10.1029/ja083ia06p02637.

[5] Rossi, Alessandro, et al. “ReDSHIFT: A Global Approach to Space Debris Mitigation.” Aerospace, vol. 5, no. 2, 2018, p. 64., doi:10.3390/aerospace5020064.

[6] Schaub, Hanspeter, and Zoltán Sternovsky. “Active Space Debris Charging for Contactless Electrostatic Disposal Maneuvers.” Advances in Space Research, vol. 53, no. 1, Jan. 2014, pp. 110–118., doi:10.1016/j.asr.2013.10.003.

[7] National Research Council. 2014. 3D Printing in Space. Washington, DC: The National Academies Press. https://doi.org/10.17226/18871.

[8] Werner, Debra. “3D Printing Saving Satellite Builders Time and Money.” SpaceNews.com, Space News, 9 Mar. 2017, spacenews.com/3d-printing-saving-satellite-builders-time-and-money/.

Acknowledgements

Claro would like to thank:

The Contributing Students, whose scholarly pursuits exemplify the best of RRCC's interdisciplinary achievements and commitment to excellence.

The Contributing Instructors, whose innovative assignments and discerning tastes provide Claro with quality content year after year.

The RRCC Foundation, whose grant made the initial issue of Claro a reality.

Founder of Claro
Stina French